Report MDC A3304
15 March 1975

Copy No. 31

EXPANSION OF FLIGHT SIMULATOR CAPABILITY FOR STUDY AND SOLUTION OF AIRCRAFT DIRECTIONAL CONTROL PROBLEMS ON RUNWAYS

Phase I

Final Report

FOR NASA INTERNAL USE ONLY

National Aeronautics and Space Administration
Langley Research Center
Contract NAS 1-13378

MCDONNELL AIRCRAFT COMPANY
Box 516, Saint Louis, Missouri 63166 · Tel. (314)232-0232

MCDONNELL DOUGLAS CORPORATION

TABLE OF CONTENTS

TABLE OF CONTENTS (Continued)

LIST OF PAGES

LIST OF FIGURES

LIST OF TABLES

ABBREVIATIONS AND SYMBOLS

ABBREVIATIONS

AGL	Above ground level
APCS	Approach power compensation system
ARI	Aileron rudder interconnect
BLC	Boundary layer control
CDC	Control Data Corporation
EOM	Equation of motion
HML	Hinge moment limits
MAC	Mean aerodynamic cord
MLG	Main landing gear
MBS	Motion base simulator
MCAIR	McDonnell Aircraft Company
MDC	McDonnell Douglas Company
NLG	Nose landing gear
SAS	Stability augmentation system
SFC	Secondary flight controls

SYMBOLS

$C_{D,f}$	Tire fluid drag coefficient
C_{M_α}	Pitching moment due to angle of attack change
$C_{M_{\dot\alpha}}$	Pitching moment due to rate of angle of attack change
C_n	Yawing moment coefficient
C_{n_r}	Yawing moment due to yawing velocity
C_{n_p}	Yawing moment due to rolling velocity
C_{n_β}	Yawing moment due to sideslip
$C_{n_{\delta_a}}$	Yawing moment due to aileron deflection
$C_{n_{\delta_R}}$	Yawing moment due to rudder deflection

ABBREVIATIONS AND SYMBOLS (Continued)

C_M	Dynamic pitching moment coefficient
C_{m_q}	Pitching moment due to pitching velocity
$Cl_{\delta a}$	Rolling moment due to aileron deflection
C_{Lq}	Lift coefficient due to pitching velocity
Cl_r	Rolling moment due to yawing velocity
Cl_β	Rolling moment due to sideslip
C_L	Lift coefficient
$Cl_{\delta R}$	Rolling moment due to rudder deflection
C_{l_P}	Rolling moment due to rolling velocity
C_D	Drag coefficient
C_T	Skid control brakes on-off ratio
C_{y_r}	Side force due to yawing velocity
d_1	Runway fluid depth
FGN	Vertical force on tire
FSN	Strut spring force
FNY	Nose strut side force
FD	Total strut damping force
FVN	Strut viscous damping force
FV^2N	V^2 damping force
K_T	Tire heating factor, provided by NASA
N	Number of tires
N_y	Aircraft lateral acceleration
N_Z	Aircraft vertical acceleration
P_r	Tire rated pressure

ABBREVIATIONS AND SYMBOLS (Continued)

Q	Dynamic pressure
S	Displacement
$\dot{S}$	Velocity
$\ddot{S}$	Acceleration
T	Time
V_g	Ground velocity
V_{side}	Component of MLG strut velocity parallel to axle
V_{total}	Total resultant MLG strut velocity
$V_{N_{side}}$	Component of NLG strut velocity parallel to axle
$V_{N_{total}}$	Total resultant NLG strut velocity
W	Tire width
$\bar{Y}_R$	Tire hydroplaning parameter
Y_{cmb}	Lateral motion of simulator
$\ddot{Y}_{cmb}$	Lateral acceleration of simulator
Z_{cmb}	Vertical motion of simulator
$\ddot{Z}_{cmb}$	Vertical acceleration of simulator
α	Aircraft angle of attack
δ/d	Tire deflection/diameter ratio
θ	Simulated aircraft pitch angle
μ_{max}	Maximum coefficient of friction
μ_{eff}	Effective coefficient of friction
μ_s	Coefficient of friction perpendicular to line of motion
μ_D	Coefficient of friction in line of motion
τ	Time constant
ϕ	Simulated aircraft roll angle
ψ	Angle tire makes with line of motion
ψ_N	Angle nose tire makes with line of motion

ABBREVIATIONS AND SYMBOLS (Continued)

ψ_M	Angle main tire makes with line of motion
ψ_A	Aircraft yaw angle
ρ	Fluid mass density

1.0 SUMMARY

This report describes the study performed by McDonnell Aircraft Company (MCAIR) under National Aeronautics and Space Administration (NASA) Contract NAS 1-13378 titled "Expansion of Flight Simulator Capability for Study and Solution of Aircraft Directional Control Problem on Runways." Principal investigators were William Macy, Robert Palmer, Harry Passmore and Dave Rolston. The program was managed by Mark Thorpe.

The objectives of this contract were to define and demonstrate the hardware and computer software necessary to expand current flight simulator capability for study and solution of aircraft directional control problems on runways. The USAF-MCAIR F-4 aircraft was selected for this study since its performance and system parameters are well documented. The MCAIR five-degree-of-freedom motion-base simulator (MBS) was used in combination with a six-degree-of-freedom aircraft mathematical model to demonstrate the simulation adequacy on dry, wet, flooded and icy uncrowned runways with steady state and gusty crosswinds. Known aircraft parameters were used where possible to increase program credibility. Tire-runway friction models were coordinated with personnel of NASA, Langley Research Center. Three F-4 experienced pilots representing NASA, FAA, and USAF participated in the 130 approach-touchdown-rollout demonstration and verified the simulation adequacy. This report represents the completion of the feasibility demonstration phase of the total investigation of the simulator use for ground handling studies.

We at MCAIR appreciate the program contributions of many people especially John McCarty, Walter Horne, and Thomas Yager of NASA, Langley Research Center.

2.0 INTRODUCTION

Aircraft operational safety margins are reduced by slippery runways, crosswinds, reduced visibility, extended touchdown points, excessive velocity, insufficient directional control, equipment malfunction and aircraft configuration constraints and limitations.

In past years, research and development efforts have concentrated almost exclusively on optimization of the braking portion of landing and have neglected the equally critical directional control element of the ground handling problem. Airplane performance during takeoff and landing is traditionally explored when the aircraft is in the flight test phase, at which time indicated changes are expensive to incorporate. In addition, only part of the directional control characteristics envelope can be safely examined in flight testing. Thus, the object of this contract was to expand the same techniques used to simulate aircraft in flight to include the runway rollout portion of flight operations.

This program is the first step in developing an effective simulation as a design and evaluation tool for safely exploring aircraft directional control and braking performance under adverse runway conditions. Once this simulation capability is developed, the potential applications include,

- Aircraft configuration trade-off studies in the aircraft design phase.
- Establishing safe operational limits for existing aircraft.
- Optimizing pilot techniques on adverse runways.
- Defining regulatory requirements for aircraft and runway design.
- Training pilots for adverse runway conditions.

3.0 PROGRAM DESCRIPTION

3.1 Objectives

The principal objective of this contract was to define and demonstrate the hardware and computer software necessary to expand current flight simulator capability for study and solution of aircraft directional control problems on runways. The primary effort was to model the landing gear system of an F-4 and to add this subroutine to the existing flight related aircraft simulation.

3.2 Approach

3.2.1 General Simulation Approach - The approach, touchdown, and rollout environment of aircraft operations was examined during this study using a six-degree-of-freedom simulation program in conjunction with a five-degree-of-freedom motion-base simulation (MBS) cockpit. Runs which do not include the approach phase result in control problems which are not typical of the aircraft because the pilot is uncertain as to what initial control inputs to provide. The aircraft touchdown simulation included characteristics due to yawed or wing-low landing.

In modeling the simulation, information from analytical studies, flight tests, laboratory tests and runway friction tests was incorporated as follows:

- F-4 Category II "Wet Runway Testing" and the Edwards AFB "Raintire" flight test data was used to quantitatively verify simulator performance and to correlate the effective tire-runway friction models.
- Qualitative data from pilot experience provided information on runway braking and directional control performance.
- Laboratory strut drop test results were used to determine landing gear strut dynamics (damping and friction).
- NASA, LRC test track data was used in conjunction with NASA empirical equations to formulate the tire-runway friction models.

The resulting total simulation used software models of the aerodynamic environment and the aircraft characteristics, including controls, engine, landing gear and tire dynamics. The simulation was run on the motion-base simulator, using video visual displays of a terrain map runway.

3.2.1.1 Motion Base Simulator (MBS) - The MBS, shown in Figure 3-1, was chosen for studying directional control on the runway, based on providing the pilot with as many visual and motion cues as possible.

The MBS provides the added dimension to the simulation by providing acceleration onset cues to the pilot. Yaw mode skidding onset and "fish-tailing", both phenomena experienced by aircraft on wet runways, are mainly "felt" rather than "seen" during that initial critical control period. A diagram of the motion base simulators operation is presented in Figure 3-2.

The MBS response can match the aircraft response for only a short time period due to displacement limitations, thereafter the command signals must be "washed out" to prevent the MBS from driving to its physical limit. The washout is a trade-off between the minimum pilot perception rate and the time required to project an acceptable level of motion cue. Washout rates are discussed in Section 5.1.3, motion drive washouts.

3.2.1.2 Software Programs - The software for the simulation consists of an executive routine and several subroutines as presented in Figure 3-3. The executive routine is used to provide program control and to call the subroutines in the appropriate order.

The aerodynamic, control system, engine system, gear system and wind subroutines were used to determine the forces and moments which are input to the six-degree-of-freedom equations of motion (EOM). Integrations to determine the velocities and positions of the aircraft center of gravity are performed in the EOM routine. Details of software are found in Section 5.0.

3.2.2 Aircraft Selection

The F-4 aircraft was selected for this simulation study for the following reasons:

1) Simplicity - The F-4 has single braked-wheel struts which simplified the initial modeling effort.

2) Commonality with other aircraft - The F-4 has pilot selectable nose wheel steering, several generations of skid control, multi-engines and auxiliary drag devices. These are items which are common to more complex aircraft.

3) Available qualitative data - The F-4 ground handling characteristics are well known due to numerous landings experienced under various adverse runway and surface wind conditions.

4) Available quantitative data - The F-4 has an extensive amount of documented aircraft data. The aircraft parameters are well known; i.e., aerodynamic coefficients, landing gear spring and damping constants, engine and control system characteristics, and aircraft tire-to-runway parameters. Existing aircraft runway related programs which were utilized included the Wallops Island "Grooved-Runway Studies", the Edwards AFB "Raintire Program" and the RF-4C Category II "Wet Runway Testing." In addition, NASA, LRC has conducted landing loads track test programs to verify the F-4 tire friction mechanics and skid control system performance.

5) Previous simulator modeling - The F-4 has previously been modeled in the "in-air" mode for motion and fixed-base simulators.

3.2.3 Modeling - The landing phase portion of the previous MBS aerodynamics model was used for this study. All other portions were omitted to make more computer core available for detailed modeling of the strut dynamics and tire friction. See Section 5.0 for details of software models.

3.2.4 Demonstration and Evaluation - The aircraft ground handling simulation was quantitatively and qualitatively evaluated. During the program demonstration, which took place on 18 and 19 November 1974, representatives of NASA, FAA, and USAF participated. The demonstration consisted of having three pilots "fly" the MBS, during which they compared the feel of MBS to that of the real aircraft. Quantitative data such as stopping distance and velocity were recorded for comparison to actual flight data.

3.2.4.1 Qualitative Results - The qualitative results were given in two forms; general comments and a numerical rating of various aspects of the simulation. Figure 3-4 is a sample form which was used by the pilots to provide an evaluation of this simulation. The rationale associated with their numerical grading is illustrated in Figure 3-5. The pilots were instructed to evaluate how well the MBS simulated the actual aircraft.

3.2.4.2 Quantitative Results - Comparisons of simulation data outputs to the actual flight test results of the "RF-4C Category II Wet Runway", the F-4 "Raintire", and Wallops Island "Grooved Runway" test programs were conducted (See Figure 6-11).

3.3 Program Schedule

The program schedule is shown in Figure 3-6. The only significant change in the proposed schedule was the extension of Task III, Simulation Development and Verification. The extension was intended to further tune the simulation and study the sensitivity to changes in some of the models resulting from the various comments and discussions during the Task IV Simulation Demonstration.

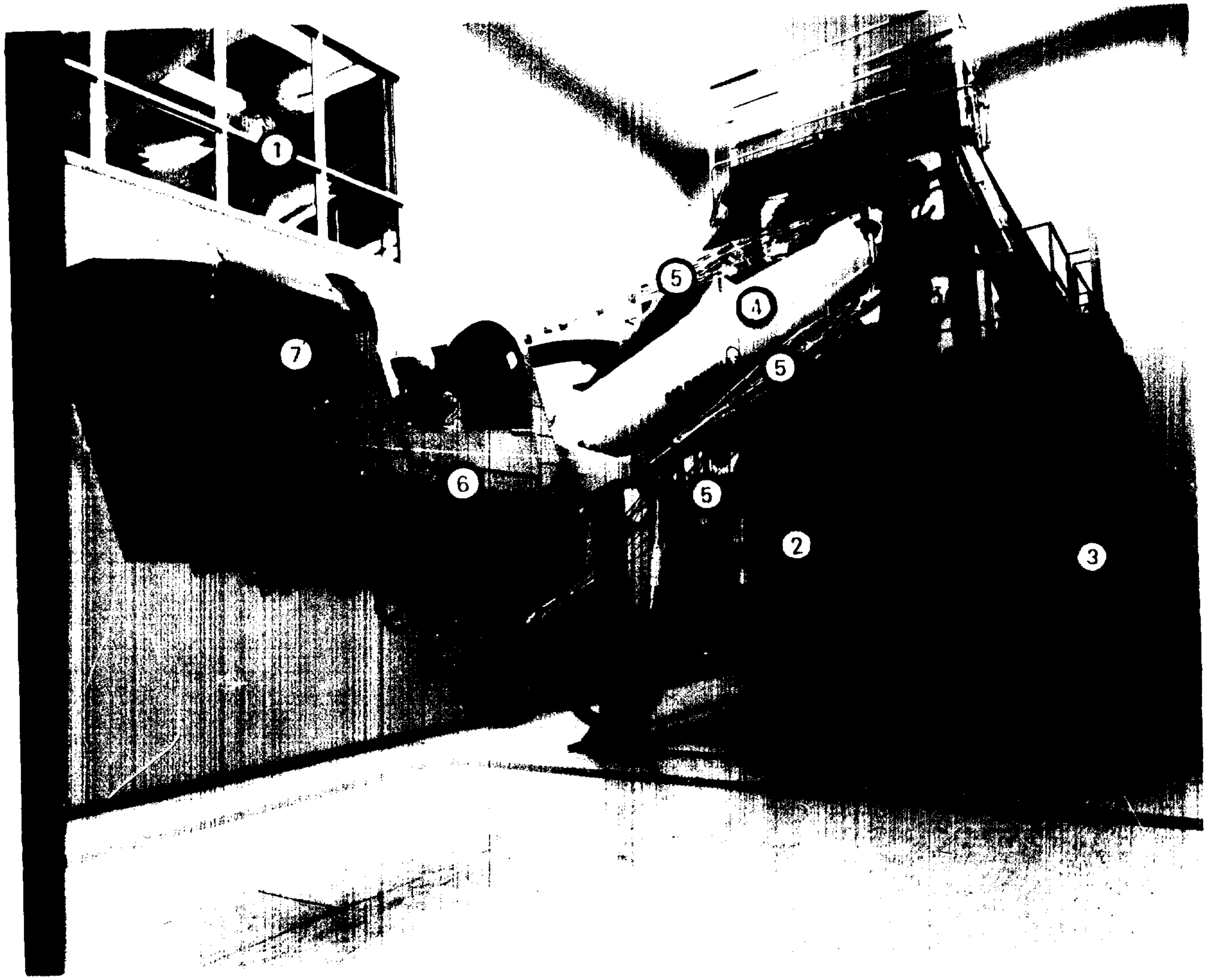
1
5
4
7
5
6
5
2
3

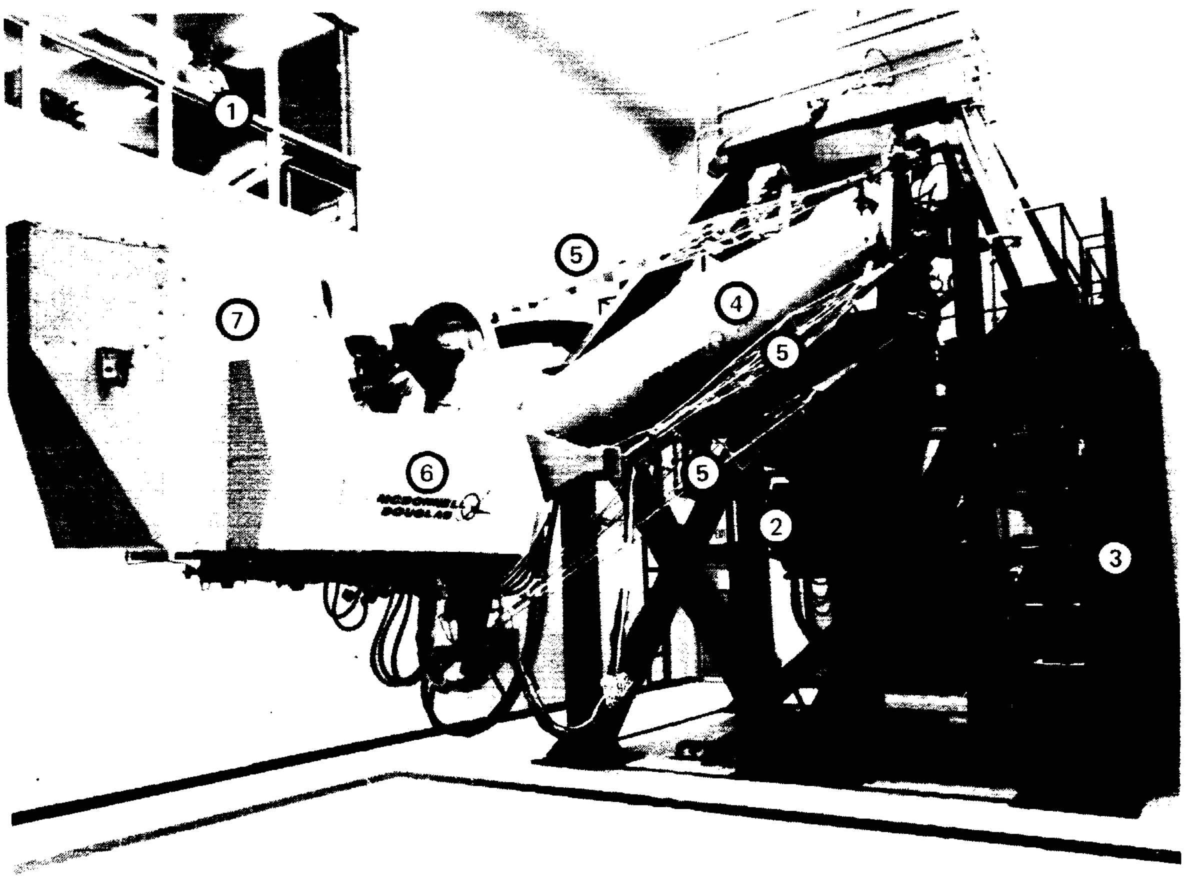

1. Control Console
2. Vertical Motion Actuator
3. Hydraulic Accumulator
4. Boom
5. Pitch-Roll-Yaw Mechanism
6. Cockpit
7. Visual Display System

FIGURE 3-1
MOTION BASE SIMULATOR (MBS)

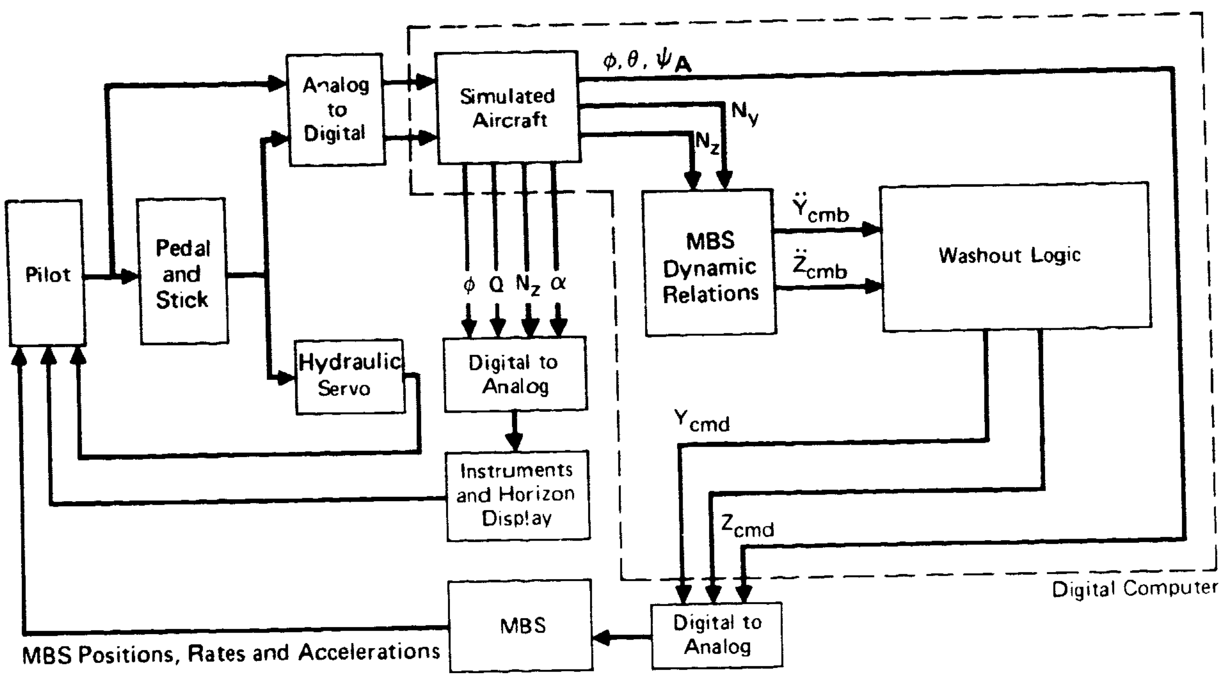

FIGURE 3-2
MOTION BASE SIMULATION DIAGRAM

GP75 0072 21

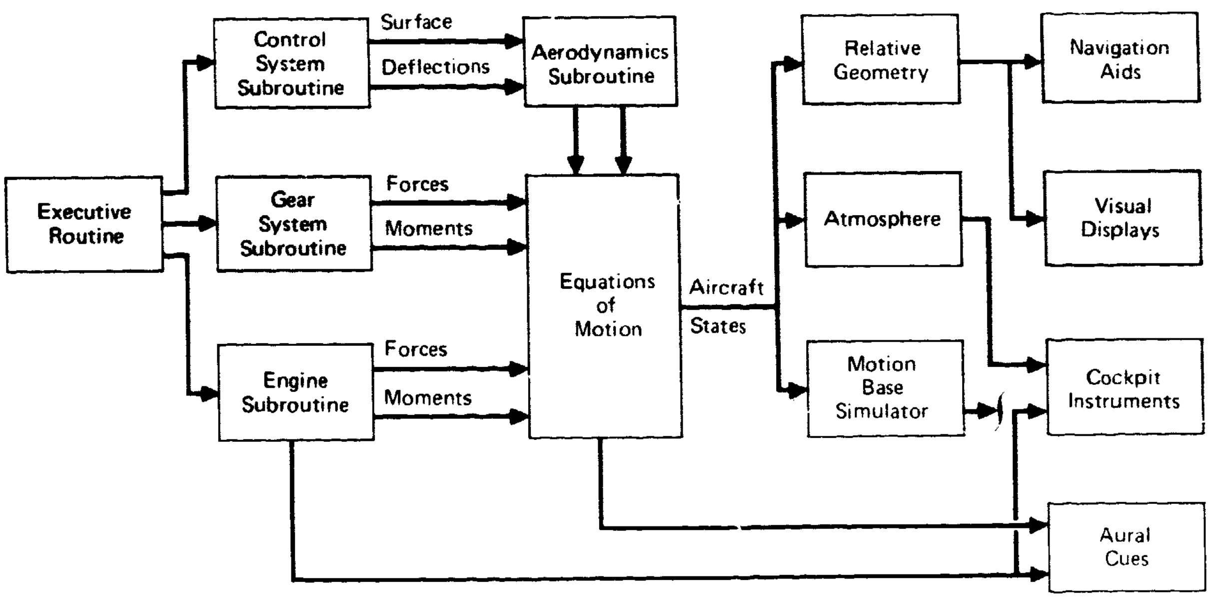

FIGURE 3-3
MAJOR SOFTWARE MODULES

GP75-0072-22

Pilot: ______________________

Runway Condition: Dry ______ Wet ______ Flooded ______ Icy ______

Item	Rating (Excellent) 1	2	3	4	5	6	7	8	9	(Poor) 10
1. Aerodynamic Steering										
2. Nosewheel Steering										
3. Combined NW & Aero Steering										
4. Braking Effectiveness										
5. Crosswind										
6. Yaw Control										
7. Yaw Stability										
8. Drag Chute										
9. Other										

Comments:

FIGURE 3-4
MOTION BASE SIMULATION RATING SHEET

GP75 0072 13

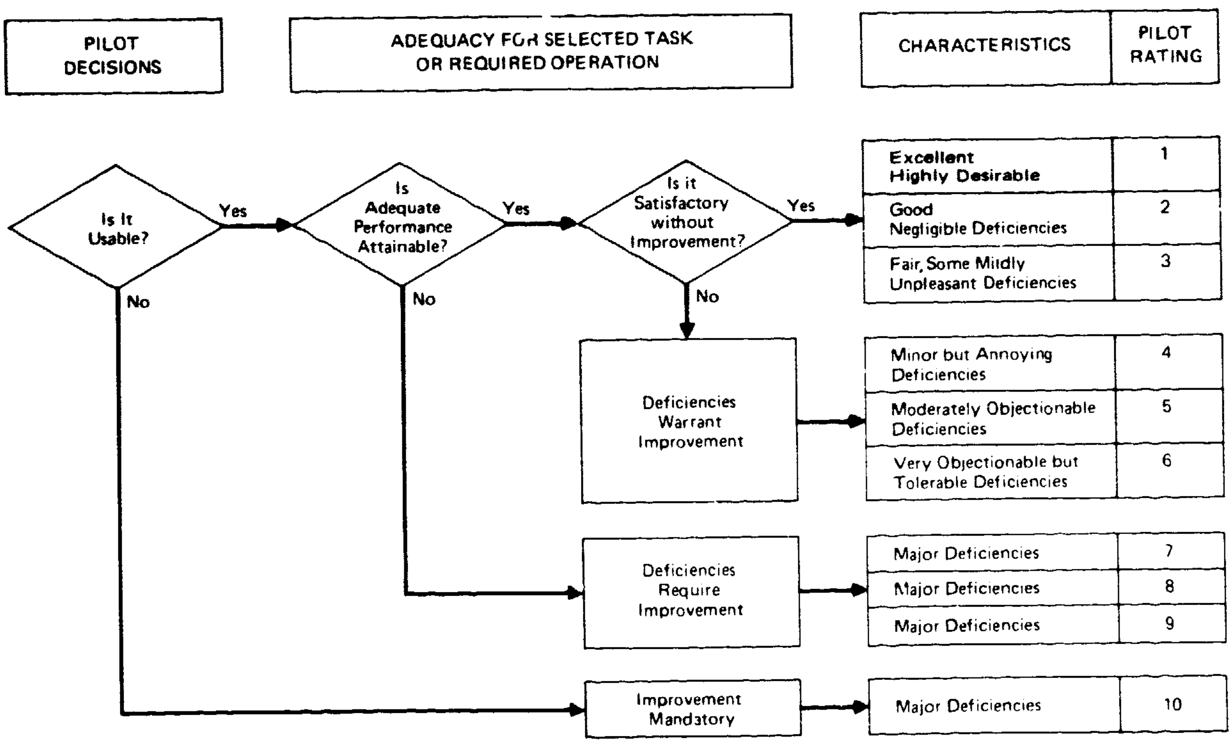

FIGURE 3-5
PILOT RATING CRITERION

GP75-0072-3

ORIGINAL PAGE IS
OF POOR QUALITY

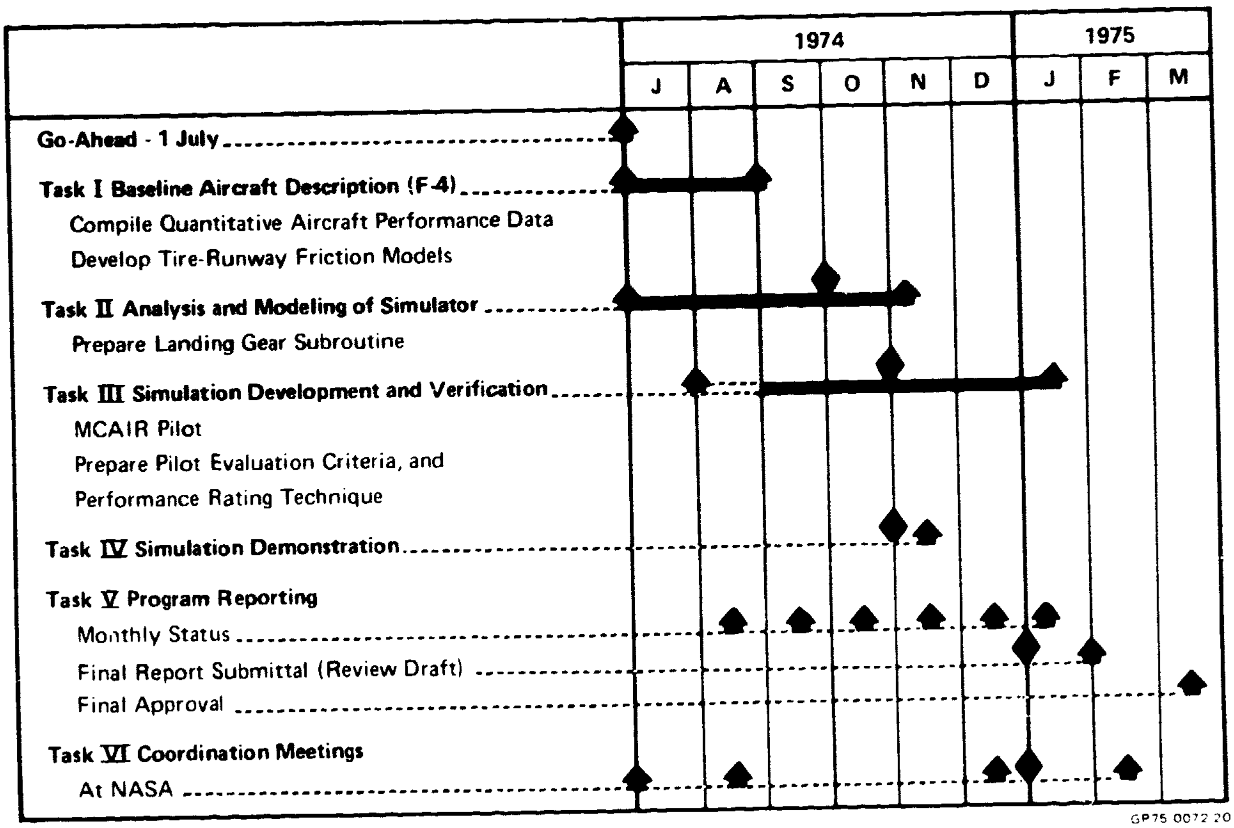

Key:

- Scheduled Milestone
- Actual Milestone
- Originally Scheduled (on Proposal) but Revised
- Task Scheduled, Work not in Progress
- Work in Progress

FIGURE 3-6
PROGRAM SCHEDULE

4.0 PROGRAM HARDWARE

4.1 Flight Simulation Facility

The McDonnell Aircraft Company, St. Louis, flight simulation laboratory employs a Control Data Corporation (CDC) 6600 digital computer with a modified KRONOS operating system. All computations are performed in the digital computer and signals are distributed to the various hardware locations by the Unit Interface. A Unit Controller at each location (cockpit, brush recorders, display generation area) does the analog-to-digital and digital-to-analog signal conversion. Other peripheral equipment includes three tape drives, three disks, two line printers and a card reader.

4.2 Motion Base Simulator

The MBS is a large amplitude, hydraulically powered, five-degree-of-freedom, single-cockpit, motion-base simulator with out-the-window displays. The MBS, shown schematically in Figure 4-1, is a flexible design tool which operates in conjunction with the computer and display-generating equipment.

The cockpit is mounted on the end of a 20 foot movable boom. Pitch and yaw are produced by moving the crew station mounting structure about a universal joint at the end of the boom. Roll is obtained by rotating the crew station with respect to its mounting structure. Vertical and lateral translation is provided by rotating the boom in its two-degree-of-freedom mounting while simultaneously rotating the cockpit with respect to the boom. This system essentially uncouples the cockpit angular motions from the motions of the boom.

Crew station motion is produced by hydraulic actuators. Hydraulic power for the motion system is supplied by a 150 gpm, 300 psi pump driven by a 250 hp electric motor. This supply is augmented by a 100 gallon accumulator to accommodate large transient acceleration requirements.

The following table contains the current man-rated performance specifications for the motion base simulator:

Degree of Freedom	Displacement	Velocity	Acceleration
Vertical	±8 ft	±8.5 ft/sec	+3g, -1g
Lateral	± 5 ft	±6.5 ft/sec	±1g
Pitch	±30°	±30 deg/sec	±300 deg/sec^2
Roll	±20°	±100 deg/sec	±240 deg/sec^2
Yaw	±30°	±30 deg/sec	±240 deg/sec^2

The MBS servo system contains redundant safety systems to prevent a motion limit impact in case of electrical or hydraulic failure. Dampers are incorporated at the motion limits to control deceleration forces to safe levels if the electrical safety system were to fail and allow an impact.

4.3 MBS Cockpit

The crew station is laid out in a general single place fighter arrangement, with some flexibility as to location of instruments and controls.

The MBS cockpit contains a two-axis control stick for lateral and longitudinal control. The control stick is provided with a feel system to give realistic force response to pilot inputs. The control stick hydraulic servos are driven by signals derived from mathematically solving dynamic stick response to force inputs. The forces are measured by strain gage force transducers mounted in the stick grip, which allows the stick-feel characteristics to be varied easily without hardware change. Complete flight control characteristics are mechanized, including a variable spring gradient, viscous damping, friction, and spring preload. Both the lateral and longitudinal feel systems can be manually trimmed by the pilot.

Functional rudder/brake pedals provide directional control, and feel forces are produced by a pneumatic spring arrangement connected in parallel with the rudder pedal linkage. Fully functional brake pedals are a part of the rudder pedal assembly. A throttle quadrant and speed-brake switch, similar to those found in the F-4, are provided for speed control.

Basic flight instruments in the MBS cockpit are as follows:

- Attitude director indicator
- Airspeed/Mach indicator
- Barometric altimeter
- Vertical velocity indicator
- Load factor indicator
- Engine rpm indicators (2)
- Angle of attack indicator

Other instruments, warning lights, and switches are also located in the cockpit to complete a realistic simulation. Figure 4-2 shows the MBS cockpit, instrumentation, and the visual display monitor.

Wide-spectrum noise generators were used in this program to provide sound cues of engine rpm, touchdown, skid control cycling, and runway rumble. The sound is supplied to the pilot by stereo speakers in the crew station.

The visual display system used in the motion base simulator is a dual raster/stroke cathode ray tube and optical system mounted in front of the pilot. It provides an out-the-window 45 degree forward field of view.

4.4 Terrain Map and Translator

The TV image used for take-off and landing studies is generated by the terrain map and translator equipment shown in Figure 4-3. The three-dimensional terrain map (20 ft x 40 ft) is a 1000:1 scale representation of both natural and cultural features, including hills, rivers, trees, roads, bridges, a factory, a village, and 10,000 feet of runway, with associated taxiways, hangar, control tower, parked aircraft, and approach lights.

Translational limits of the camera are 40,330; 8,750; and 9,660 scale feet in the north-south, east-west, and vertical directions, respectively. Pitch limits are ±60 degrees; yaw limits are ±170 degrees; and roll freedom is unlimited.

There are several significant limitations to this system as applied to this simulation. First, the lowest possible scale distance from pilot eye to runway surface is about 25 ft, due to the size of the TV probe mirror and support structure. The actual distance for the F-4 is about 11 ft. The other significant problem is the inability of the translator to track speeds smoothly below about 50 knots, where the motion becomes erratic and jerky. A new map and translator is currently under construction which should eliminate these problems.

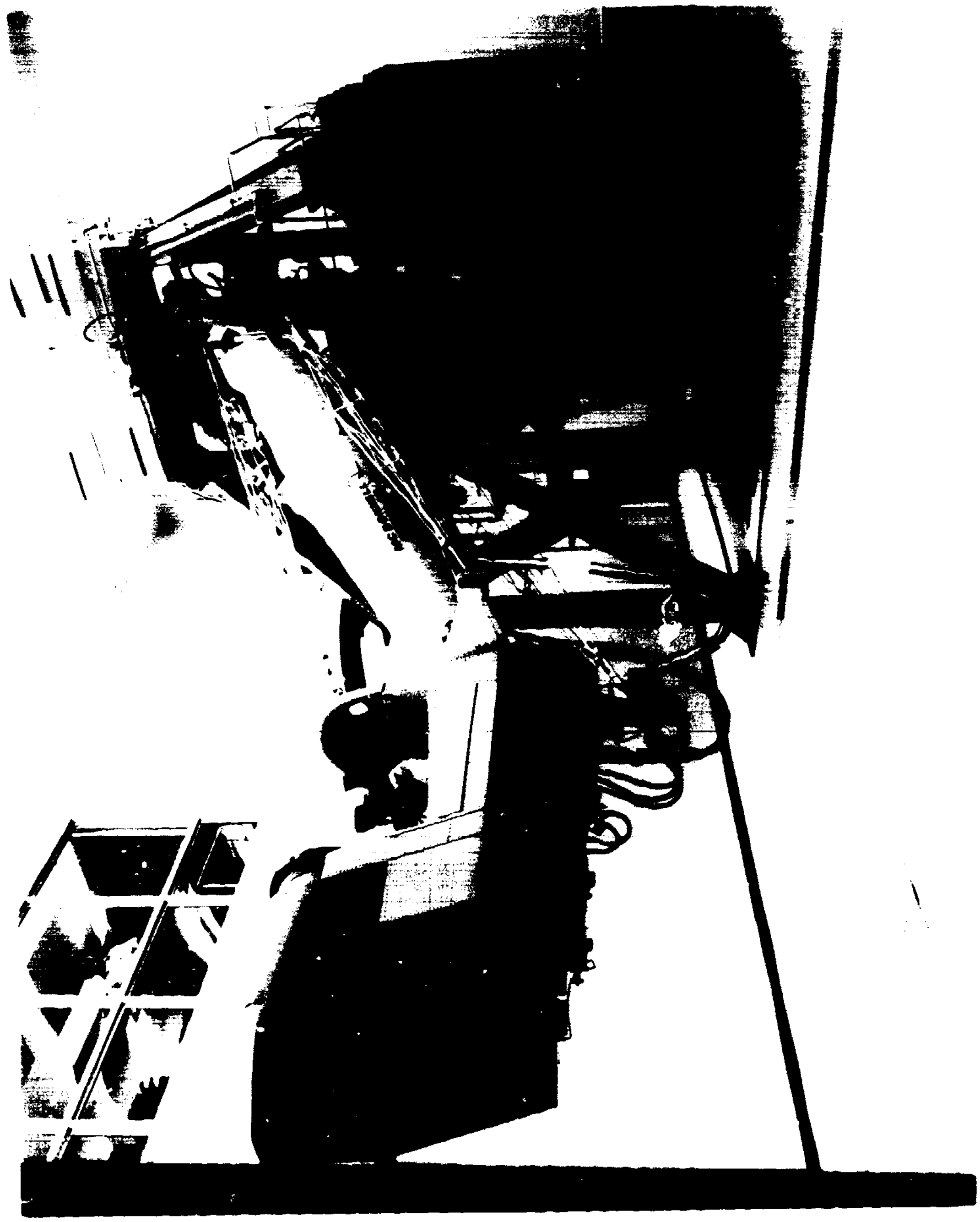

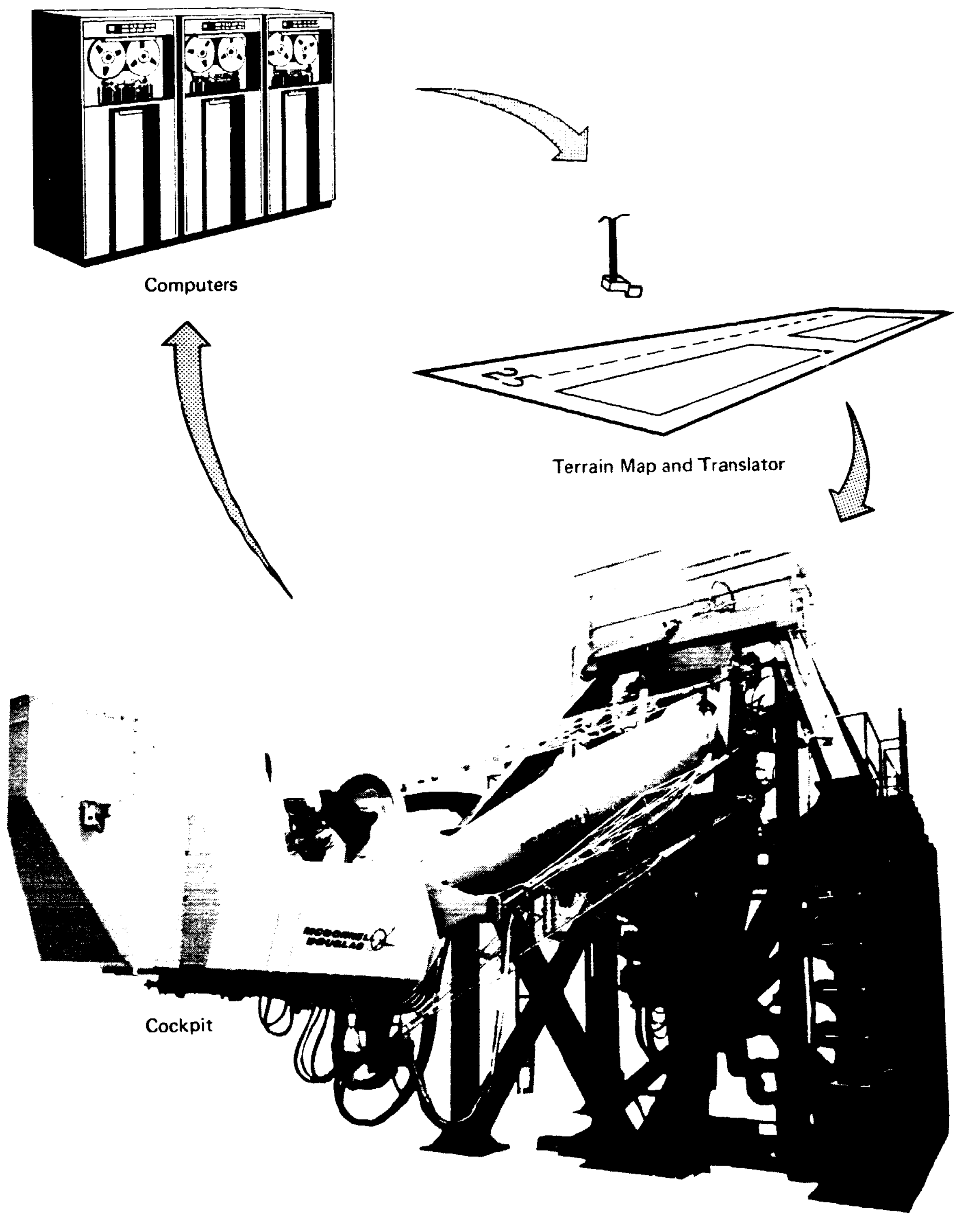

FIGURE 4-1
MOTION BASE FLIGHT SIMULATOR

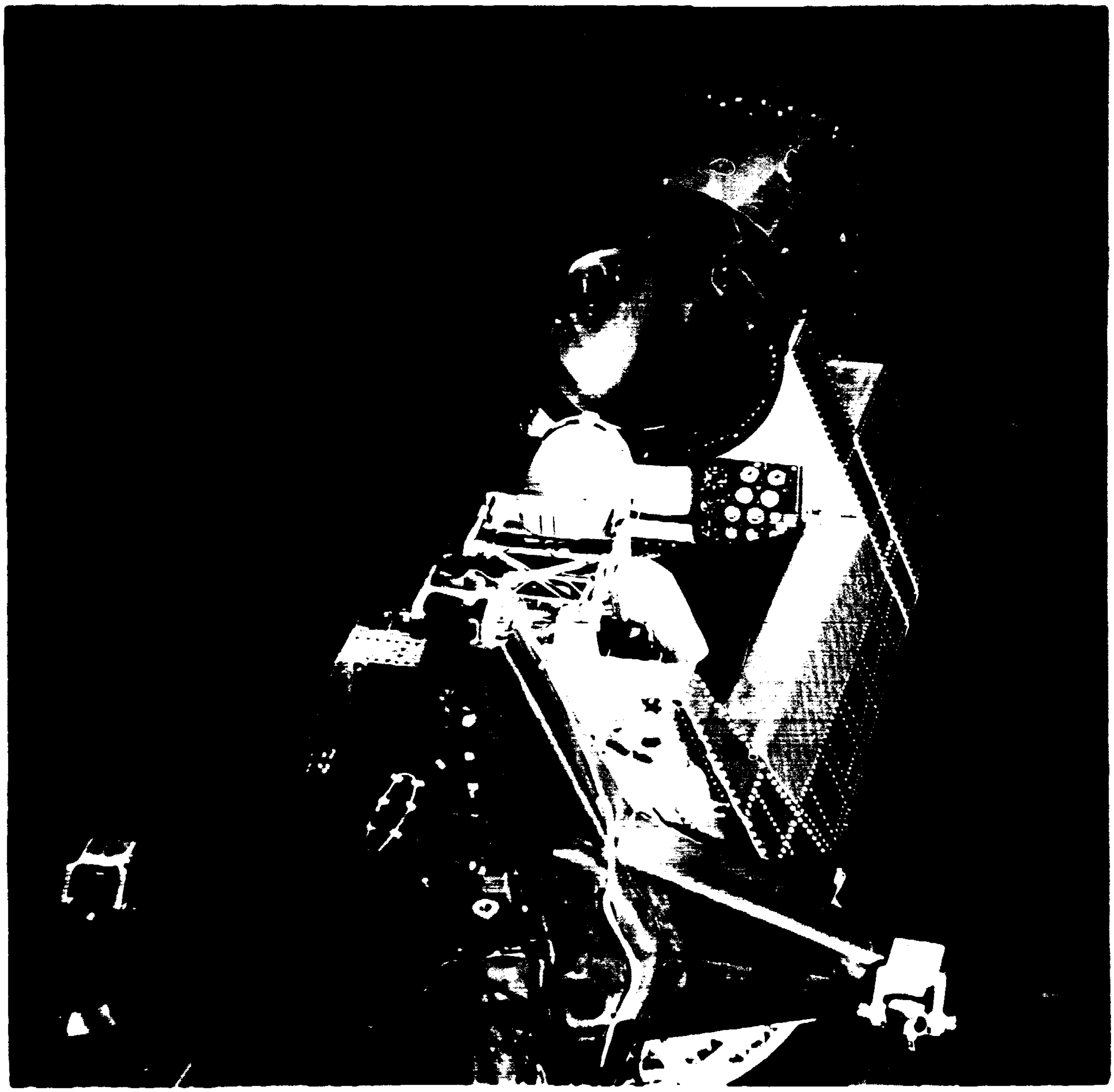

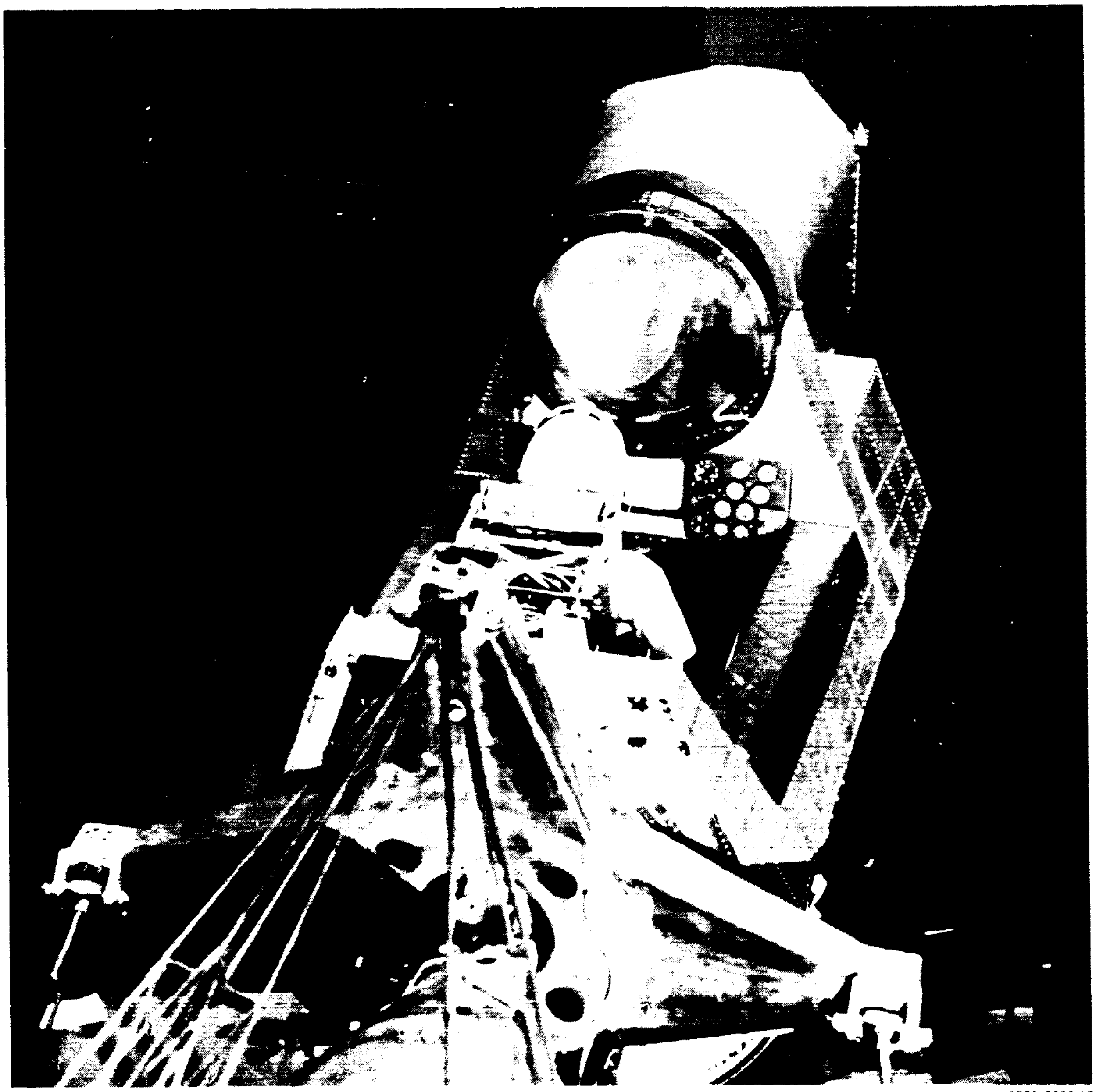

FIGURE 4-2
MOTION BASE SIMULATOR COCKPIT

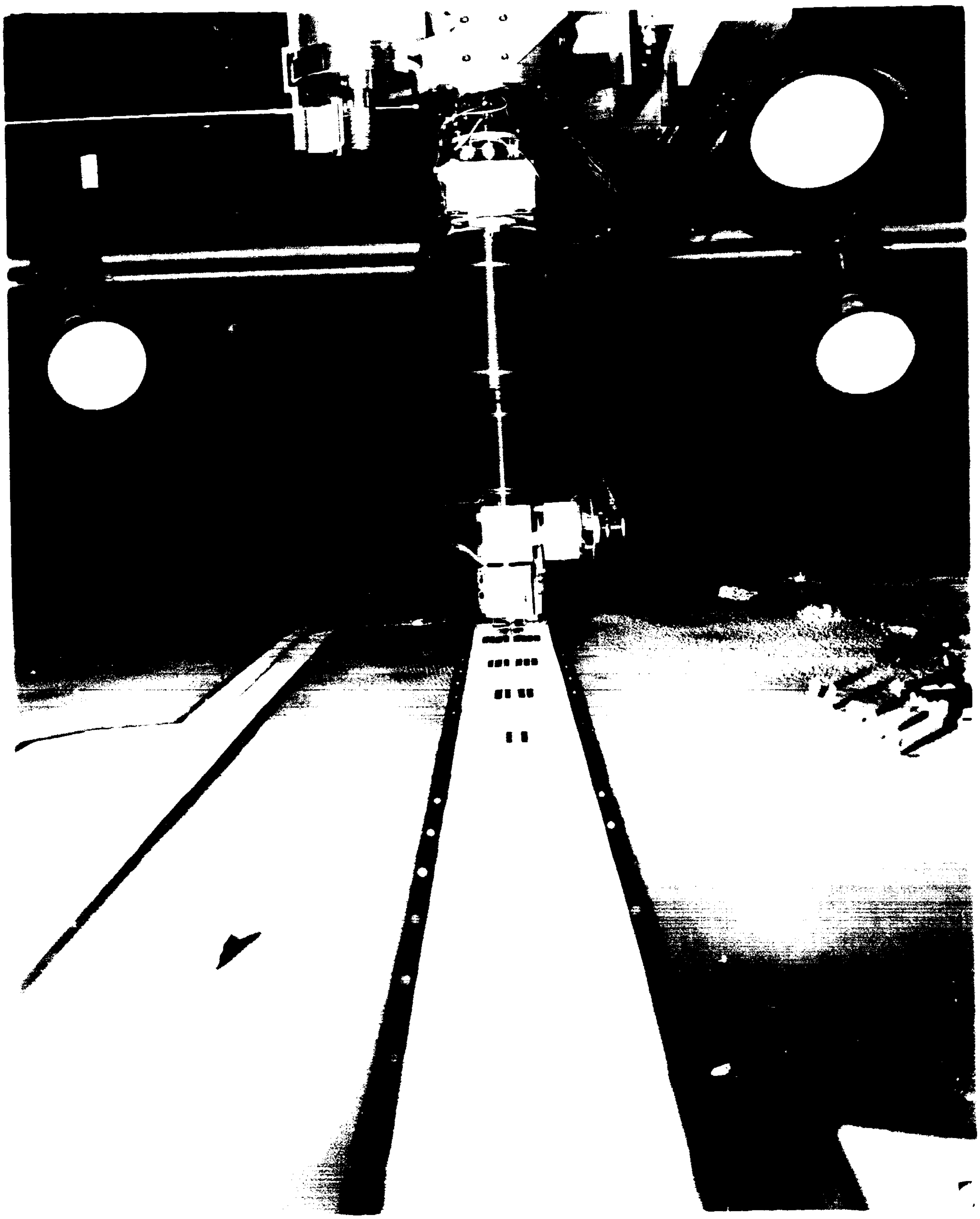

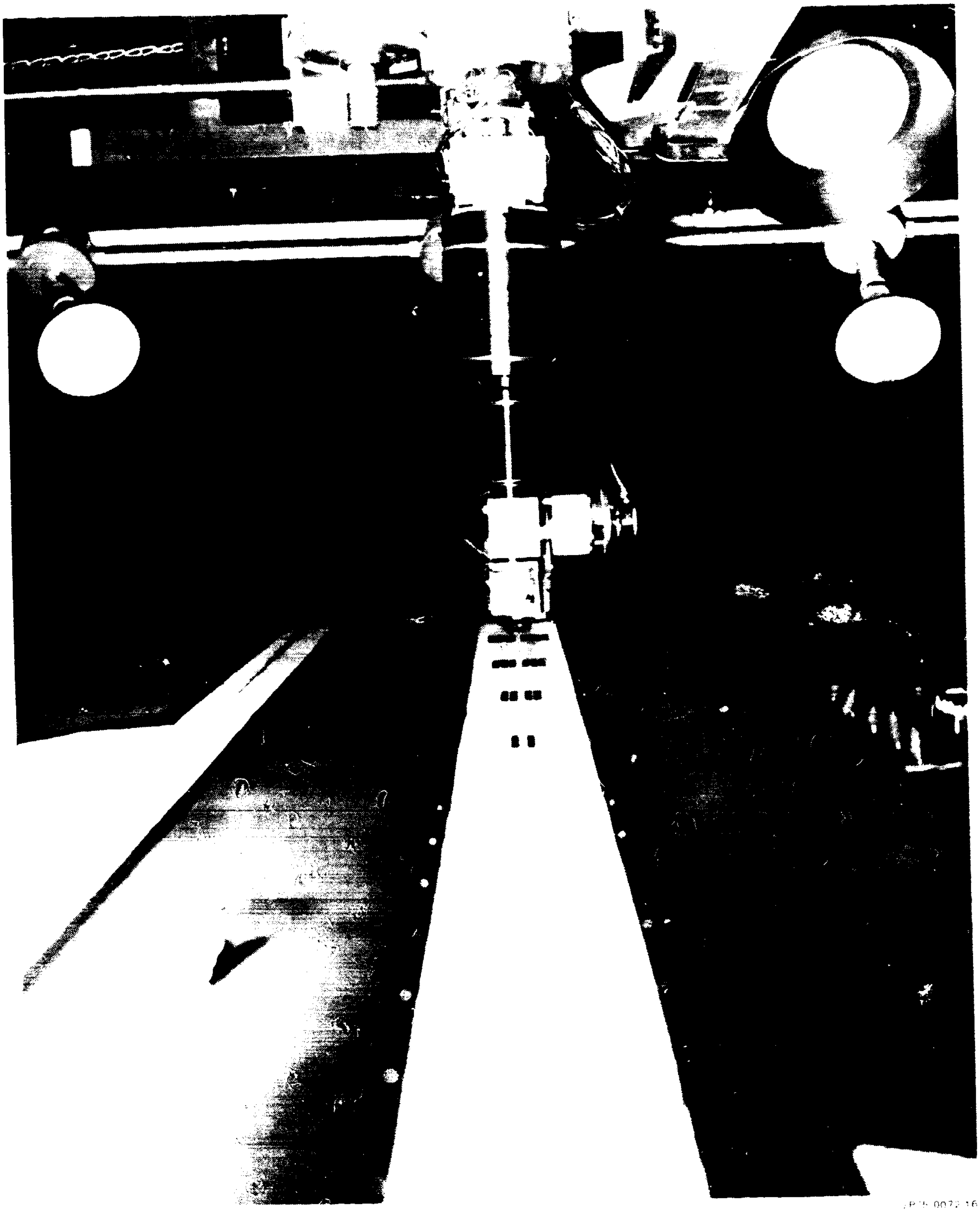

FIGURE 4-3
TERRAIN MAP AND TRANSLATOR

ORIGINAL PAGE IS
OF POOR QUALITY

5.0 SOFTWARE

5.1 Basic Software

Systems software is a basic CDC system modified to facilitate real-time simulation. Applications software is structured into modular subprograms which can be classified as either standard or study-dependent modules. Standard modules, such as equation of motion, atmosphere and hardware drives, have been optimized with respect to time and core, and provide an off-the-shelf capability to any program. The subroutines for wind, turbulence, atmospheric conditions, the translational equations of motion (TEOM1, TEOM2) and rotational equations of motion (REOM1 and REOM2) are written in assembly language. The rest of the program was written in Fortran. This modular approach is used to implement the software, and a common array is used to interface the various subprograms. Subprograms can be added or deleted to change the simulation configuration. The result is versatile, reliable software which is easy to change and check out.

5.1.1 Executive Program - This standard routine contains the basic structure of the simulation program. The initial program load is accomplished through a RW211 computer display station which provides many options as to the aircraft and configuration to be flown and simulator crew stations to be occupied. Once the proper program is loaded, the executive program is activated in a "low field length" mode where further options, such as data output and display requirements, can be selected. The time-critical "high field length" program is then activated in a reset mode where the flight conditions and special effects such as wind, turbulence, motion system modes, etc., are initialized. Control is transferred to the Simulator Remote Control Box where the simulation engineer can "operate", "reset", "hold" or "drop" the program or revert to a lower field length mode.

The simulation run is started by selecting "operate". The executive program samples cockpit inputs, calls all of the required subroutines in a logical looping sequence, and outputs the digital-to-analog signals before the end of each time iteration (.025 sec for this program). Figure 5-1 is a simplified flow chart of the subroutine calling sequence.

It should be noted that there are sub-executive routines for the aircraft, crew station and displays. Due to the high frequency dynamics of the tire/strut/aircraft model, some special looping was required in the aircraft executive program and landing gear subroutine. These features are shown on flow charts of those routines.

5.1.2 Equations of Motion (EOM) - The integration of the aircraft EOM is accomplished in a standard subroutine using the third order Adams-Bashford numerical integration scheme. The angular equations are integrated using quaternion rates rather than Euler angles to avoid singularity problems. An oblate spheroid rotating earth model is used. Speed of sound and density data come from the US Standard Atmosphere of 1962, prepared under the sponsorship of NASA.

The basic inputs to the EOM routine are forces and moments from aerodynamics, engine and landing gear routines, as shown in Figure 5-4. Outputs are latitude, longitude, altitude, Mach number, dynamic pressure, true airspeed, body axis components of translational and rotational acceleration and velocity, Euler angles, direction-cosine matrix, angle-of-attack, and sideslip.

5.1.3 Motion-Drive Washouts - The motion drive algorithm is normally tuned to give the pilot acceleration onset cues and wash out the low frequency components. For this study, where pitch attitude and heading are normally held within certain bounds, the motion drive routine was modified to drive the MBS crew station pitch and yaw position directly with aircraft pitch and heading angles. This provides the pilot with one-for-one aircraft motion information and precludes the possibility of improper pilot action due to false cues from washout movements.

Vertical, lateral, and roll accelerations were washed out so that only motion onset cues were transmitted to the pilot in those axes. Vertical acceleration and roll cues are not important after the touchdown, as those motions are slight and do not contribute much to the directional control task on roll-out. However, lateral accelerations of the sustained (or low frequency) variety are important cues to the pilot as to the skid and cornering state of the aircraft. The lateral washout break frequency was set quite low so that the pilot did receive usable lateral acceleration onset cues. The lateral motion fidelity was reasonably good on the dry runway, where the response to steering and skids was quick and of fairly large magnitude. On slick surfaces the lateral accelerations were of such low frequency and amplitude that very little motion came through the washout filters.

An improvement in the sustained lateral acceleration cue should be possible by tilting the crew station, at a roll rate below pilot perception threshold, to give a component of gravity in the lateral axis. This possibility may be explored in any follow-on study.

The longitudinal deceleration cue is the sixth degree of freedom which is missing from the five-degree-of-freedom MBS, so the pilot's only deceleration cues were airspeed indicator and runway movement with ground speed.

5.1.4 Environment

5.1.4.1 Winds - The wind and turbulence model are as defined in Reference 1. A modification was made to the steady wind model to achieve a "wind shear" effect. If a steady surface wind of some magnitude was desired a value of 10 knots higher was established at 500 ft above ground level (AGL) and was varied linearly to the desired value at 50 ft. This value was maintained below that point.

5.1.4.2 Runway Surfaces - The runway surface used had the following characteristics:

(a) Smooth, uncrowned and zero slope. The MCAIR simulator has the capability to simulate runway roughness, crown and slope; however, such variations were beyond the scope of this contract.

(b) Surface frictions, dry, wet, flooded, icy (Reference Paragraph 5.3.3).

(c) Runway size: 10,000 x 200 ft.

5.1.4.3 Atmospheric Conditions - All runs were made for standard day, sea level pressure and temperature.

5.2 F-4 Aircraft Software

5.2.1 Configuration - The aircraft simulation included weight and inertia data for a basic F-4E with the gear down and four fuselage mounted Sparrow missiles. The landing weight was 34,230 lb, representing 30% internal fuel remaining. The C.G. was 27% MAC. All mass properties were held constant for the duration of the run (fuel flow was not integrated to reduce weight, etc.). The final approach speed for this configuration was 134 knots.

5.2.2 Aerodynamics - All aerodynamics data was extracted from Reference 2 plus F-4E and F-4J addendum. Only full flap data (with gear down and jet effects included) was programmed. The effects of speedbrakes, ground effects, and engine RPM dependent boundary layer control were also included.

The aerodynamic data is stored in tables at the required degree of granularity. The aerodynamic coefficients and stability derivatives required to calculate the forces and moments are determined through special table look up routines in the AERO subroutine. C_{l_r}, C_{n_r}, C_{y_r}, C_{L_q}, C_{M_q}, C_{l_p}, C_{n_p}, $C_{l_{\delta a}}$, $C_{n_{\delta a}}$, C_{n_β} and C_{l_β} are all stored in one-dimensional functions of angle of attack. C_D, C_L and C_M are stored in two-dimensional tables as functions of angle-of-attack and stabilator deflection, $C_{n_{\delta_R}}$ and $C_{l_{\delta_R}}$ are functions of the angles of attack and yaw. The contributions due to extending the speedbrakes or the landing gear or deploying the drag chute are treated as delta increments on the appropriate coefficients. All lateral directional coefficients are expressed in body axes prior to incorporation in the program. The C_L and C_D transformation to body axes is performed after the terms are "looked up."

Once the "look ups" are complete and the coefficients are determined for the given flight condition and control surface positions, the coefficients are combined with the appropriate state conditions. Further combinations are made with the geometrical constants of the airplane, such as wing area, chord length, and c.g. position. These combinations are then used to calculate the total aerodynamic forces and moments, using expressions formulated in the aircraft body axis system.

The drag chute was also incorporated in the aerodynamics routine using a drag coefficient of .1875, based on a wing area of 530 sq ft. The force was applied in the direction of the local relative wind at the attach point on the tail so that the resultant forces and moments would be correct. For the initial demonstration runs, the force was delayed one second after drag chute handle actuation, and then faded in on a one second ramp.

5.2.3 Control System - The programmable stick feel system in the MBS was set up as an F-4E, including the variable gradient and bobweight effects. The control system data is contained in Reference 2. The surface actuators and motion sensors were accurately modeled in the control system subroutines.

Non-linear effects such as friction, rate limits, position limits and hinge moment limits were included. The stability augmentation system (SAS) and aileron rudder interconnect (ARI) were also modeled and were in operation for all test runs. The ARI gives 3.65 degrees of rudder per inch of stick with SAS "off" and 5.32 with SAS "on". Full stick throw is 3.75 inches. Trim was functional for the longitudinal axis only, to prevent any possibility of directional effects from out-of-trim rudder or ailerons.

5.2.4 Engines - Both engines were operated from the pilot's right throttle so that there could be no directional effects from differential thrust. The full-flap thrust data (vs. airspeed and rpm, BLC on) from Reference 2 was utilized. The idle thrust at touchdown speed was about 270 lb per engine; below 100 knots the idle thrust was 470 lb per engine. A second order lag thrust response (frequency = 6.66, damping = 1.0) model was used. An F-4J auto-throttle Approach Power Compensation System (APCS) was programmed and used for all runs even though the F-4E does not have that system. This ensured that all landings were accomplished at very nearly the same airspeed and angle of attack.

5.2.5 Landing Gear - The main effort for this study was directed toward the landing gear and the related parameters. The details of the landing gear model are given in Section 5.3, landing gear subroutine.

5.3 Landing Gear Subroutine - Basic data for modeling the F-4 landing gear, such as gear geometry, strut orifice, damping constants, air spring, tire geometry, tire spring rates, nose wheel steering, etc., was obtained from F-4 program engineering data. The tire-runway side force and braking friction coefficients, along with a skid control effectiveness model, were formulated in coordination with NASA. The math flow charts (Figures 5-5 through 5-10) of the landing gear show in some detail how these models were implemented in the software.

5.3.1 Strut Model - The F-4 main gear strut is a dual-chamber arrangement which has a stroke-dependent orifice area for velocity squared damping and landing energy dissipation. The strut also has a stroke-dependent air chamber volume which results in a nearly fully compressed strut and a very stiff air spring after the initial touchdown compression. This condition allows very little main strut stroke action after touchdown. The nose gear air spring is softer and permits slight rocking action during rollout on the simulator. Some linear (viscous) damping was added to the nose and main strut model (nose = 500 lb/in/sec, main = 200 lb/in/sec) to more nearly duplicate the aircraft. The strut model did not include any friction, compression limits, or bending. The main strut inclination from vertical (5.29°) was set to zero to eliminate some geometry matrix manipulations and save on critical computation time. The aircraft was considered to be a rigid body for this study.

5.3.2 Wheel-Tire Model - Rotational inertia of the wheel and tire was neglected so there were no spin-up forces during touchdown. The tire was considered to be a simple massless spring and damper whose forces are exerted on the strut axle in a direction normal to the ground plane. Braking and cornering forces were applied directly to the axle in directions along and perpendicular to the axle velocity in the ground plane. The main tire spring rate was 16530 lb/in. The nose tire spring rate is a double gradient and is described in Nose Gear Detail Note (3) Figure 5-8. The damping on both nose and main tires was assumed to be 50 lb/in/sec. This tire damping number was used because it was the lowest number that would damp out a very low frequency oscillation which was present in the tire model.

5.3.3 Tire-Runway Friction Model - The tire runway friction models shown in Figures 5-11 through 5-16 were developed in coordination with NASA-LRC. Friction models were developed from runway data as follows:

Dry	Edwards Air Force Base	non-grooved rough texture concrete
Wet	Edwards Air Force Base	
Flooded	Miami International	non-grooved, rubber coated asphalt
Icy	.05 coefficient of friction effective	

The friction curves which were used for this study were constructed as straight line approximations for the ease of programming. The curves were based on a mix of analytical and test data from References 3 through 8 and were computed as follows:

5.3.3.1 Unbraked Cornering Friction - The variation of the cornering force friction coefficient μ_s with yaw angle ψ for the unbraked condition was computed as follows:

μ_s increases linearly from zero (at ψ=0°) with increasing ψ at a slope which corresponds to the cornering power computed for that tire from the empirical equations developed in Reference 3, and reaches a maximum at the intersection of this line with the curve generated by the generalized expression:

$$\mu_s = (0.93-0.0011p) \cos\psi \cdot K_T \cdot \bar{Y}_R$$

where: p is the tire inflation pressure

K_T is the tire frictional heating factor which on wet or flooded surfaces is assumed equal to unity (because of water cooling effects) and on a dry surface is considered to be a function of the tire slip velocity. Figure 5-17 shows the relationship between K_T and the slip velocity as provided by NASA. (Note that for pure yaw the slip velocity is the product of the ground speed and the sine of the yaw angle).

$\overline{Y}_R$ is termed a hydroplaning parameter which is equal to unity on a dry surface and on a wetted surface, is assumed to be a function of the surface texture, the extent of wetting, and the ratio of ground-to-hydroplaning speed for the tire in question. Figure 5-18 presents the relationship between $\overline{Y}_R$ and the speed ratio as derived by NASA for two runways of different texture. For the purpose of this study, $\overline{Y}_R$ for a wet runway assumed the values noted in the figure for the wet Edwards AFB runway. For the flooded runway case, $\overline{Y}_R$ values were based upon measurements taken on the wet, rubber-coated section of runway 9R/27L at Miami International Airport prior to grooving.

The equation on the previous page describes the cornering friction coefficient for yaw angles in excess of that of $\mu_{s_{max}}$ and up to 90°. However for ease in programming, the curves were approximated by two straight line segments between $\mu_{s_{max}}$, μ_s at ψ=30°, and μ_s=0 at ψ=90°.

Landing loads track data was used to adjust the calculated friction to give results more consistent with the specific tire.

Figure 5-11 presents the results from calculations for the nose gear tire from 0 to 150 knots in 50 knot intervals. It should be pointed out that since no data, empirical or experimental, existed to aid in defining the wet and flooded friction coefficients at 30° yaw, those data points were approximated by reducing the peak of their respective curves by the same proportion as the 30° point on the dry curves for the same velocity.

The curve for the icy surface was selected as being representative of previous test data observed from NASA landing loads track tests.

The main tire cornering curves with no braking are presented in Figure 5-12. These curves were calculated in the same manner as the nose tire curves however the available test points were observed to differ significantly from those calculated. This difference can perhaps be explained by noting that the basis of the theory was a Type VII tire. The F-4 nose tire is a Type VII, however, the main tire is a Type VIII. Therefore the main tire curves were dropped proportionately to correspond to the test data.

5.3.3.2 Combined Cornering and Braking Friction - The curves for combined cornering and braking were determined in the following manner.

(1) The μ_D values at ψ=0 were determined first.

μ_D (dry) values were taken from Reference 6.

μ_D (wet and flooded) values were taken from Reference 9.

μ_D (wet-high speed and icy) values were set equal to rolling resistance.

μ_D (flooded-high speed) values were set equal to fluid drag from the following NASA provided formula.

$$\mu_{\text{fluid drag}} = \frac{C_{D,f}\,\rho W d_1 N\, V_g}{F_Z}$$

$C_{D,f}$ = tire fluid drag coefficient = .75

ρ = fluid mass density = 1.938

W = tire width = 11.25 in. (main tire)

d_1 = fluid depth = .07 in.

N = number of tires = 1

V_g = vehicle speed (ft/sec)

F_Z = vertical load

(2) The μ_D values at $\psi \geq 0$ were determined as follows:

μ_D (dry) values were calculated as K_T times the value at $\psi=0$.

μ_D (wet and flooded) values were reduced from the value at $\psi=0$ by the same proportion as the dry values.

μ_D (wet and flooded high speed and icy) same value as the one at $\psi=0$.

(3) The initial slope of the μ_s curves was calculated using the same method as the no braking/cornering curves.

(4) The μ_s (dry) points were calculated by a vector approach. The value of μ_s was one component. The value of μ_D calculated at the desired ψ in item (2) was the component perpendicular to μ_s. The value of μ_D at $\psi=0$ calculated in item (1) was the total available μ.

(5) The μ_D (wet and flooded) are the values which correspond to the appropriate μ_D as found in References 7 and 8.

These curves were developed for a maximum of 16° since there is no data on combined cornering/braking friction for aircraft tires at high yaw angles. The effects of the skid control system are included in these curves, making them curves of μ_{eff}. When the skid control system math model was used the μ_{eff} values from the curves had to be modified as described in Section 5.3.4.

5.3.4 Brake System and Skid Control Simulation - The brake system and skid control models, shown in Notes 6 and 7 of Figure 5-8, provide the aircraft equivalent between the brake pedal input and the drag force at the main wheel. The simulation includes pedal deadband, hydraulic lag, brake torque gain and skid pressure limits with differential, proportional brake force metering capability. Braking forces were computed from metered pressure as limited by the available braking force determined from the braking friction coefficients and tire normal force. When less than the skid level brake pressure is metered, the "no braking" side forces were applied, when the skid level pressure is exceeded, the "braking" side force coefficients were used.

The F-4 Hytrol Mark II system was selected for modeling with brake pressure time histories provided from the Raintire program as a data base. The Figure 5-19 math model was developed which approximated the aircraft brake pressure time histories as shown in Figure 5-20. The math model operated upon the μ_{eff} curves in a cyclic fashion to result in aircraft μ_{eff} braking forces. The skid control wave form is controlled by Figure 5-21 which was computed from Raintire records. The limits of the μ_D and μ_s are defined in Figure 5-19.

5.3.5 Nose Wheel Steering Model - The nose wheel steering (NWS) model, shown in Notes 1 and 2 of Figure 5-8 provides the aircraft equivalent motion between the rudder pedals and nose wheel steering angle.

The simulation includes a pilot steering select switch, system deadband, ratio between rudder pedal and steered wheels, actuator steering rate as a function of strut load and steered wheel travel limits. The deadband was increased to a more realistic aircraft characteristic after the demonstration in response to pilot criticism that steering was too sensitive. The post demonstration comments were favorable.

5.3.6 Numerical Methods - A considerable amount of the programming and checkout time was devoted to solving the rather difficult numerical problems associated with modeling a lightly damped, high frequency physical system in a real time all-digital simulation. The first major hurdle was to limit the strut damping forces to reasonable values. This was accomplished as shown in Figure 5-9 on damping limits. The strut/wheel/tire mass was considered as a one-degree-of-freedom free body and its acceleration was integrated independently of the aircraft in the landing gear subroutine. Simple Euler integration was used (See Nose Gear Detail Note (5) of Figure 5-8) as it is simple to compute and does not require past values.

The natural frequency of aircraft motion on the tires is about 2.0 Hz in pitch and 3.5 Hz in roll. The real-time operation sample time is .025 secs (40 samples/sec) was not sufficient for accurate and stable integration of the strut motions so a multiple looping arrangement was established whereby the aircraft EOM and landing gear subroutines were called twice per sample period. Within that loop the strut forces were integrated four times per pass through the gear routine. This was a rather "brute-force" approach to the stiff system simulation problem . Therefore, it required careful balancing of the timing in the slow loops of the executive program to avoid exceeding the available computation time per sample time. (Computation time ran about .021 seconds out of the .025 seconds available).

With this experience and some time to apply more sophisticated numerical methods, it should be possible to reduce the looping and computation time considerably. The entire program took about 110,000 (octal) core locations, which is less than half of that available; if the computation time could be also reduced to about half of the sample time the computer costs to run this simulation would be reduced significantly.

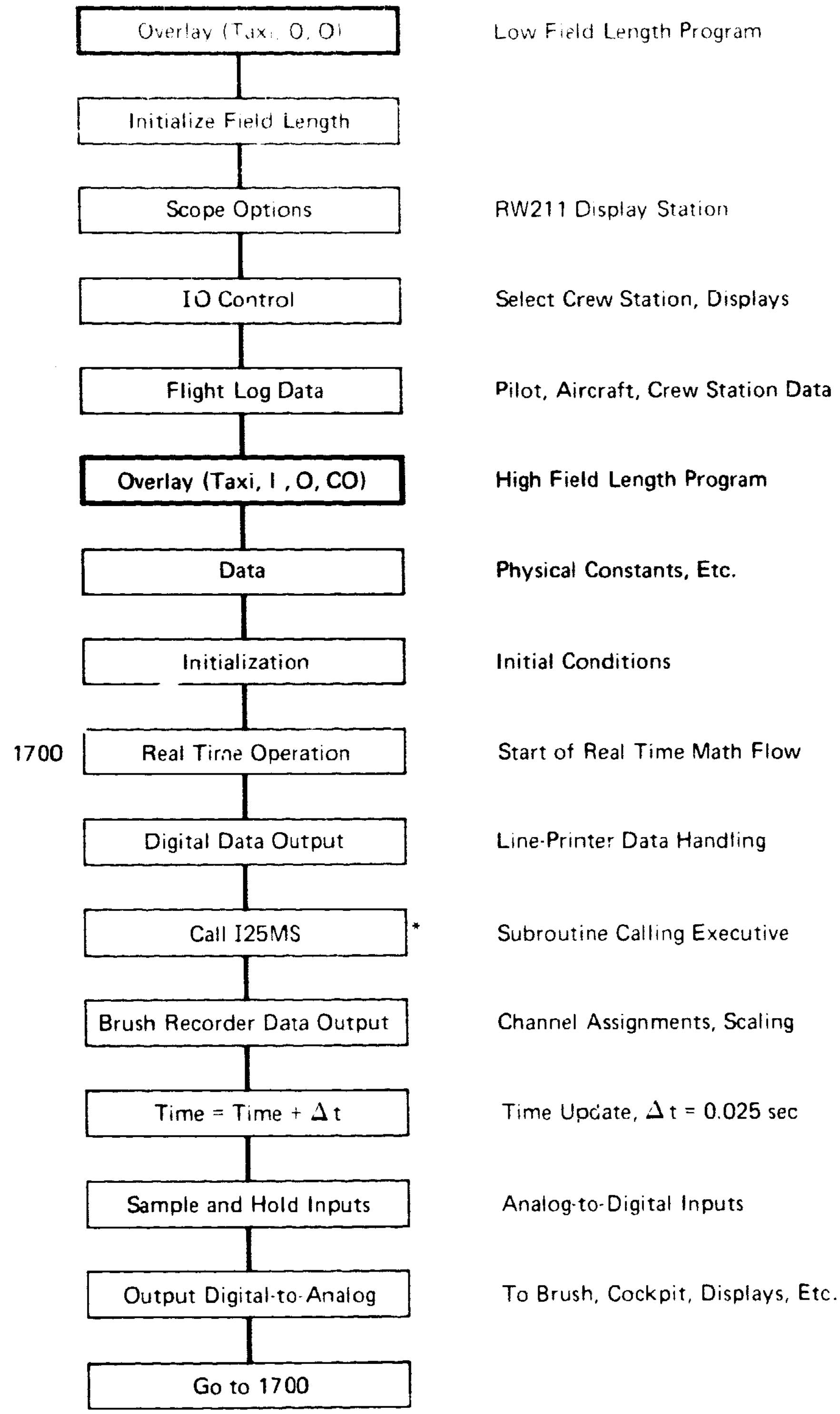

*See Figure 5-2 for details

FIGURE 5-1
EXECUTIVE PROGRAM MATH FLOW DIAGRAM

GP75 0012 54

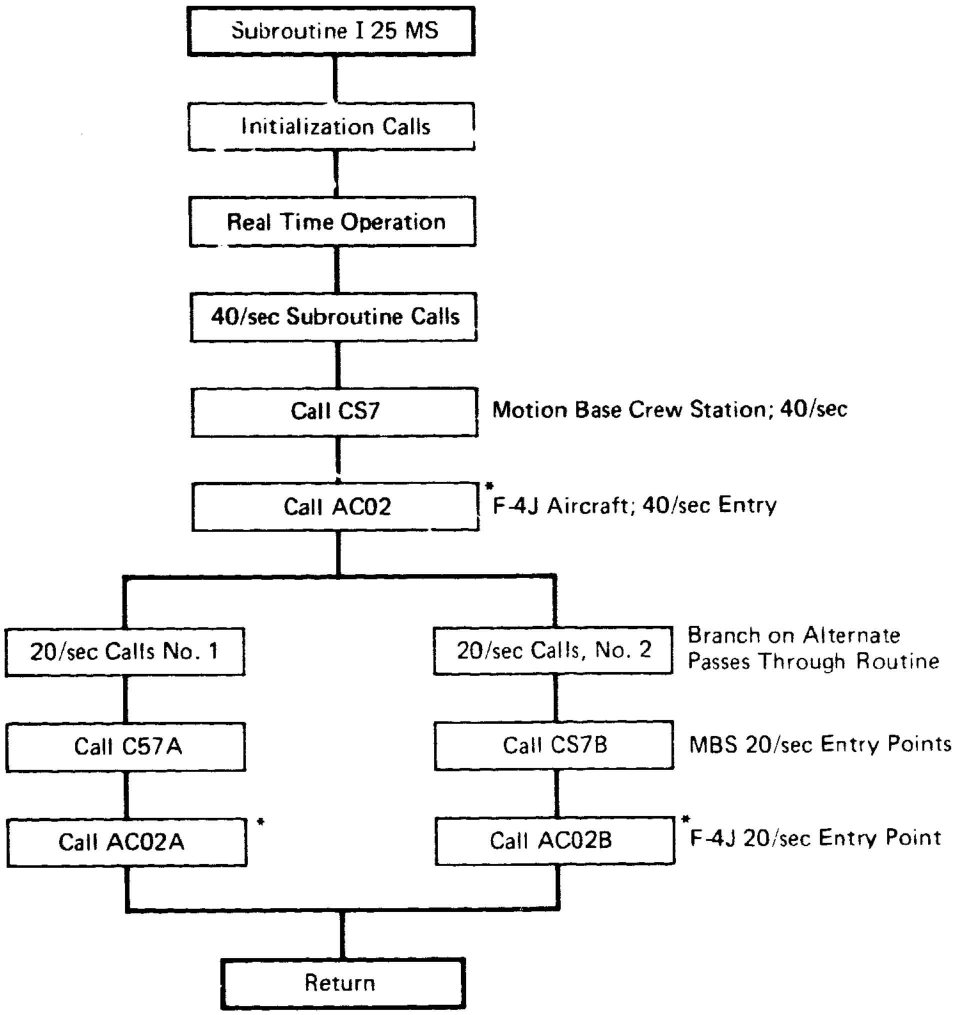

*See Figure 5-3 for details

FIGURE 5-2
SUBROUTINE CALLING PROGRAM

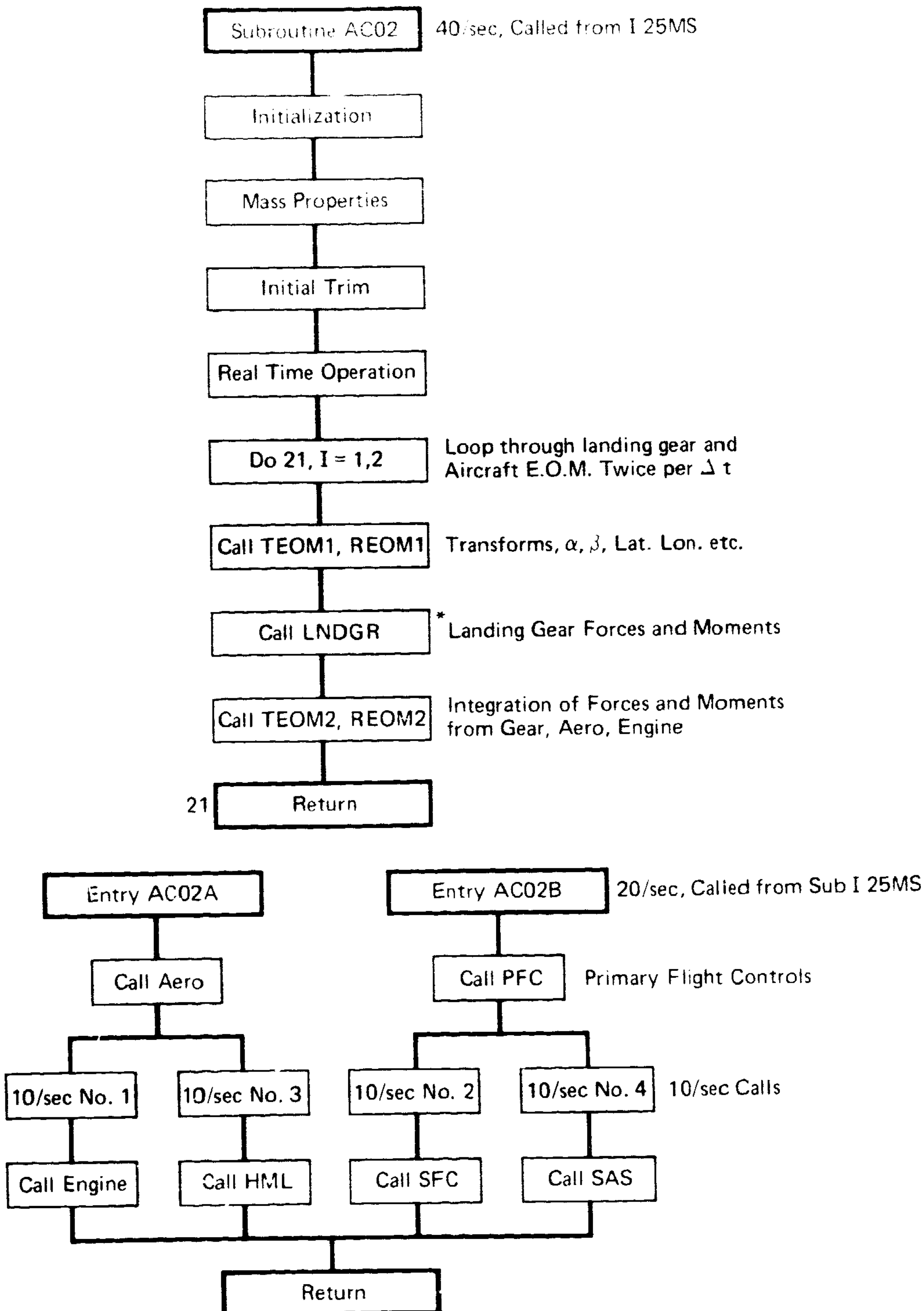

*See Figure 5-5 for details

HML = Hinge Moment Limits
SFC = Secondary Flight Controls (Gear, Flap, Speed Brake)
SAS = Stability Augmentation System

FIGURE 5-3
AIRCRAFT EXECUTIVE PROGRAM

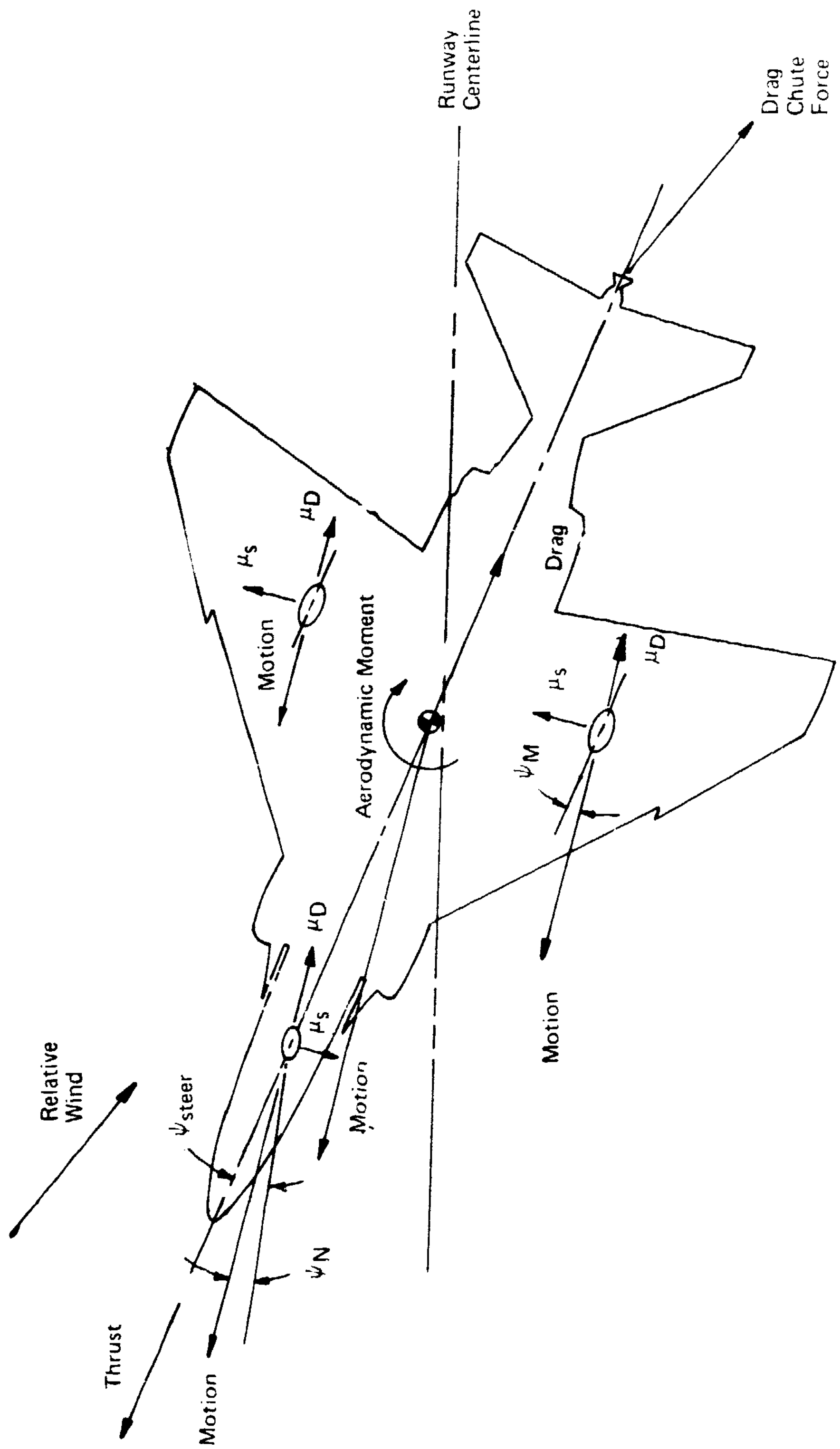

FIGURE 5-4
PRINCIPAL INPUT FORCE DIAGRAM

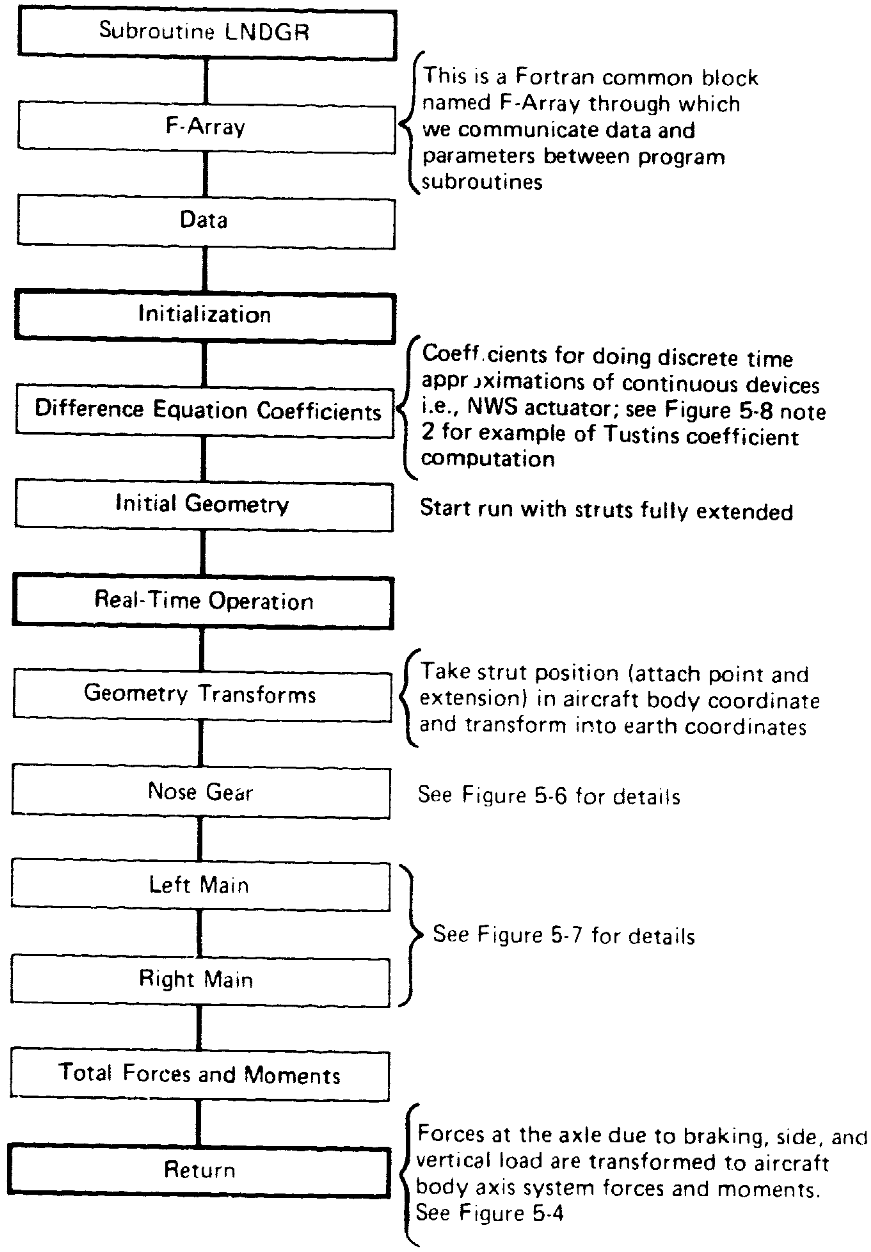

FIGURE 5-5
LANDING GEAR MATH FLOW DIAGRAM

Rudder Pedal to NWS Gearing + Deadband	See Detail Figure 5-10
Side Load Dependent NWS Rate Limit	See Note (1) Figure 5-8
NWS Actuator, Steering Angle	See Note (2) Figure 5-8
Skid Angle	$\Psi_{skid} = \sin^{-1} V_{N_{side}}/V_{N_{total}}$ (See last note on this page)
Side Force Coefficient	Table Look Up from Data in Figure 5-11
DO 149, I, = 1,4	4 Pass Integration of Strut Force
Axle Altitude	Axle position in earth coordinates is computed axle position in aircraft body coordinates (function of attach point and extension), aircraft position in earth coordinates, and aircraft attitude (pitch, roll, yaw)
Tire Deflection, Rate, Forces	See Note (3) Figure 5-8
Strut Air Spring Force	Table Look Up from F-4 Data, Reference 10
Damper Orifice Area	Table Look Up from F-4 Data, Reference 11
V^2 + Viscous Damping	See Note (4) Figure 5-8
Damping Force Limits	See Figure 5-9
Force Sum, Integration	See Note (5) Figure 5-8
149 Strut Stroke, Velocity	
Velocity at Axle	For skid angle computation in ground plane, see Figure 5-4. Velocity (labeled motion) at the axle is V_{total}; the component normal to the wheel is V_{side}

FIGURE 5-6
NOSE GEAR MATH FLOW DIAGRAM

	Step	Notes
	Skid Angle	$\Psi_{skid} = \sin^{-1} V_{side}/V_{total}$ See note on previous page
	Brake Hydraulic Pressure	See Note (6) Figure 5-8
	Anti-Skid Cycle Period; % on Time	See Figure 5-23
	Skid + Braking Coefficients	Table Look Up from Data in Figures 5-17 through 5-21
	Brake Force Cycles	See Note (7) Figure 5-8
	DO 109, I = 1,4	4 Passes through Strut Integration
	Axle Altitude	From strut stroke and aircraft position and attitude. See note on previous page
	Tire Deflection, Rate, Forces	See Note (3) Figure 5-8
	Strut Air Spring Force	Table Look Up from F-4 Data, Reference 10
	Damper Orifice Area	Table Look Up from F-4 Data, Reference 12
	V^2 and Viscous Damping	See Note (4) Figure 5-8
	Damping Force Limits	See Figure 5-9
	Force Sum, Strut Acceleration	See Note (5) Figure 5-8
109	Integration, Strut Rate, Stroke	See Note (5) Figure 5-8
	Axle Position, Velocity	For Skid Angle Computation

FIGURE 5-7
MAIN GEAR MATH FLOW DIAGRAM

1.) NWS Actuator Rate Limits (Side Load Dependent)

Positive Rate Limit = 35. - FNy x 0.00677 deg/sec
Limit (PRLIM, 12.,35.)
|Negative Rate Limit| = 35. + FNy x 0.00677 deg/sec
Limit (NRLIM, 12., 35.)
FNy = Side Load, lb

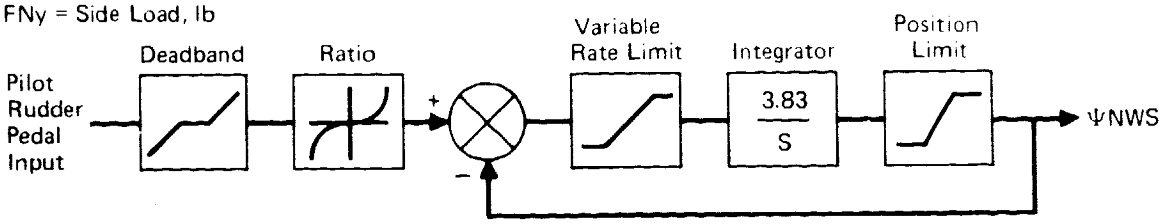

2.) NWS System

The digital mechanization of this system is accomplished as follows:

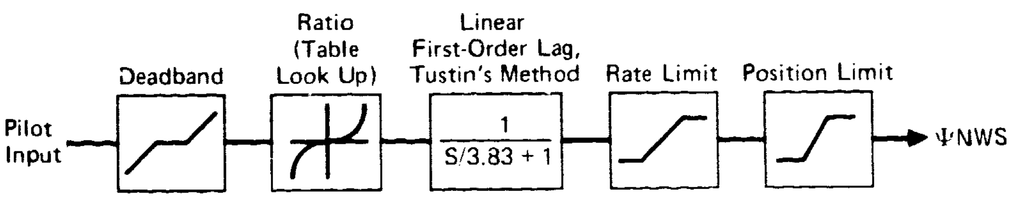

Tustin's Method for First Order Lag: $$C_m = \frac{T/2}{(\tau + T/2)} (R_m + R_{m-1}) + \frac{(\tau - T/2)}{(\tau + T/2)} C_{m-1}$$

T = Iteration Time τ = Time Constant = 1/3.83

The rate limit is imposed on the output of this difference equation by testing if the difference between the present and previous output exceeds rate limit x T.

3.) Nose Tire

Tire Spring Rate

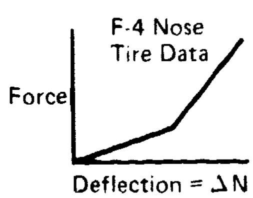

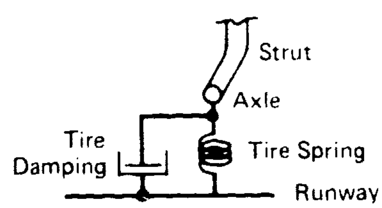

Spring Force = 16,000. x ΔN, if ΔN > 2.
FSN = 32,000 + 28,000 (ΔN - 2.)

Damping Force = 50. x ΔN lb

The tire damping coefficient was an arbitrary value which decreased the tendency of the aircraft to rock on the tires.
Tire force on strut = FGN = tire spring + damping force

FIGURE 5-8
NOSE AND MAIN GEAR MATH MODEL DETAIL NOTES
(Continued)

GP75 0012 60

4.) **Strut Damping**

$$\text{Velocity Squared Damping} = \dot{S}\,|\dot{S}|\,\frac{0.3\ (\text{nose}) - 0.5\ (\text{main})}{A^2_{orifice}}$$

$\dot{S}$ = strut stroke rate (in./sec)

$A_{orifice}$ = orifice area, table look up vs strut stroke

Viscous damping = 500. × $\dot{S}$, the viscous damping coefficient was an arbitrary value which decreased low amplitude rocking on the gear. Main strut damping was 200 lb/in./sec.

5.) **Strut Force Integration**

$$\ddot{S} = (\underbrace{FGN}_{\text{Tire}} - \underbrace{FSN}_{\text{Airspring}} - \underbrace{FVN - FV^2N}_{\text{Damping Force}})/\text{Mass}_{unsprung}$$

unsprung mass =
nose 138 lb
main 450 lb

$\dot{S} = \dot{S} + \ddot{S} \times T/4$ Euler Integration, 4 Passes/Iteration, T

$S = S + \dot{S} \times T/4$ Strut Stroke

$T = \Delta t = 0.025$ sec

6.) **Brake Pressure Cycles**

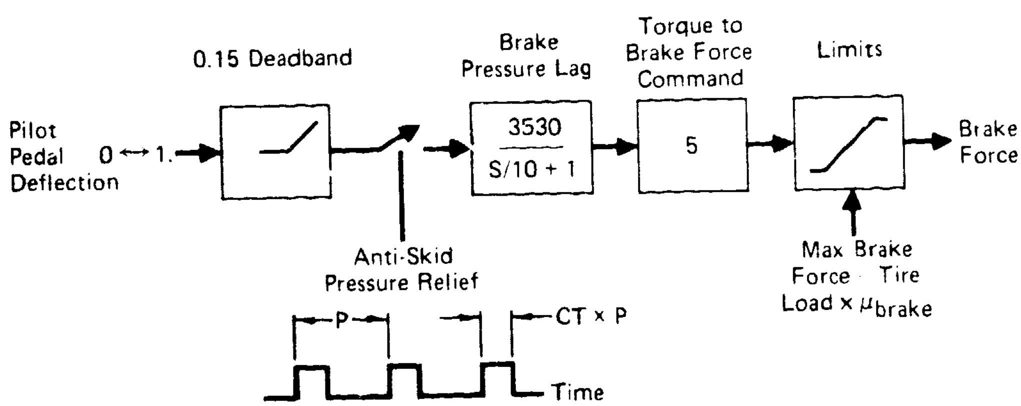

7.) **Brake Anti-Skid Cycle**

P = Cycle Period = $1.2 - 0.005 \times V_L$
Limit (Period, 0.25, 1.2) V_L = Wheel Speed

CT = Fraction on Time = $1.0 - 0.001075\, V_L$ (Dry Runway)

CT = $1.0 - 0.0047\, V_L$ (Wet, Flooded, Icy Runway) if
$V_L > 85$, CT = $0.6 - 0.002941\,(V_L - 0.05)$

FIGURE 5-8
NOSE AND MAIN GEAR MATH MODEL DETAIL NOTES
(Continued)

8) The side force on the tire is μ_S times the vertical force on the tire and the braking force is a function of μ_D (Figure 5-19) times the vertical force. The vertical force is calculated as shown in Note 3. The tire deflection (ΔN) is obtained from the axle altitude. The axle altitude is calculated in the "DO" loops of Figures 5-6 and 5-7. Therefore, the vertical force is obtained by an iterative process.

The side and braking forces on the axle are then resolved into aircraft body axis components. These forces are resolved to 3 forces acting at the aircraft C.G. and 3 moments acting about the C.G. The three forces and moments are then treated just like aerodynamic forces and moments by the aircraft EOM.

FIGURE 5-8
NOSE AND MAIN GEAR MATH MODEL DETAIL NOTES
(Concluded)

Case I - Strut Compressing (FGN>FSN)

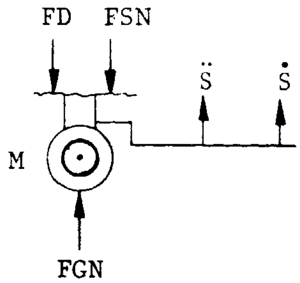

$FD = FGN - FSN - M\ddot{S}$
$FGN - FSN > 0$
therefore
$FD < FGN - FSN$

The computed damping force must be less than FGN - FSN.

Case II - Strut Compressing (FGN<FSN)

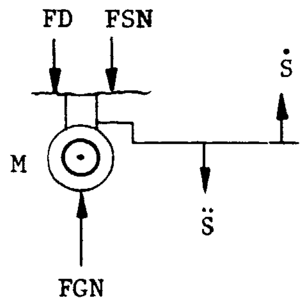

$FD = FGN - FSN + M\ddot{S}$

The computed damping force must be less than $FD_{t - \Delta t}$

Case III - Strut Extending (FGN<FSN)

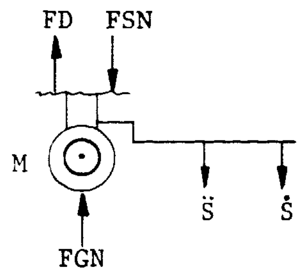

$FD = - FGN + FSN - M\ddot{S}$
$- FGN + FSN > 0$
therefore
$FD < FGN - FSN$

The computed damping force must be less than FGN - FSN.

Case IV - Strut Extending (FGN>FSN)

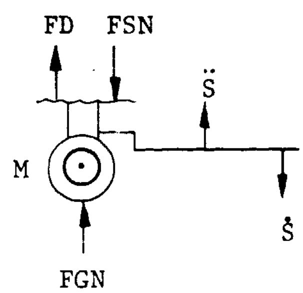

$FD = - FGN + FSN + M\ddot{S}$

The computed damping force must be less than $FD_{t-\Delta t}$

M = unsprung mass
FD = damping force
FGN = tire force
FSN = spring force

FIGURE 5-9
STRUT DAMPING LIMITS

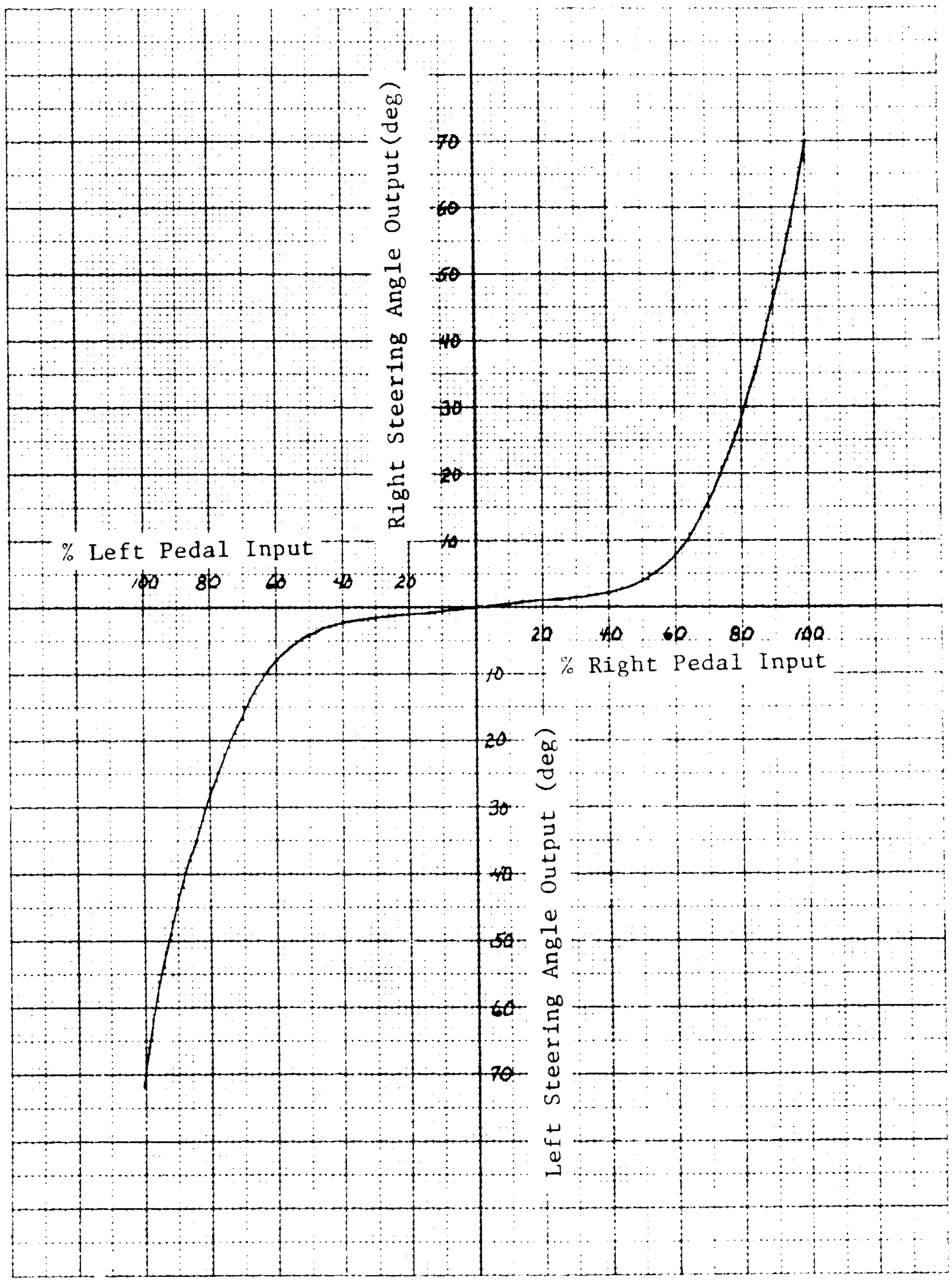

FIGURE 5-10
F-4 STEERING RATIO

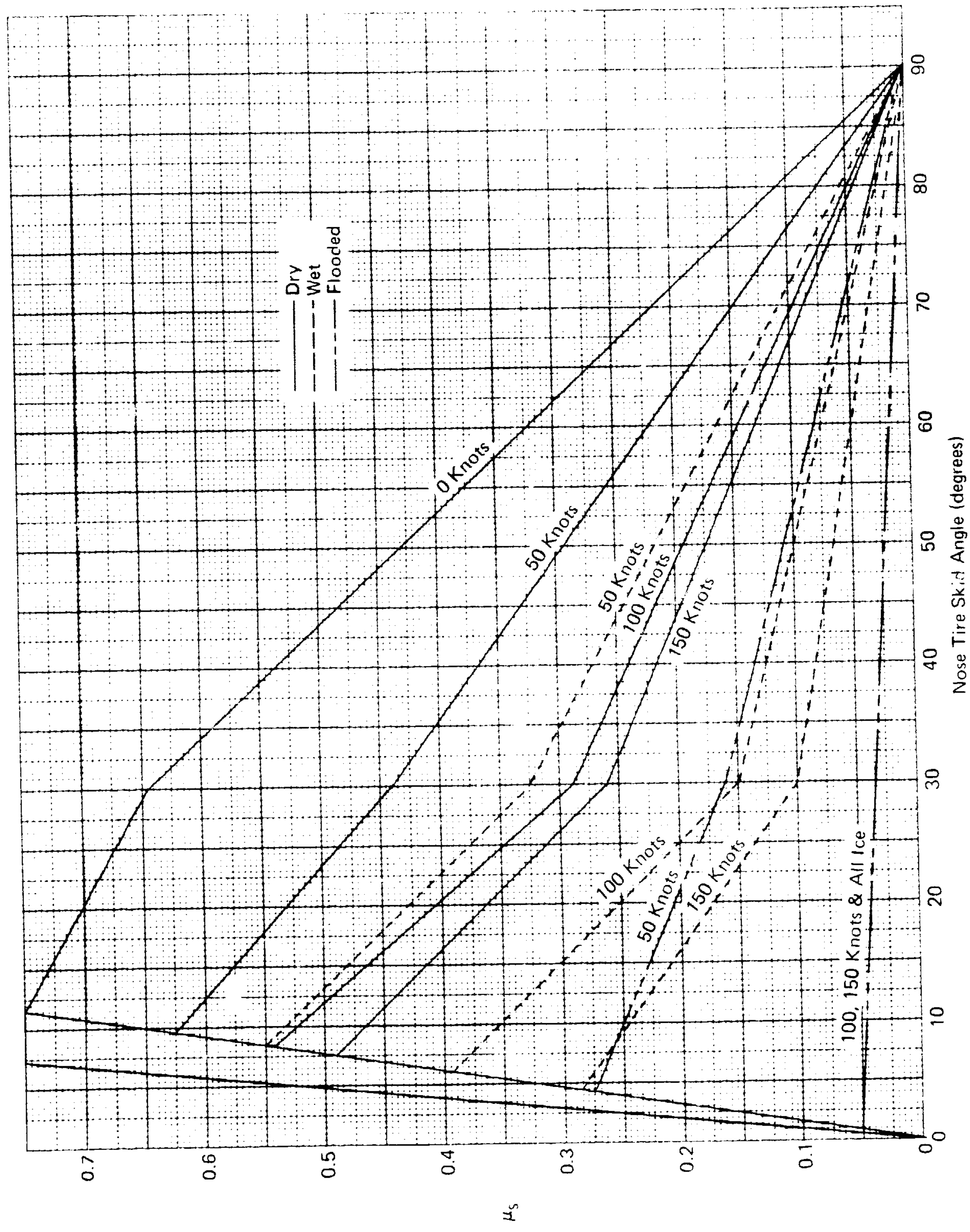

FIGURE 5-11
NOSE TIRE CORNERING COEFFICIENT

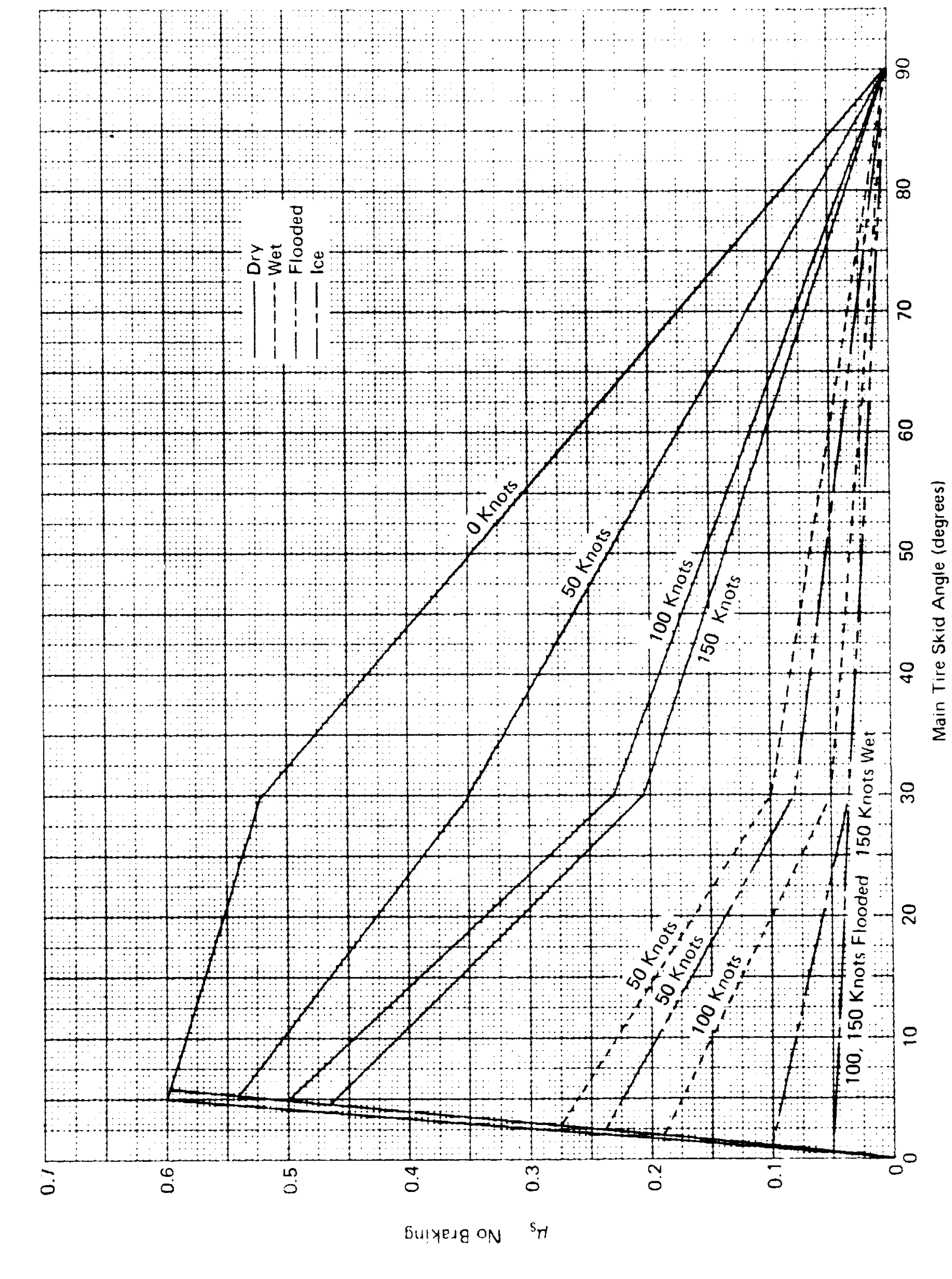

FIGURE 5-12
MAIN TIRE CORNERING COEFFICIENT

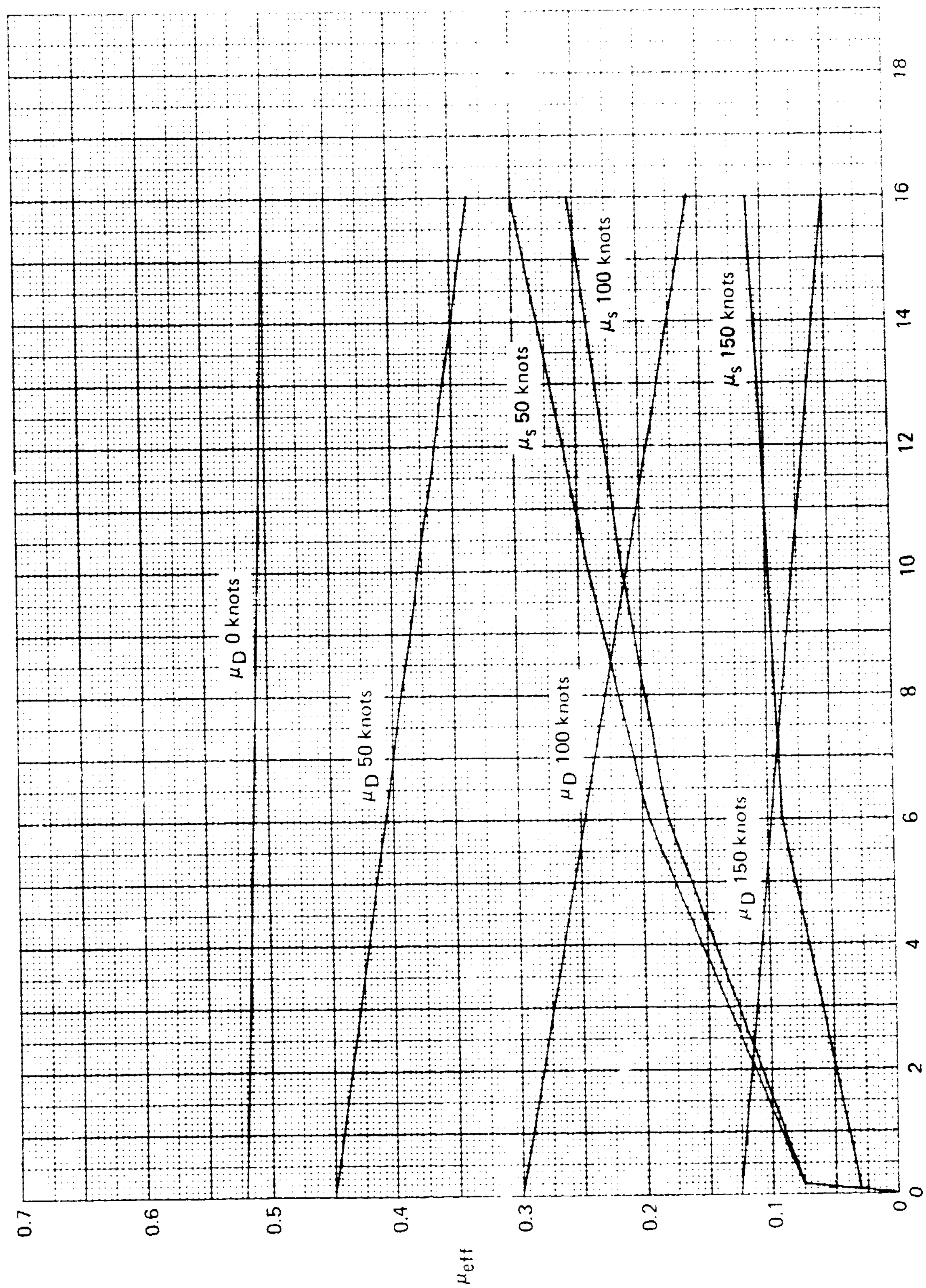

FIGURE 5-13
MAIN TIRE CORNERING/BRAKING COEFFICIENT DRY RUNWAY

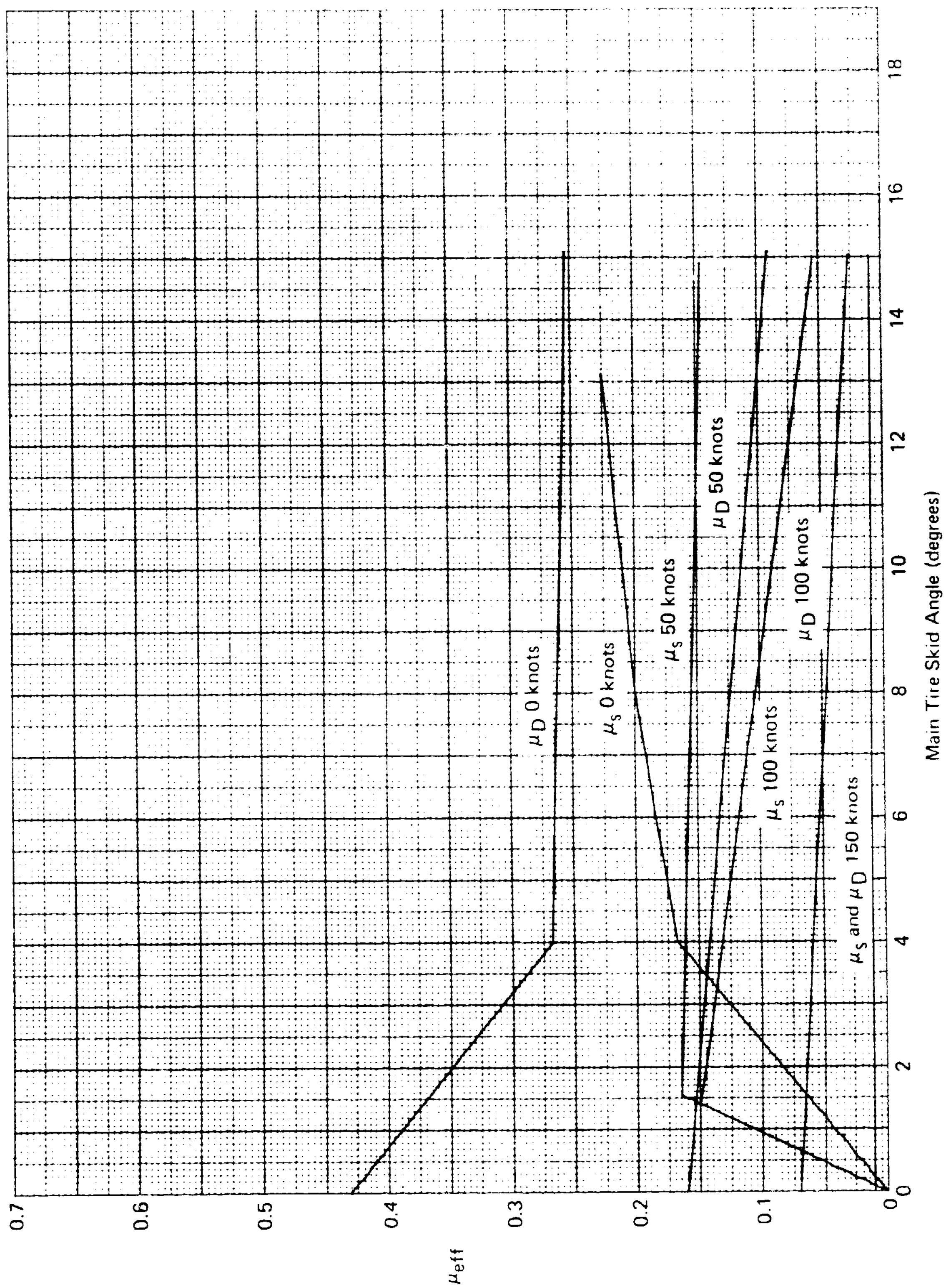

FIGURE 5-14
MAIN TIRE CORNERING/BRAKING COEFFICIENT WET RUNWAY

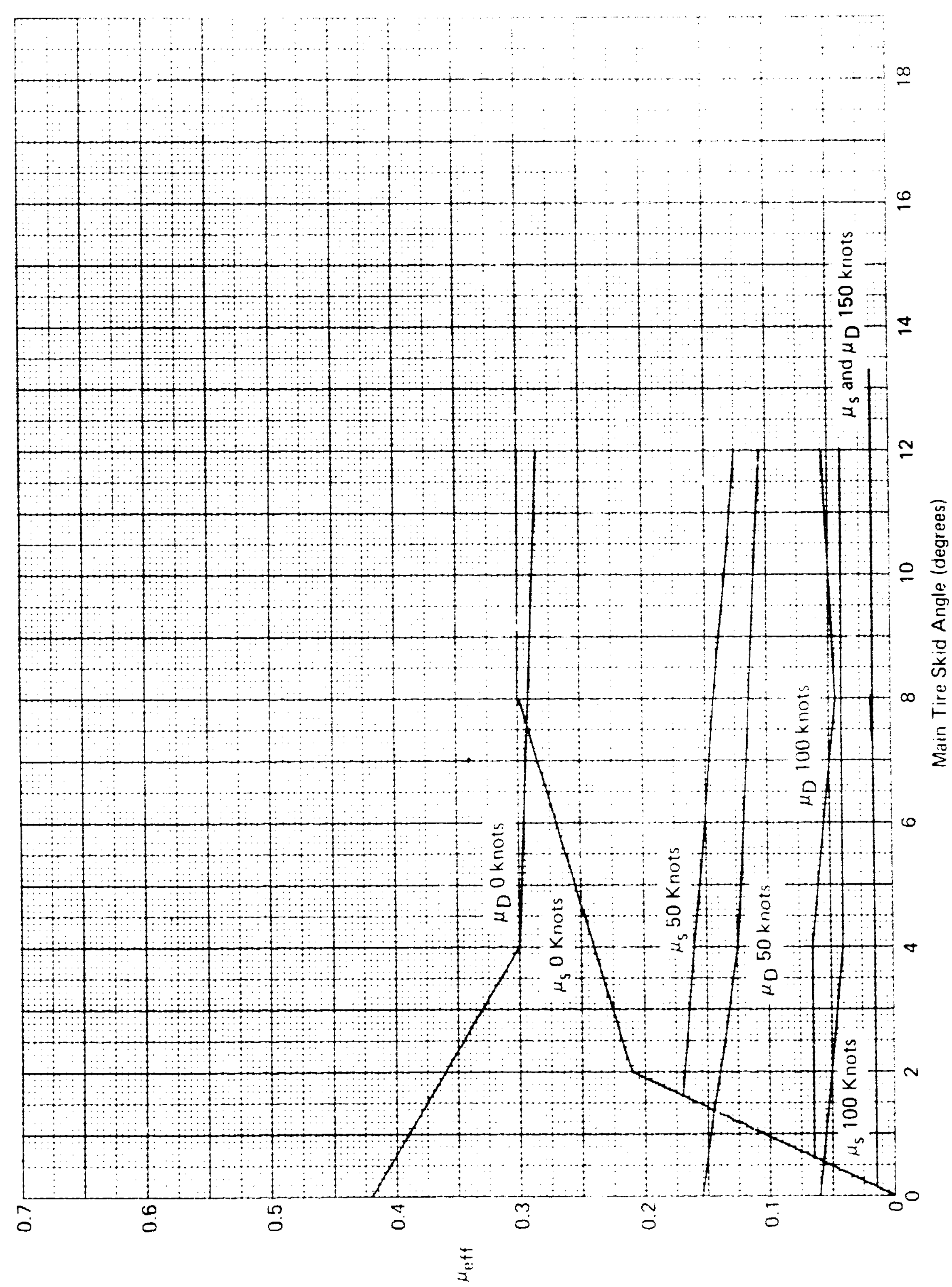

FIGURE 5-15
MAIN TIRE CORNERING/BRAKING COEFFICIENT FLOODED RUNWAY

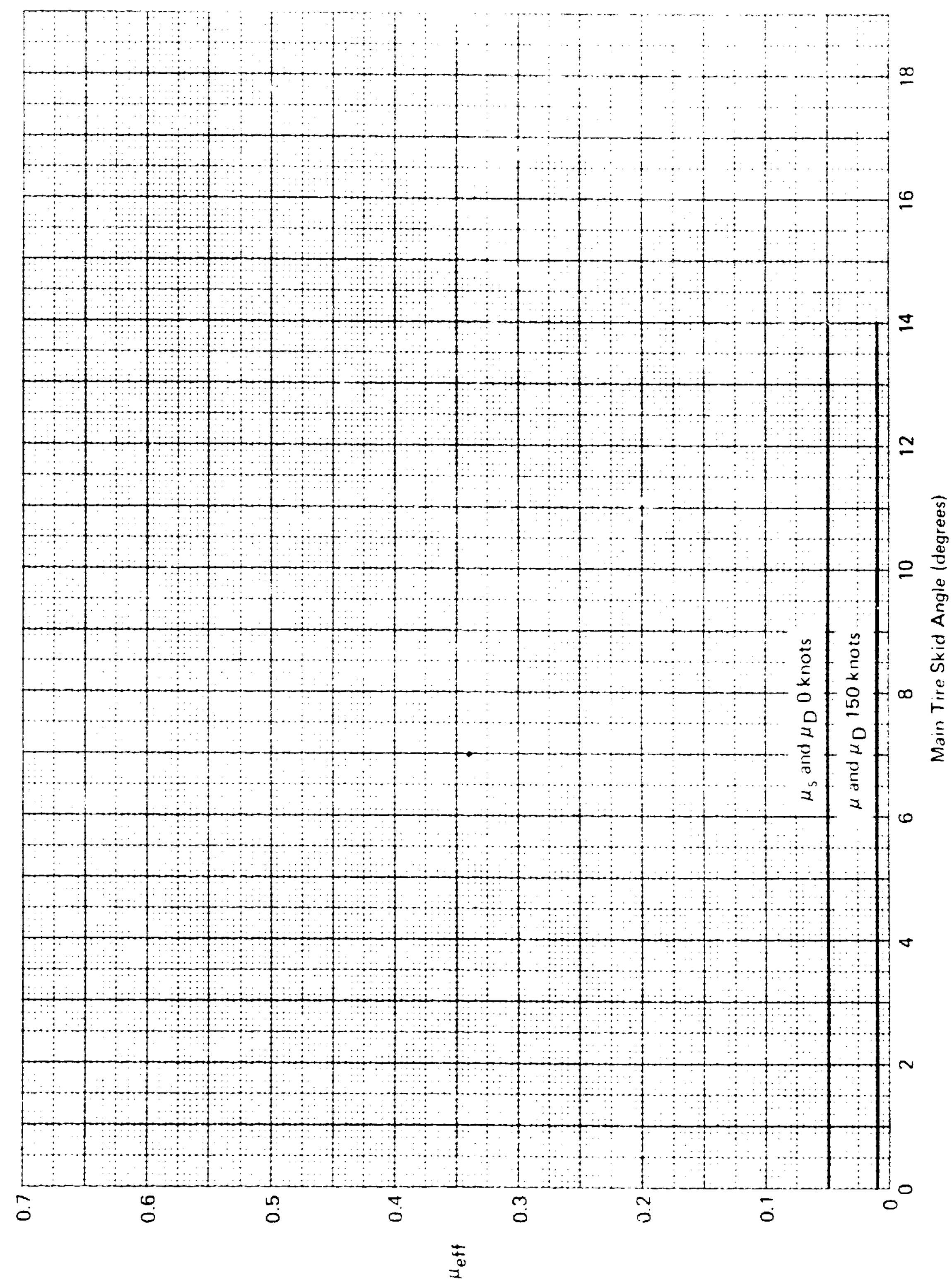

FIGURE 5-16
MAIN TIRE CORNERING/BRAKING COEFFICIENT ICY RUNWAY

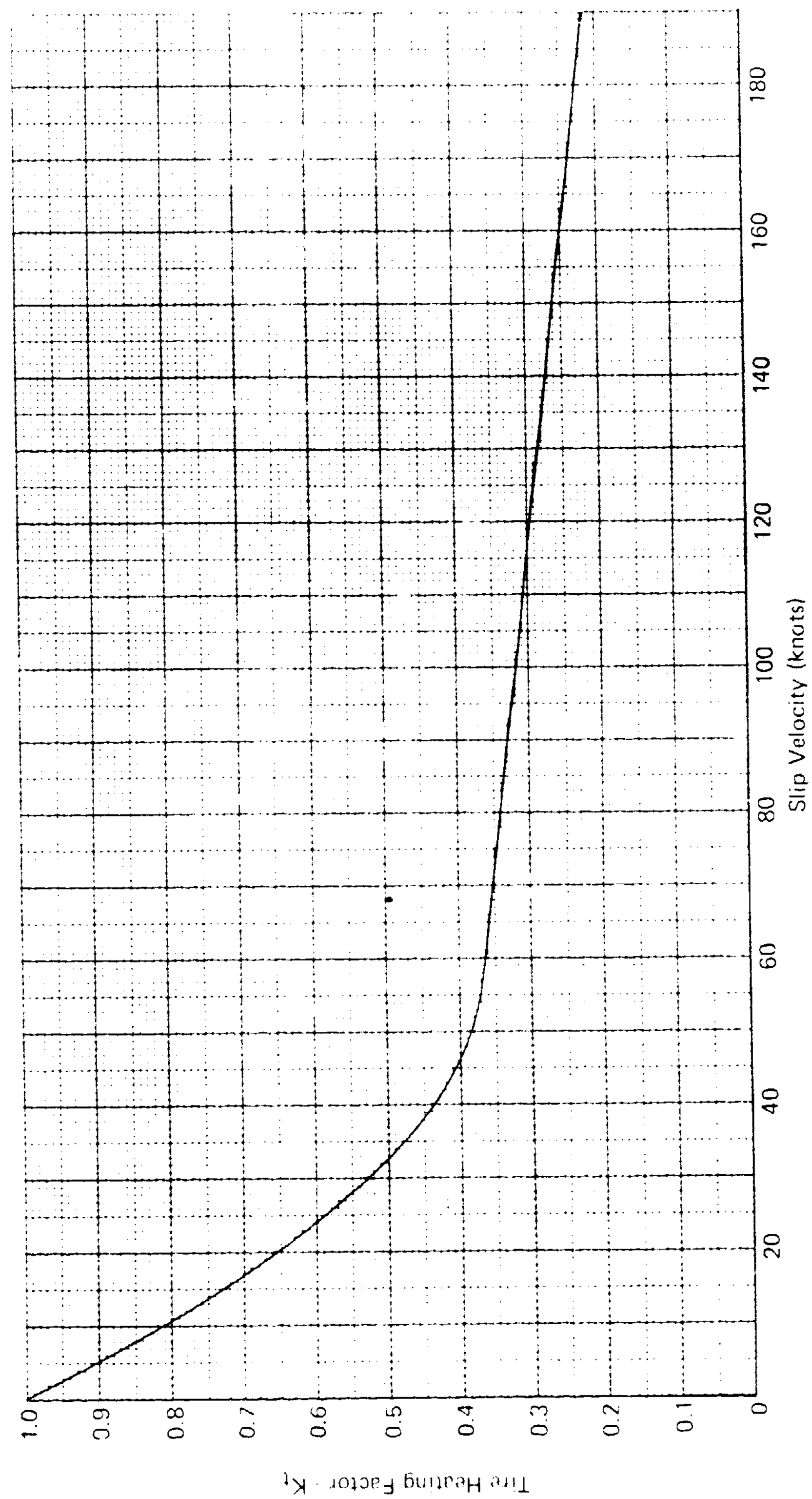

FIGURE 5-17
TIRE FRICTIONAL HEATING FACTOR - K_T

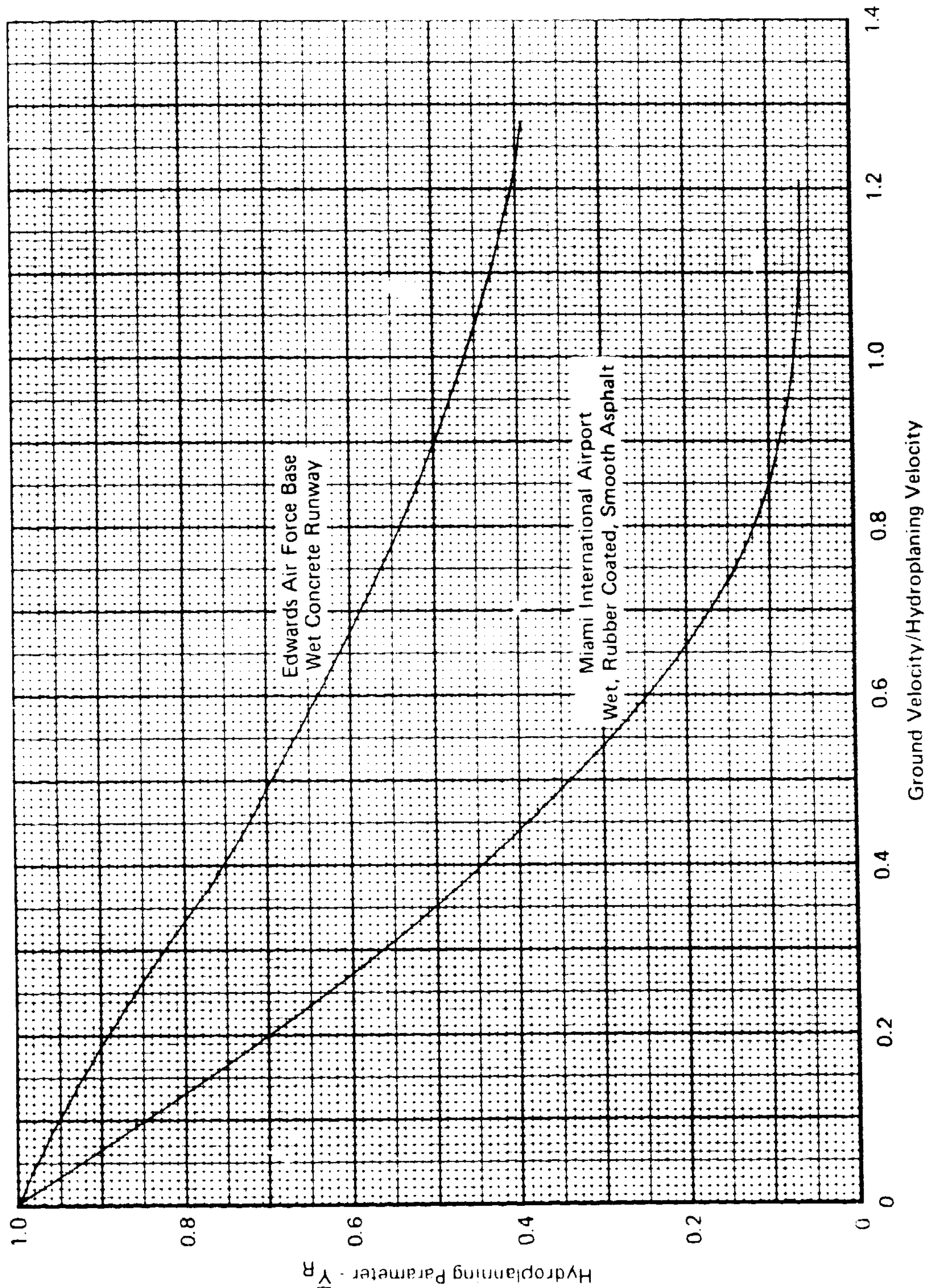

FIGURE 5-18
TIRE HYDROPLANNING PARAMETER - $\bar{Y}_R$

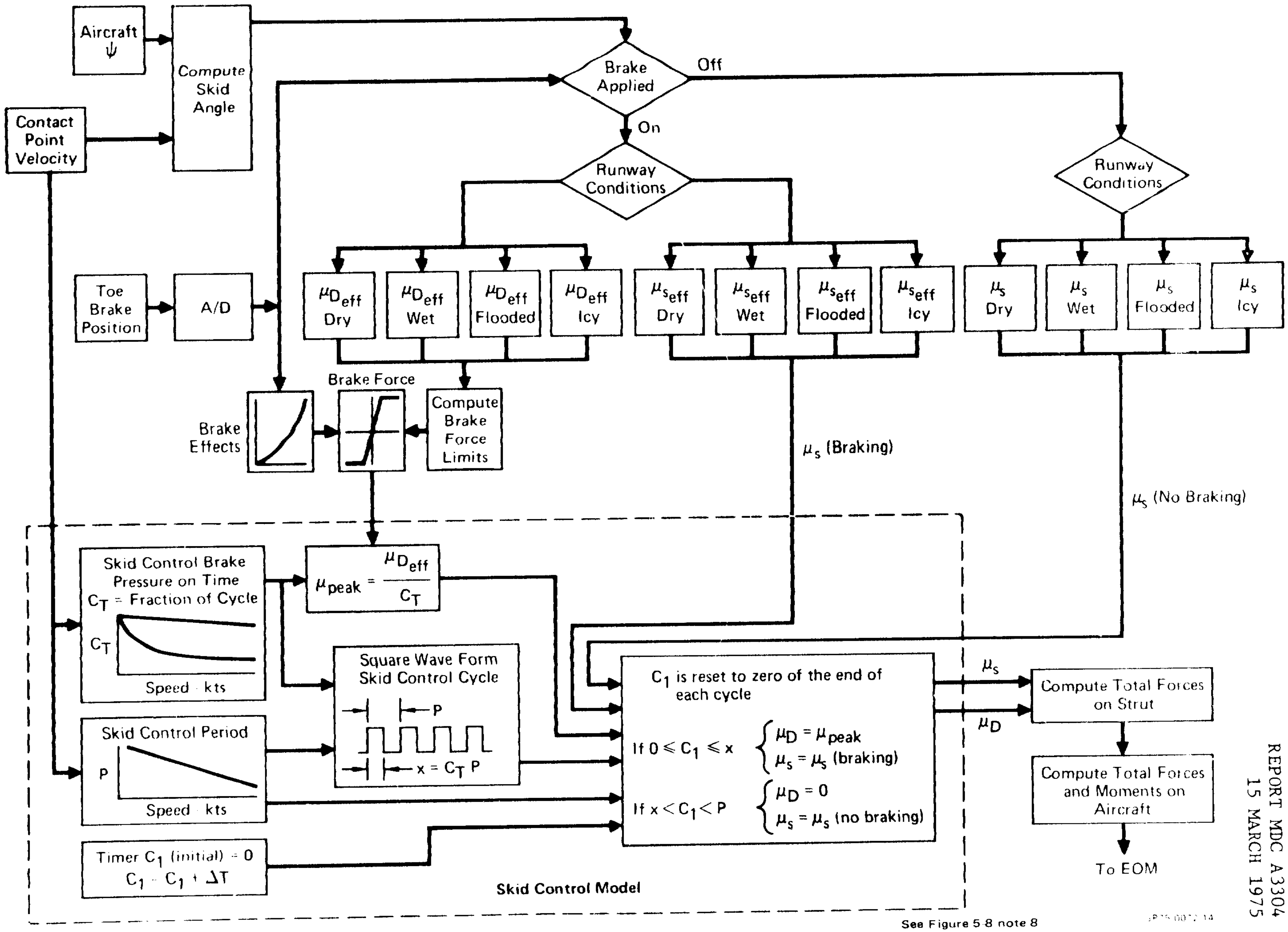

FIGURE 5-19
MAIN GEAR BRAKING AND SIDE FORCE FLOW DIAGRAM

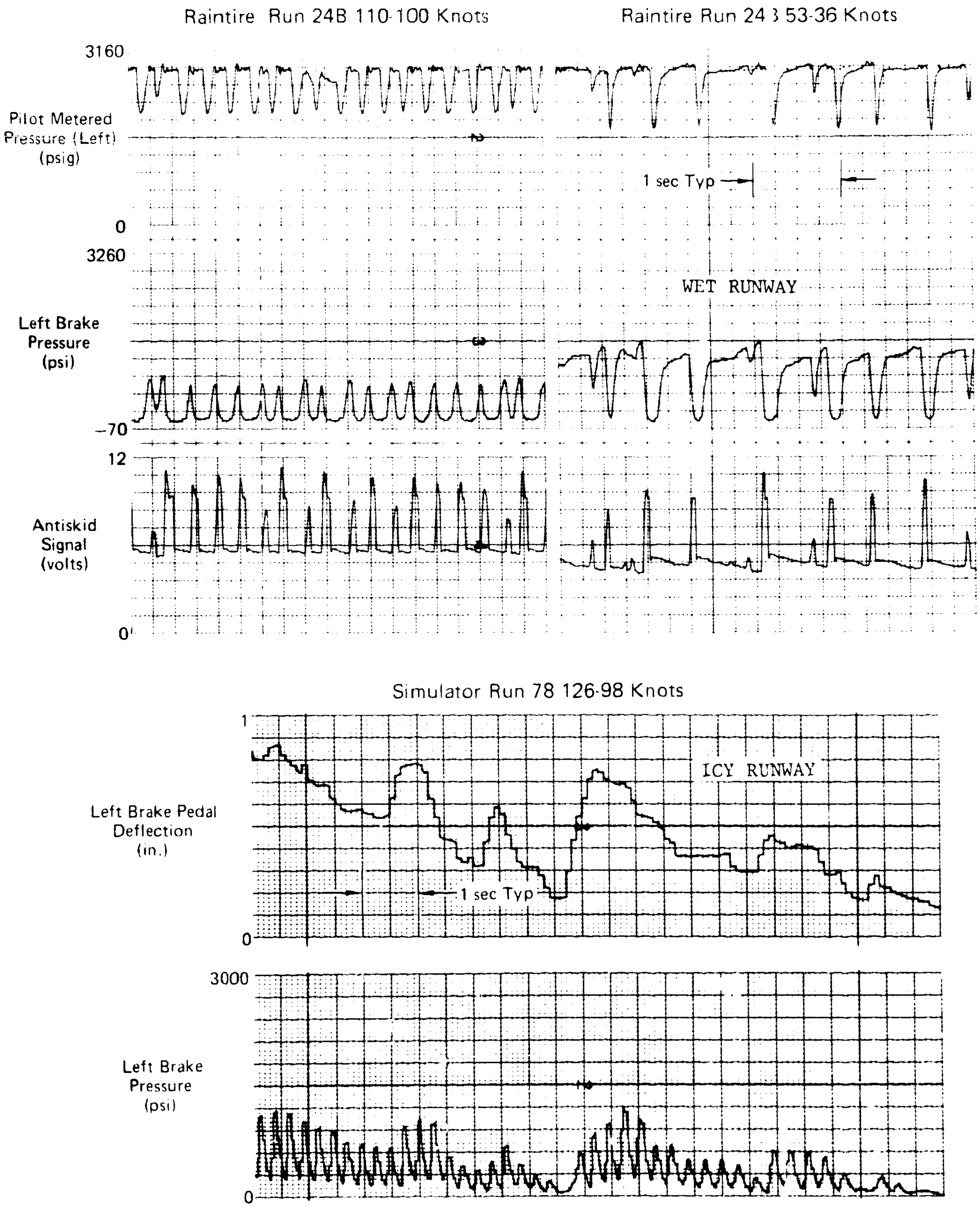

FIGURE 5-20
SKID CONTROL CYCLING COMPARISON

GP75 0072 49

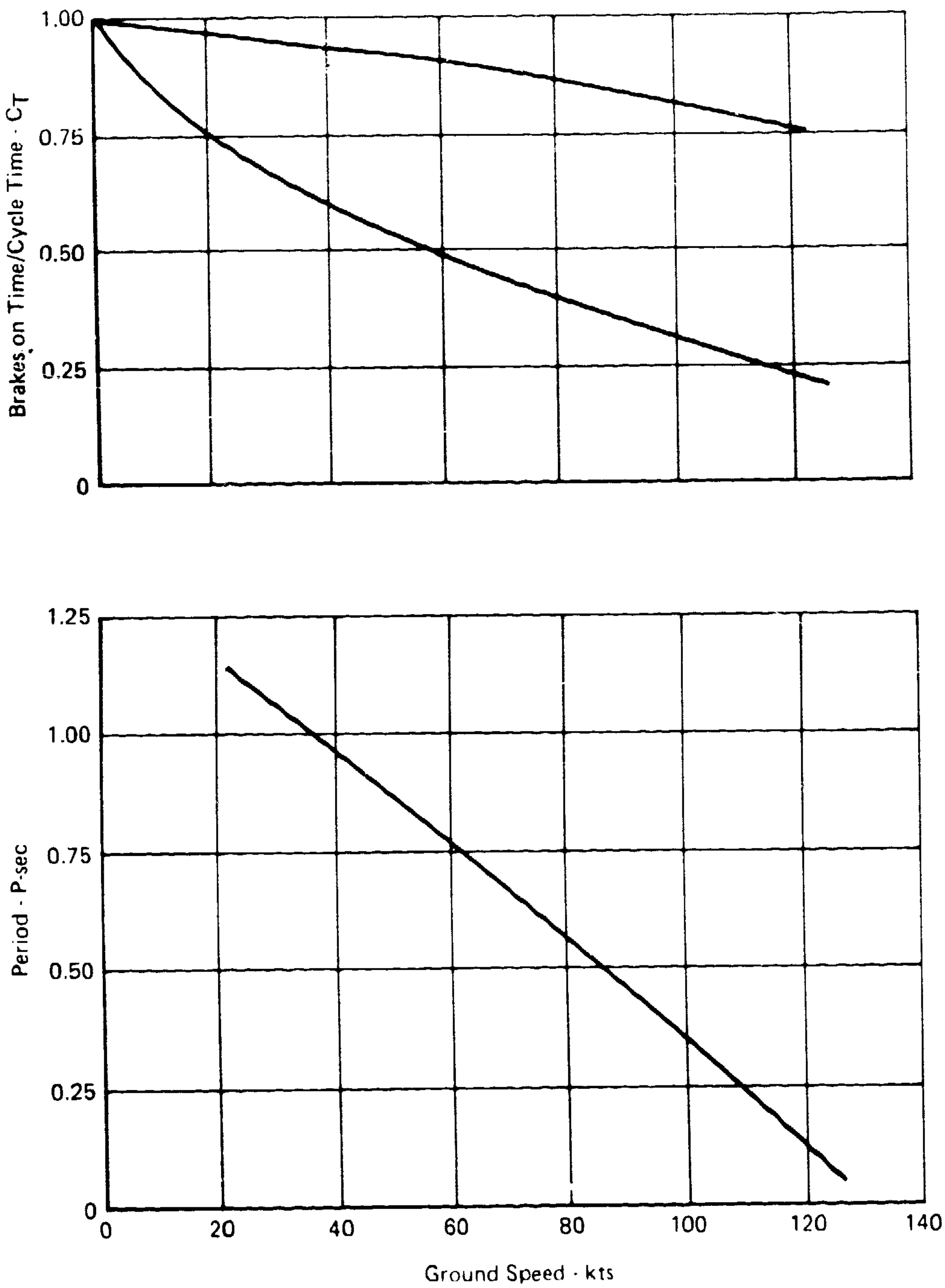

FIGURE 5-21
SKID CONTROL WAVE SHAPE CRITERIA

6.0 RESULTS AND DISCUSSION

6.1 Demonstration

6.1.1 Demonstration Summary - On 18-19 November 1974 representatives from NASA, USAF, and FAA participated in the demonstration phase of the program at MCAIR. Those attending were:

NASA: Tom Yager - NASA Program Manager
Ellis White - Computer Software Engineer

USAF: Col. George Meyers - Pilot "Raintire" Program
Maj. Joe Higgs - Pilot

FAA: Larry Andriesen - Flight Standards Engineer
Guice Tinsley - Pilot

A summary of each pilot's background and flight experience has been included in Figure 6-1.

During the two day demonstration 130 "flights" were made by the three pilots. Fifty-one of the "flights" were made on the first day for simulator familiarization and to obtain a few initial comments which might result in minor adjustments to the simulation prior to runs on the second day. These comments led to the following changes which were made before the demonstration runs on the second day.

(1) The runway "distance remaining" markers were removed from the terrain map because they hindered movement of the translator (the camera would reject when they hit the markers). Furthermore, these markers were causing visual cue problems since they were not to scale.

(2) The pitch and roll gains were adjusted for the in-air mode as noted in the following section.

(3) Gust and wind shear models were added to the wind model.

6.1.2 Pilot Evaluations

During the flights, pilot comments were recorded. Following each day's series of flights, the pilots were asked to write down their general comments and to evaluate certain aspects of the simulation on a rating scale without benefit of discussion with each other.

The rating scale which was used is shown in Figure 3-5. The results of the ratings are given on Figures 6-2 through 6-5.

A general discussion of the ratings and rating differences from each day is given below:

(1) Aerodynamic Steering - Generally rated very good

Maj. Higgs: Aerodynamic steering too effective at low speeds. (Both days)

(2) Nosewheel Steering - generally rated very good.

Col. Meyers:
- Not sure response is representative at high speed - dry (day 2)
- Too responsive - wet & flooded (day 2)

Maj. Higgs:
- Not responsive enough - wet & flooded (day 2)

Author:
- The cornering power for the nose tire on dry payment was changed after the first day to be more representative of the aircraft loads being simulated. This is probably the reason Maj. Higgs' rating changed from 6 (day 1) to 2(day 2) for the dry condition.

(3) Combined Nose Wheel and Aerodynamic Steering - generally rated good.

(4) Braking Effectiveness - generally rated moderate.

Col. Meyers:
- Nose did not fall as hard as actual aircraft.
- Simulation could be improved by adding additional cues.

G. Tinsley.
- Visual cues do not give sufficient deceleration effect.

Maj. Higgs:
- Unable to tell rate of deceleration from visual cues.
- Braking action should be better at slower speeds on wet & flooded.

Author: The jerky motion of the translator at low speeds probably added to problems in this area.

(5) Crosswind - Two pilots rated the crosswind simulation very good on the second day.

Col. Meyer:
- Not enough turn into wind when deploying chute.

G. Tinsley:
- Not enough turn into wind when deploying chute.

Author: The improved rating from day 1 to day 2 is probably due to the gusts added to the wind model.

Runway crown simulation may make this more realistic.

(6) Yaw Control - Generally rated good.

Maj. Higgs: Day 2 better than day 1.

(7) Yaw Stability - Generally rated good to moderate.

Maj. Higgs:
- Day 2 better than day 1.
- On 2 runs (day 2) yaw control became unstable below 70 knots possibly due to turbulence.

(8) Drag Chute - Two pilots rated the drag chute poor on both days.

(Same comments as those for item (5)).

Author:
- Drag chute input was changed from a ramp to a step after the demonstration flights.
- Currently, simulator does not produce any motion deceleration which might be associated with chute deployment.

(9) Other -

Col. Meyers:
- Roll control on approach is not realistic.
- Roll control better on day 2 than day 1, but not as good as the rest of the simulation.
- Touchdown simulation is excellent.

Author:
- Roll gains were changed slightly from day 1 to day 2.

There was some pilot opinion that the drag chute deployment was not giving a sufficiently abrupt initial force. So, for the final week of simulator runs, the ramp was replaced with a step. The two MCAIR pilots who tested that mechanization had no adverse comments on the aircraft reaction to drag chute deployment and jettison.

First day pilot comments on airborne handling qualities indicated that the simulator response to control inputs was sufficiently different from the pilot's experience in the F-4 to warrant some modifications to the published data. Published data on pitch stability with jet effects shows very slight negative static stability, whereas the aircraft in flight exhibits very good longitudinal stability. The published data for the F-4J is more recent, more accurate and more stable, according to F-4 project engineers, consequently, that data was incorporated during checkout. Changes after the first day evaluation included a -.002/deg CM_{α} increment, 1.5 $CM_{\dot{\alpha}}$ and C_{M_q}. The F-4J lateral response is reduced due to the drooped ailerons, therefore, roll response was increased by 1.3 $C_{l_{\delta_a}}$ and 1.3 C_{l_p}. These changes were acknowledged as reasonable improvements by the F-4 project engineers. The pilots also agreed that those changes resulted in handling qualities which were very close to that of the actual aircraft. Aerodynamic response to controls (pitch and directional) during touchdown and rollout was rated as very good by all pilots. The longitudinal deceleration information was probably the weakest point of the simulation. The current translator becomes jerky below a simulated speed of 50 knots due to mechanical limitations, and it is physically limited to a 25-foot minimum simulated altitude. The new terrain map and translator will be an improvement in the visual display because it will be capable of a lower altitude (13 ft) and, lower speeds (less than 10 knots), and will have the added realism of a color display.

Other possible ways to provide more deceleration cues include using a sound and/or peripheral flashing light which would decrease in frequency with decreasing ground speed, and tilting the crew station in pitch once the aircraft is on the ground. A pitch of 17° will produce a .3g force which will adequately simulate braking deceleration.

General comments on the overall simulation are given in Figure 6-6.

Since the pilots "flew" about 20 runs each time they were in the simulator, their verbal comments were recorded during each run so the comments could easily be associated with the specific run conditions. Table 6-1 shows a matrix of the parameters used for each tests and Table 6-2 lists the run number and any pilot comments which might have been recorded.

The general opinion of the pilots was that the simulation was representative of the aircraft's actual performance and handling characteristics. The pilots rated the existing motion cues as very good for all phases and excellent for the touchdown phase. It was generally agreed that high fidelity motion cues were very important (if not essential) for valid training or evaluation in this phase of flight.

6.1.3 <u>Numerical Data</u> - During the demonstration, strip chart records were made of selected parameters. Four 8-track pen recorders were used. Samples of the recorded output data are shown on Figures 6-7 through 6-10. Figure 5-20 shows a comparison between the cycling brake pressure of an actual aircraft during skid control cycling and the cycling of μ to simulate the skid control on the MBS.

Braking and steering were both studied during the demonstration. A large portion of the runs were made without brakes in order to examine the steering characteristics. The steering relations between aircraft and MBS were not quantitatively evaluated and are best compared by the qualitative comments from the pilots.

The braked runs were performed with differential, intermittent, or hard braking[1]. The hard braking runs were quantitatively compared to actual aircraft data as in the plot of stopping distance versus brakes-on speed (see Figure 6-11). As can be seen, good correlation with experimental data was achieved.

6.2 Post Demonstration Runs

6.2.1 Changes Made to Simulation - Following the demonstration NASA and MCAIR representatives decided to make additional changes in the simulation for this phase. The following items were studied.

(1) Deadband was increased in the rudder pedal - steering model.

(2) The parabrake fade-in ramp was changed to a step input.

(3) The nose tire cornering power was revised to be more consistent with the average aircraft loads.

(4) Comparisons were made between skid control model operative (cycling μ) and inoperative (average μ).

(5) Runs were made using a Wallops Island Runway friction model (begin braking on dry and change to wet conditions). These runs were modeled to match the aircraft at Wallops Island where an F-4 made several landings on a dry runway and brakes were applied prior to entering a wetted test section. Severe yaw occurred with crosswinds on a few of the actual aircraft runs under these conditions.

6.2.2 Pilot Comments - On January 24 and 27 two MCAIR pilots (Charlie Plummer and George Mills) flew 53 runs on the simulator after the above modifications. Major Higgs was not available for these tests, as originally planned. A matrix of their flights is shown in Tables 6-3 and 6-4. During Mr. Plummer's debriefing, he stated that the effects of steering deadband were barely detectable; the skid control operative versus inoperative was not detectable; and he did not have much of a problem with a dry to flooded (Wallops Island) model.

[1]When the pilot maintained brake pressure at a level which caused the skid control model to activate, the run was considered to be conducted with hard braking.

George Mills' comments are recorded in Figure 6-12. His runs were flown fixed base, and a Wallops Island model dry-to-ice was added to his test spectrum. His rating of the simulation is in Figure 6-13.

The Wallops Island model was accomplished by changing the μ value from dry to flooded or ice at a selected velocity[2]. The intention of this model was to demonstrate the aircraft performance experienced during braking tests performed by NASA at Wallops Island. Figure 6-14 shows aircraft simulation performance on a "dry-to-icy Wallops model". For this run the wind is blowing from the right to left. Negative values of lateral offset represent distance to the right of the runway centerline. Positive values of all the other terms (steering angle, heading, etc.) represent motion to the right.

The run in Figure 6-14 shows the typical aircraft weather vaning into the wind, however, the aircraft tracks toward the upwind side of the runway, which occasionally occurs in actual aircraft experience due to oversteering when no parabrake is used. This may mean that the cornering/braking tire friction curves need further refinement or that excessive aircraft yaw was input by the pilot.

6.3 Simulation Benefits

The simulator offers the following benefits over the actual flight testing of the aircraft.

6.3.1 Time - In actual flight testing the aircraft must fly around between each landing with gear down to cool the brakes. This results in at best three landings/hour for an actual aircraft test on a wet runway, whereas an average of 25 landings/hour can be performed on the simulator.

[2] Three velocities were tested and are shown on Table 6-3.

6.3.2 Cost - The cost of operating a fully instrumented flight test F-4 aircraft is approximately $20,000 per hour, or about $6700 per landing for ground handling studies. The MBS cost is approximately $20 per landing.

6.3.3 Safety - For this type of study, where the limits of control are being examined, there is a high risk of pilot injury and aircraft damage. Use of a simulator eliminates this risk.

6.3.4 Modification - Runway conditions and aircraft configuration changes can quickly and easily be made in comparison to the actual aircraft.

6.3.5 Data Retrieval and Measurement - The simulator quickly and accurately records aircraft speed, roll distance, yaw angle, and lateral offset compared to the time consuming data reduction process from current photographic techniques used during actual flight test. Details of runway friction and wind velocity are known.

6.3.6 Controlled Test Conditions - With the simulator, a landing can be examined at any instant of time or repeated many times at exactly the same condition. For example, there is no problem of the wind or runway water depth changing from run to run.

Flight Experience:

	George Meyers		Guice Tinsley		Joe Higgs	
	Aircraft	Hours	Aircraft	Hours	Aircraft	Hours
	F-4	800	T-33	800	F-89	100
	F-106	700	C-118	3000	F-101	1100
	F-102	450	C-135	2700	F-4	3000
	F-104	350	C-141	1000	F-15	40
	U-2	360	F-4	600		
	F-86	100	Other	1600		
	Other	1740				
	Total	4500	Total	9700		

Simulator Experience:

Tinsley - Instructor in C-135 C-141 Simulators - Link Motion Based 6 degree of Freedom.
Currently flying C-135 low visibility simulation & T-39 MLS Flight Profile Simulation.

Higgs - USAF Instructor F-101 - F-4 simulators
G.D. TEWS/F-15 Development Simulation
G.D. F-15 Threat/Evasive tactics devel. simulator
MDC - F-15 air combat performance eval.

General Experience:

Meyers - 4500 total time in mainly fighter type aircraft. Combat tour RF4's 1967. Graduate of Aerospace Research Pilot School 1968. Flew 90% of the Air Force rain tire test program in 1973 to evaluate 5 tire tread designs and compare the MK II and MK III anti skid systems on dry and wet runways.

Tinsley - Present job - Chief of Terminal Navigation Branch FAA Hg.
Current Test Projects - T-39 MLS Flight Profile Investigation
C-141 Low Visibility Landing Investigation
B-737 Terminal Area Control Investigation
& Evaluation of SST CRT Displays

Higgs - 3 yrs in Air Defense Command flying F-89 and F-101.

7 yrs in TAC flying F-4, 3 combat tours in SEA and N. Vietnam.

Instructor pilot and academic instructor in replacement training wing at George AFB, Calif. 5 yrs - maintenance check pilot, aircombat tactics/F4 aerodynamics instructor.

4 1/2 yrs at AFPRO MDC as operations officer in military flight test. Flying F4/F15 acceptance test flights. Present Duty.

FIGURE 6-1
PILOT BACKGROUND SUMMARY

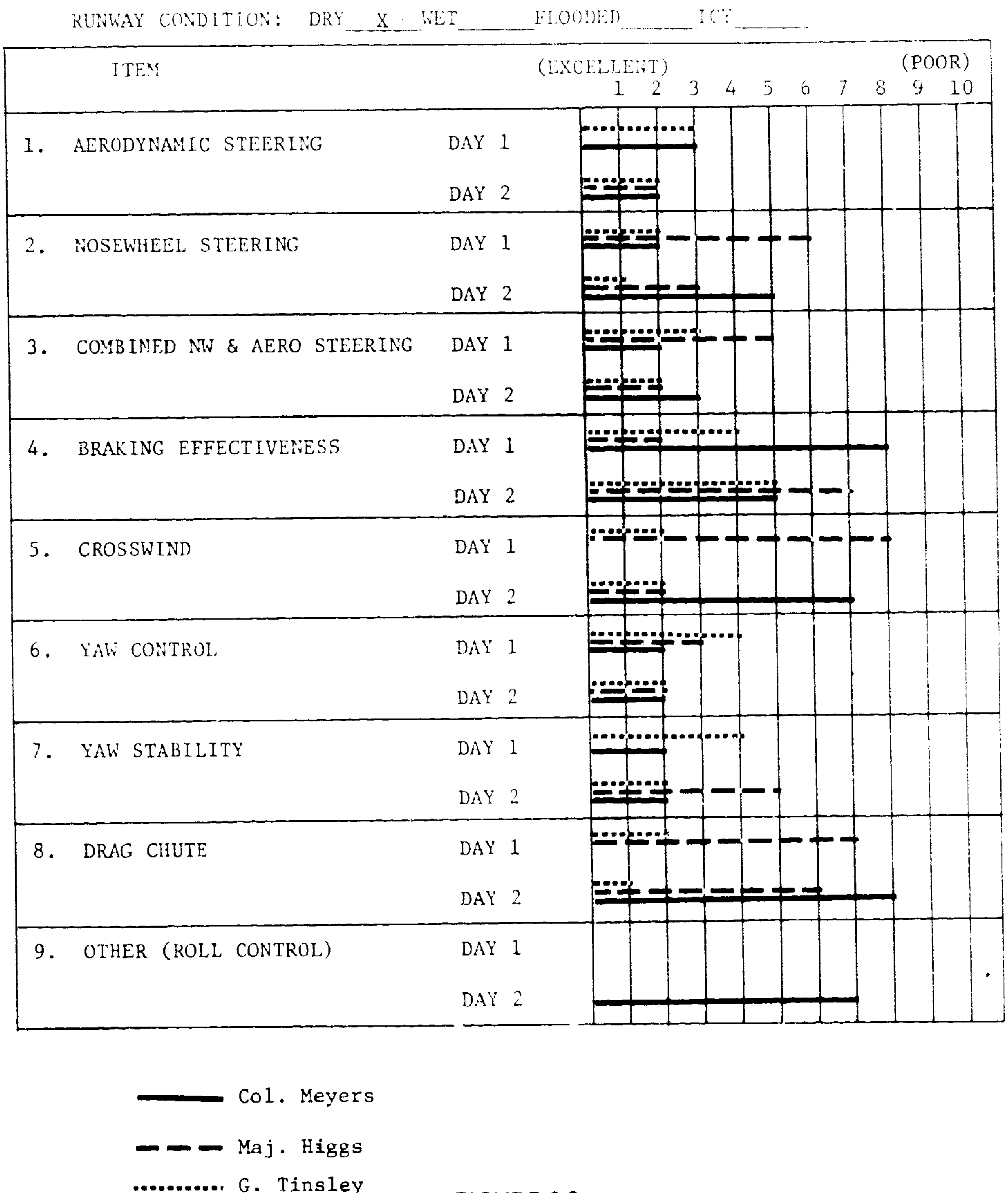

FIGURE 6-2
PILOT RATINGS - MBS DRY RUNWAY

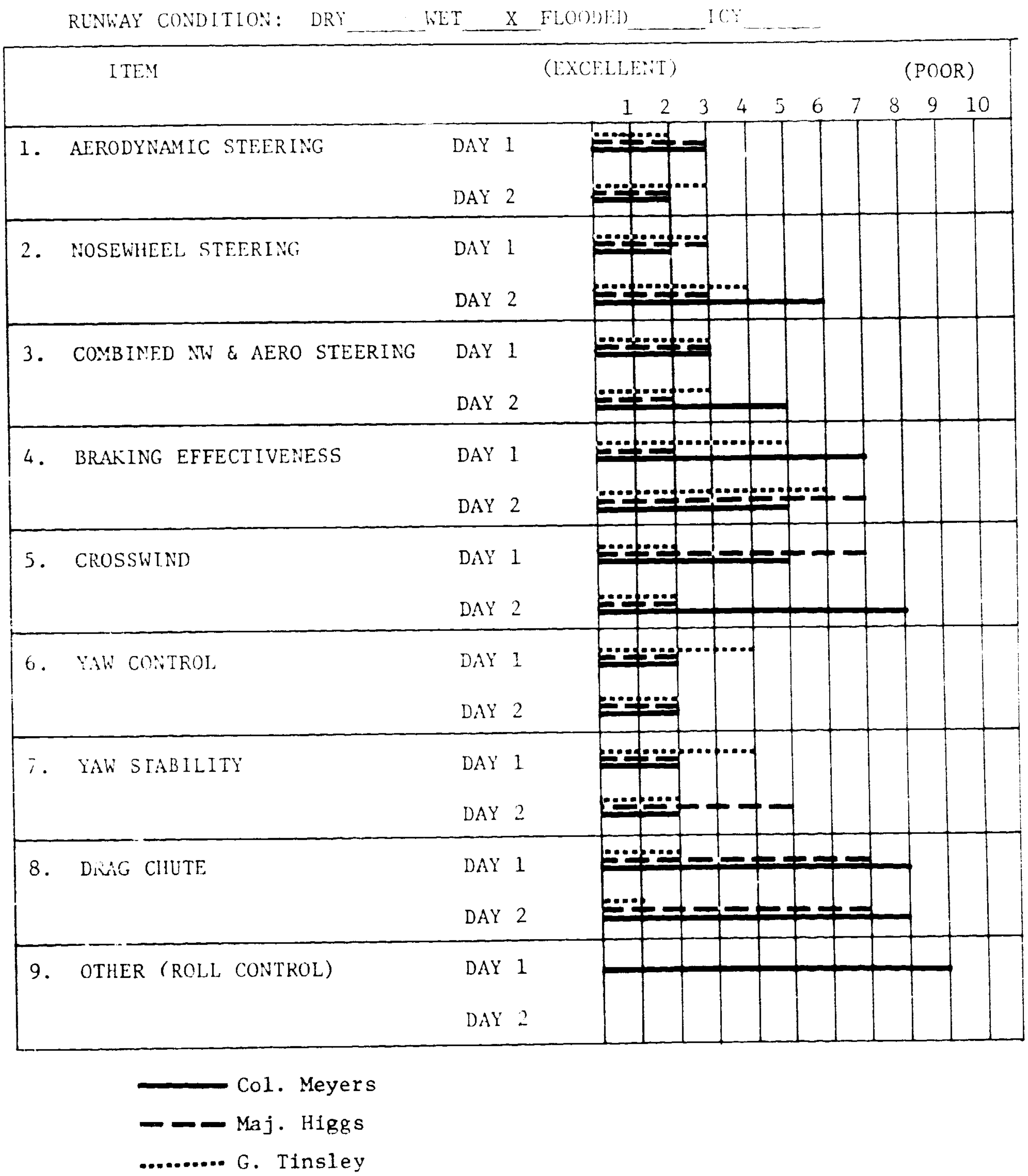

FIGURE 6-3
PILOT RATINGS - MBS WET RUNWAY

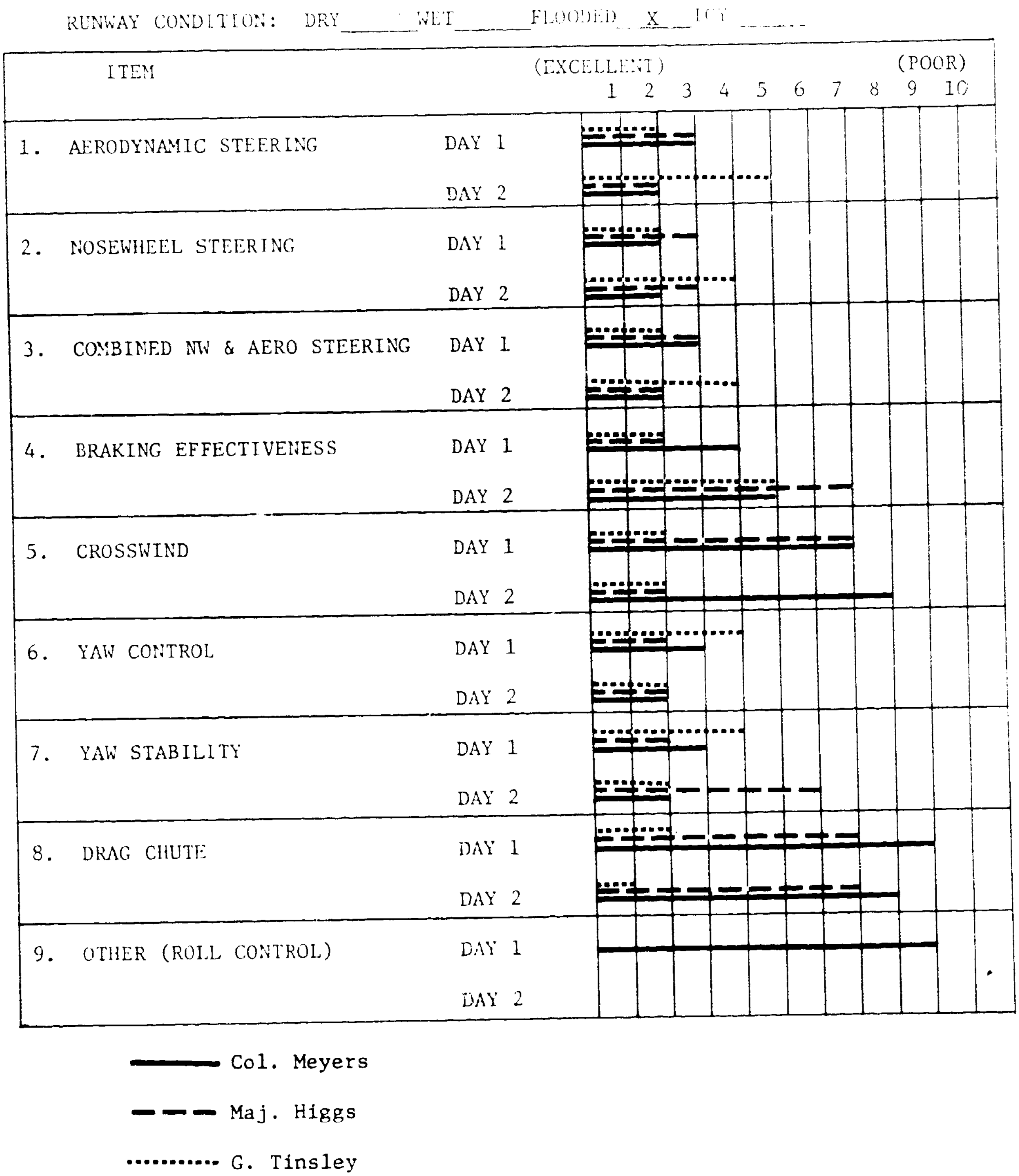

FIGURE 6-4
PILOT RATINGS - MBS FLOODED RUNWAY

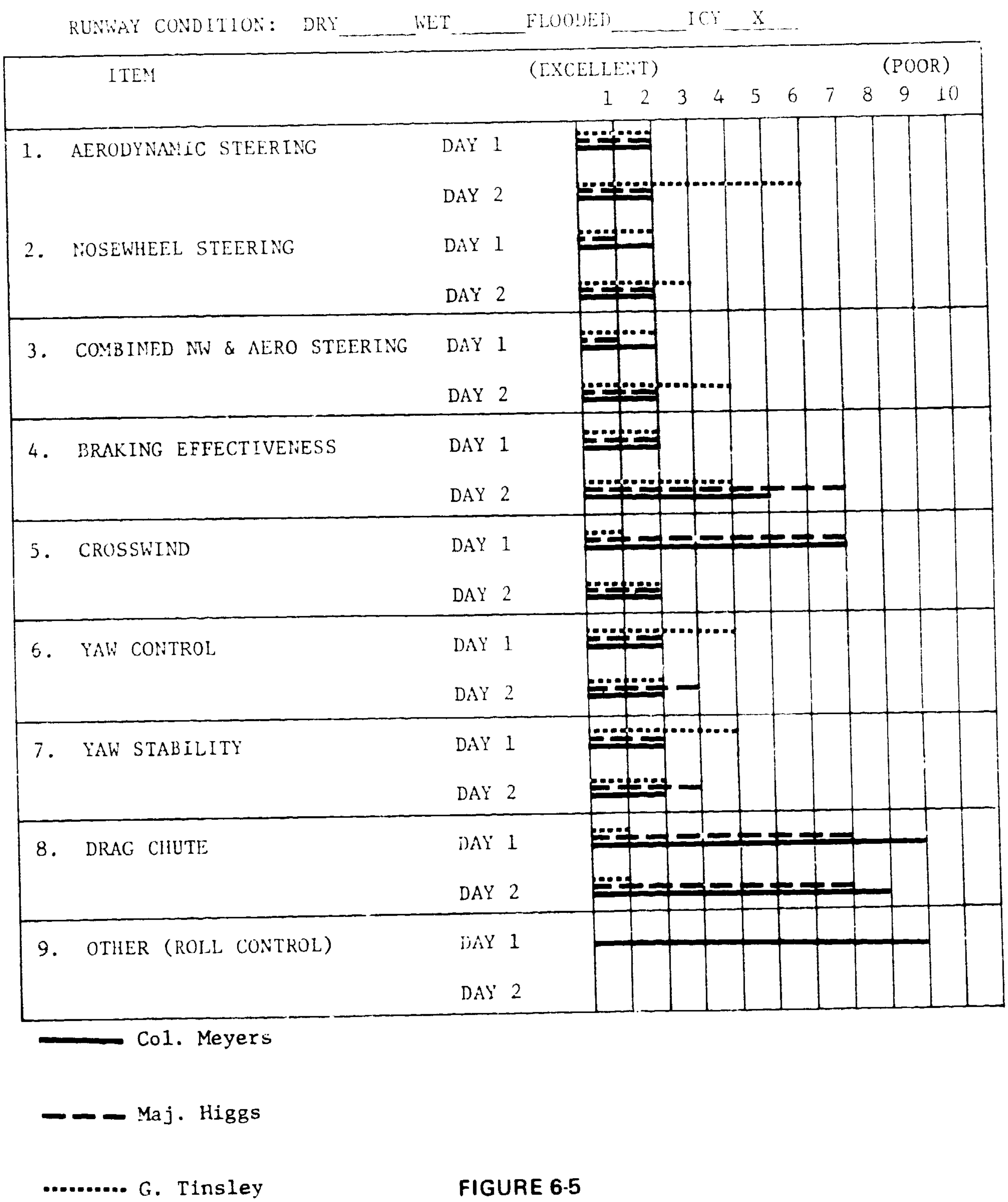

FIGURE 6-5
PILOT RATINGS - MBS ICY RUNWAY

"Overall this is a good simulation of the F-4 during the landing roll under various runway conditions. The final approach to landing could be improved by improving the handling qualities to closer mat : the aircraft response. This does not however detract that much from the overall effectiveness of the simulation. The touchdown portion of the simulation is excellent. The lack of enough deceleration cues detracts from the overall simulation. The nosewheel steering appears too sensitive on the wet runway simulation in the high speed portion of the roll. It appeared good during the flooded and icy portion. The pitch response of the simulator during deceleration is excellent in this configuration. The nose lowering is a good indicator of brake effectiveness."

Col. George Meyers: USAF

"Airborne handling qualities adequate to establish various touchdown conditions. Aircraft touchdown very realistic and varied as actual flight conditions would be. Single weakest area is no adequate visual reference that gives the proper impression of deceleration. This characteristic goes from bad to worse as speed slows to below 60 kts. Ground turbulence effect may or may not be realistic but I do question the magnitude of the resultant yaw (without drag chute) due to turbulence. Aerodynamic steering rudder and aileron seem to be very realistic. Removal of R/W markers a definite improvement. In general, I think the program has a high level of realism and except for the speed cue deficiency only minor improvements are needed."

Guice Tinsley: FAA

"This is a very good simulation of the landing phase. The touchdown realism is outstanding as is the feel and motion of flight. Visual cues are very good for forward field of view only, and are adequate to accomplish the test objectives. The airborne handling qualities of the simulation are much improved in roll over previous flights, however, pitch control is very marginal, the pitch rate is a good approximation of the F-4; however the aircraft is too slow to respond and is too sensitive to stick forces. This makes it difficult for the pilot to solve some of the anticipated landing problems by making a controlled touchdown - however, during this test the type of touchdown and conditions at last stage of final approach did not appear to affect the landing rollout in a realistic manner such that anyway to get it on the ground produced the same results. This simulation would be very useful in training but needs considerable improvements in the aircraft handling qualities and visual deceleration rates or simulation. Drag chute performance after deployment is extremely realistic."

Maj. Higgs: USAF

FIGURE 6-6
PILOTS COMMENTS ON SIMULATION

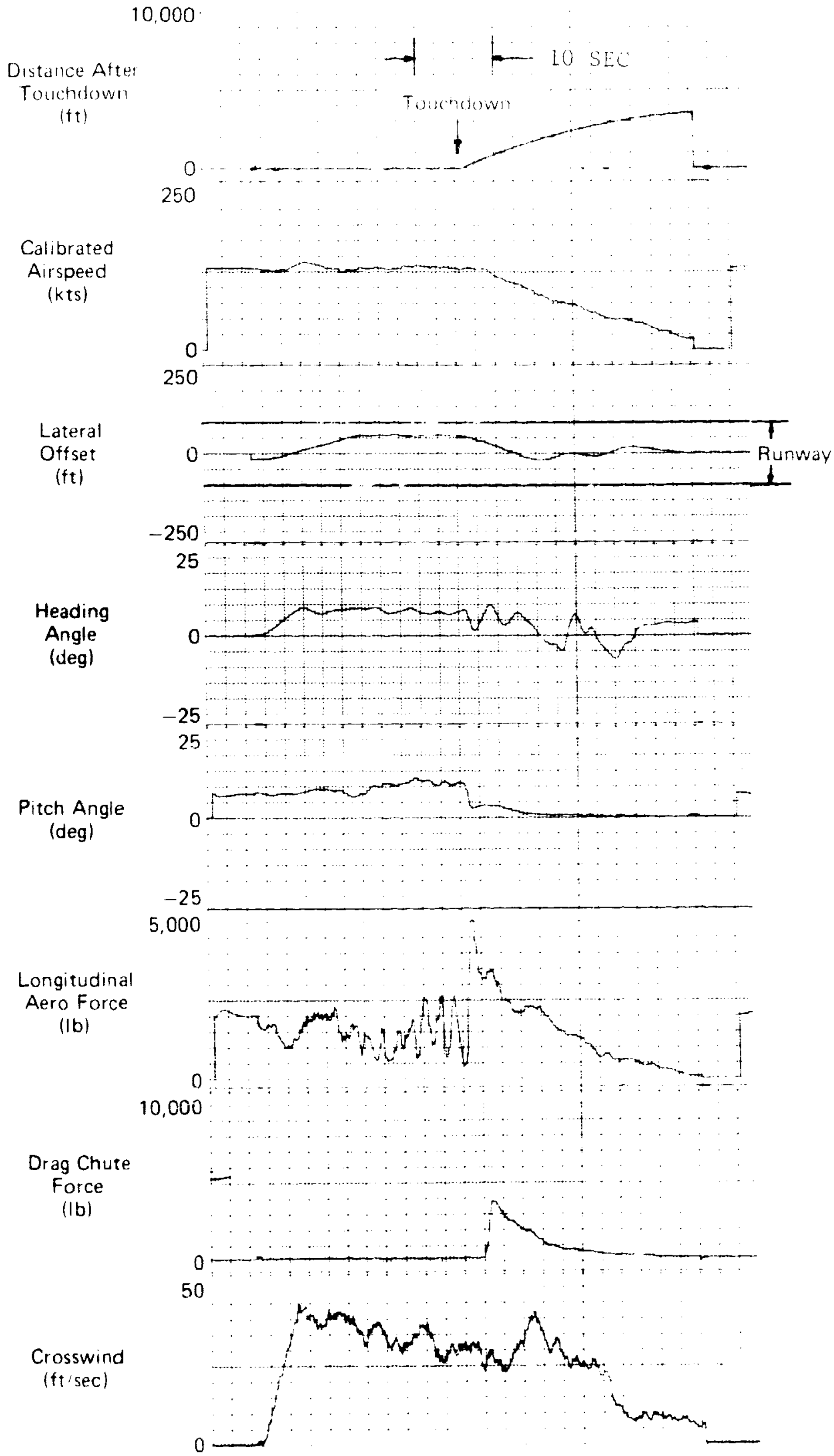

FIGURE 6-7
TYPICAL LANDING ON DRY RUNWAY
Demonstration Run No. 85 See Table 6-1

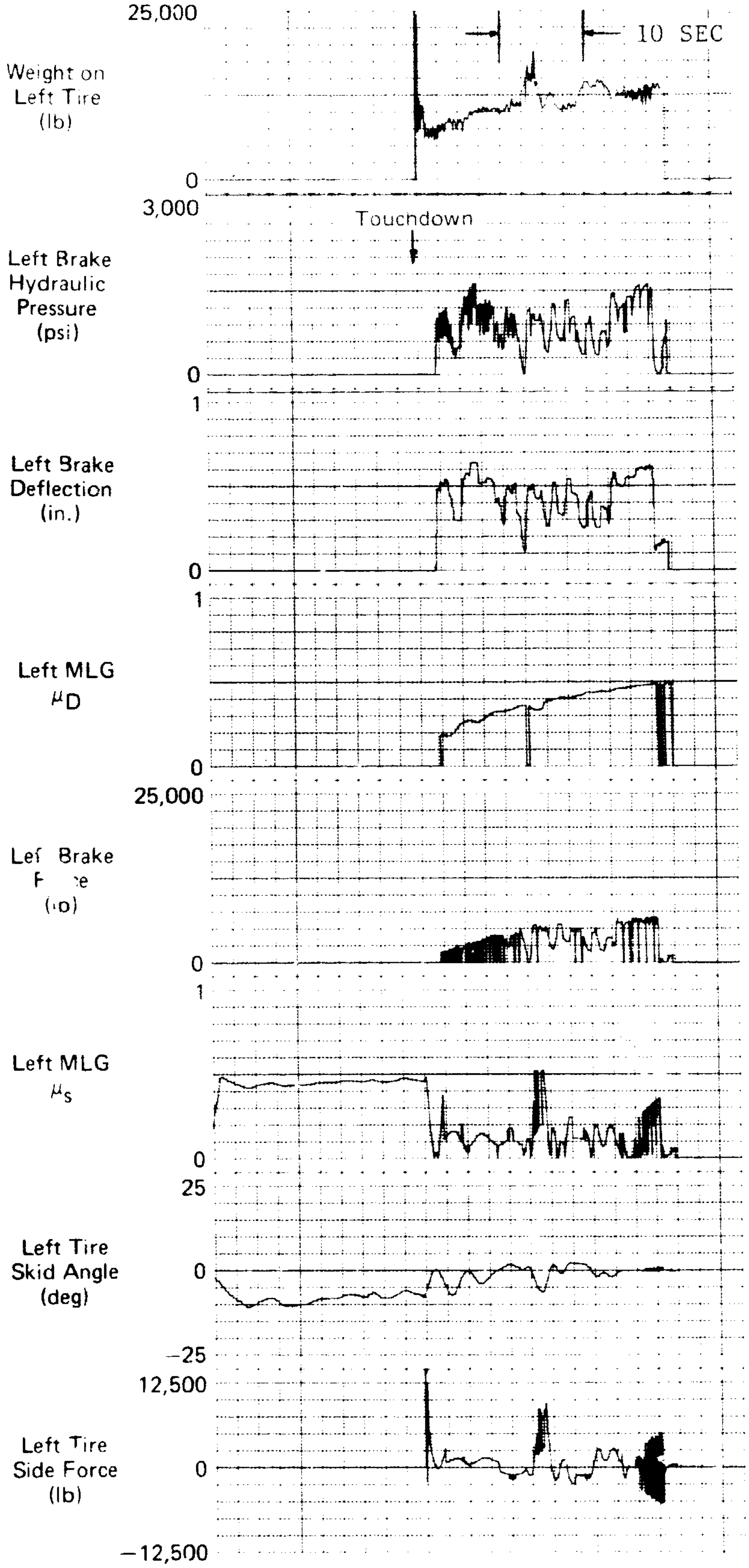

FIGURE 6-7 (Continued)
TYPICAL LANDING ON DRY RUNWAY
Demonstration Run No. 85

GP75 0072 29

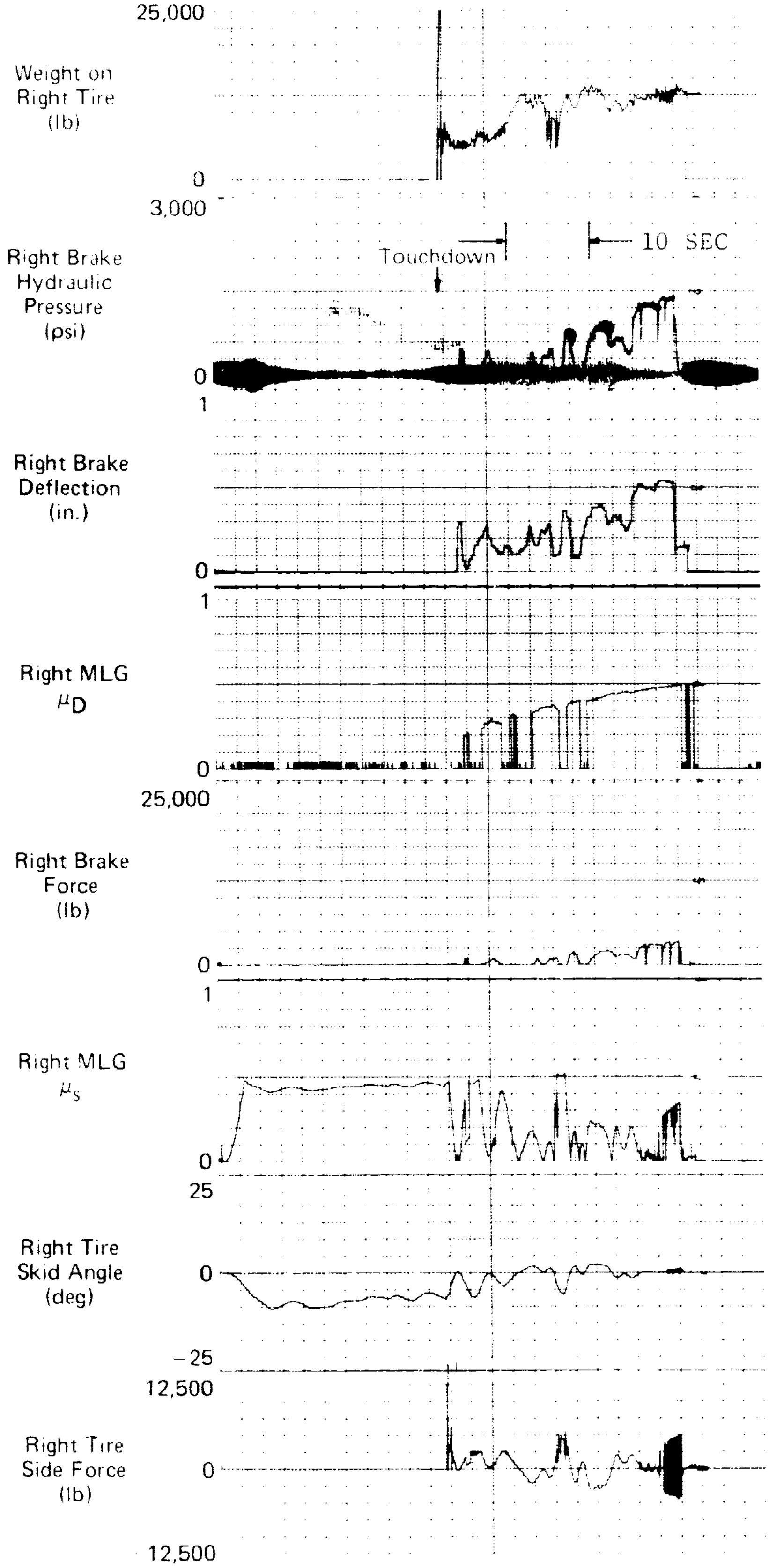

FIGURE 6-7 (Continued)
TYPICAL LANDING ON DRY RUNWAY
Demonstration Run No. 85

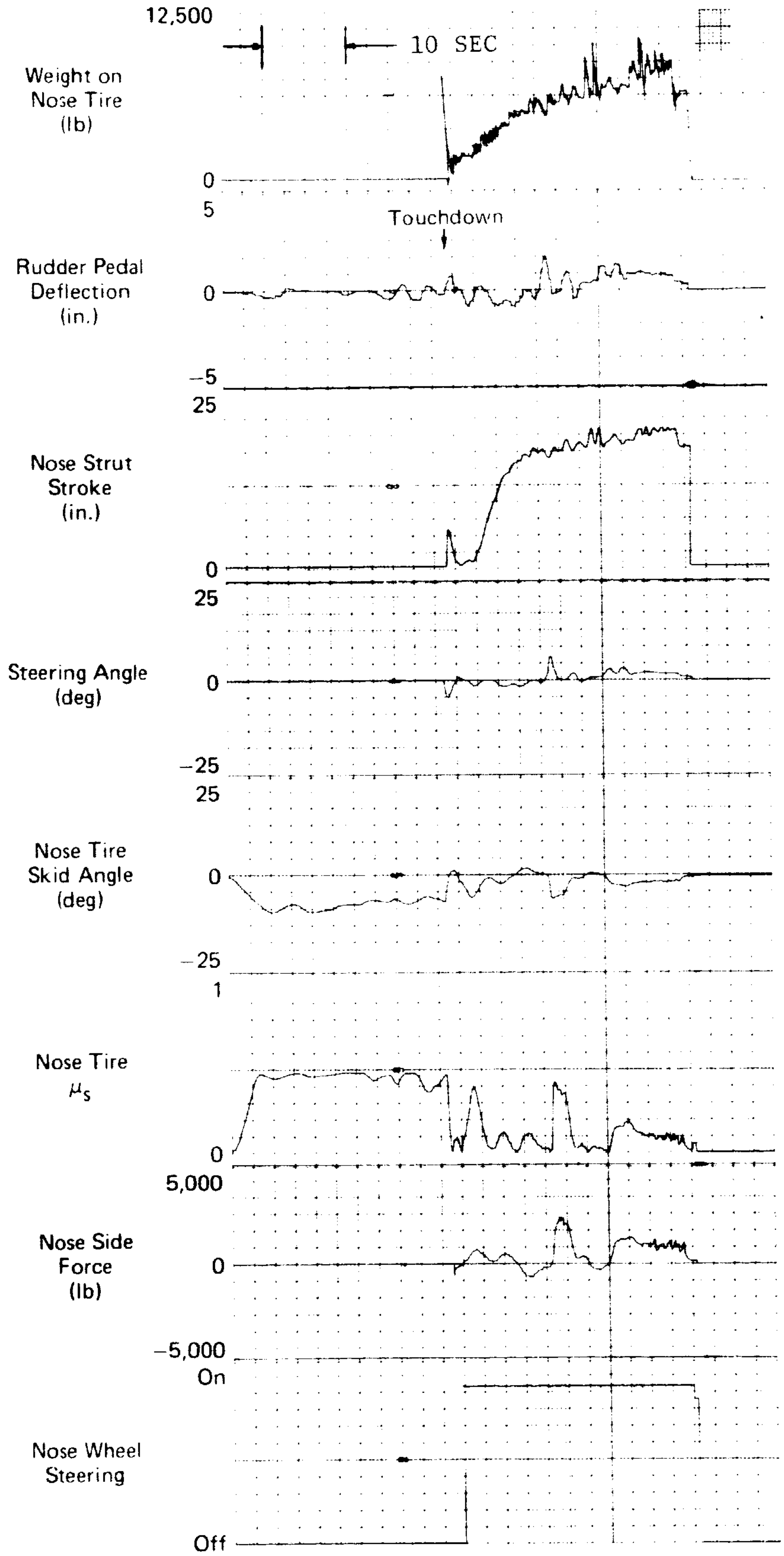

FIGURE 6-7 (Concluded)
TYPICAL LANDING ON DRY RUNWAY
Demonstration Run No. 85

GP75 0072 31

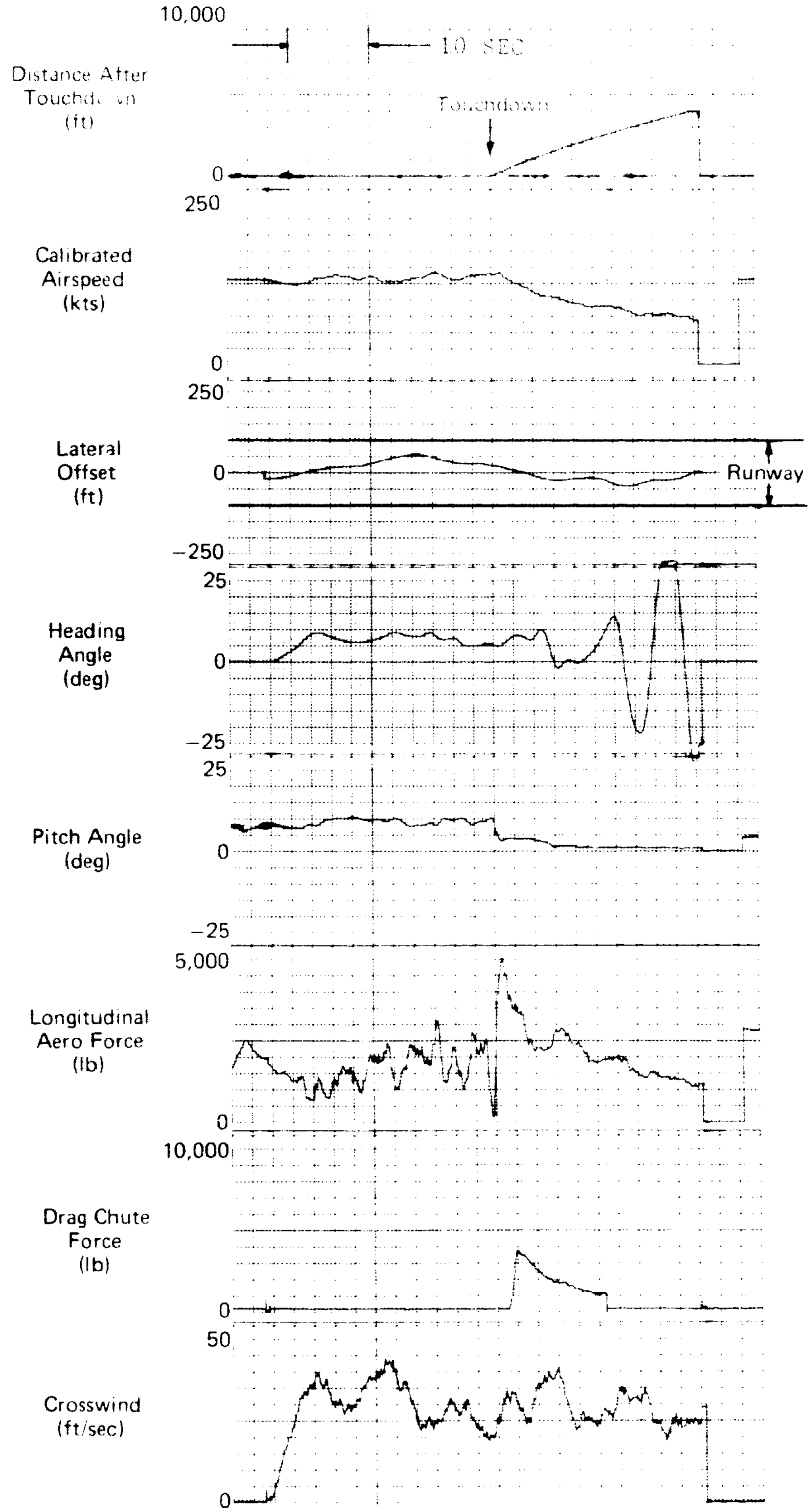

FIGURE 6-3
TYPICAL LANDING ON WET RUNWAY
Demonstration Run No. 90 See Table 6-1

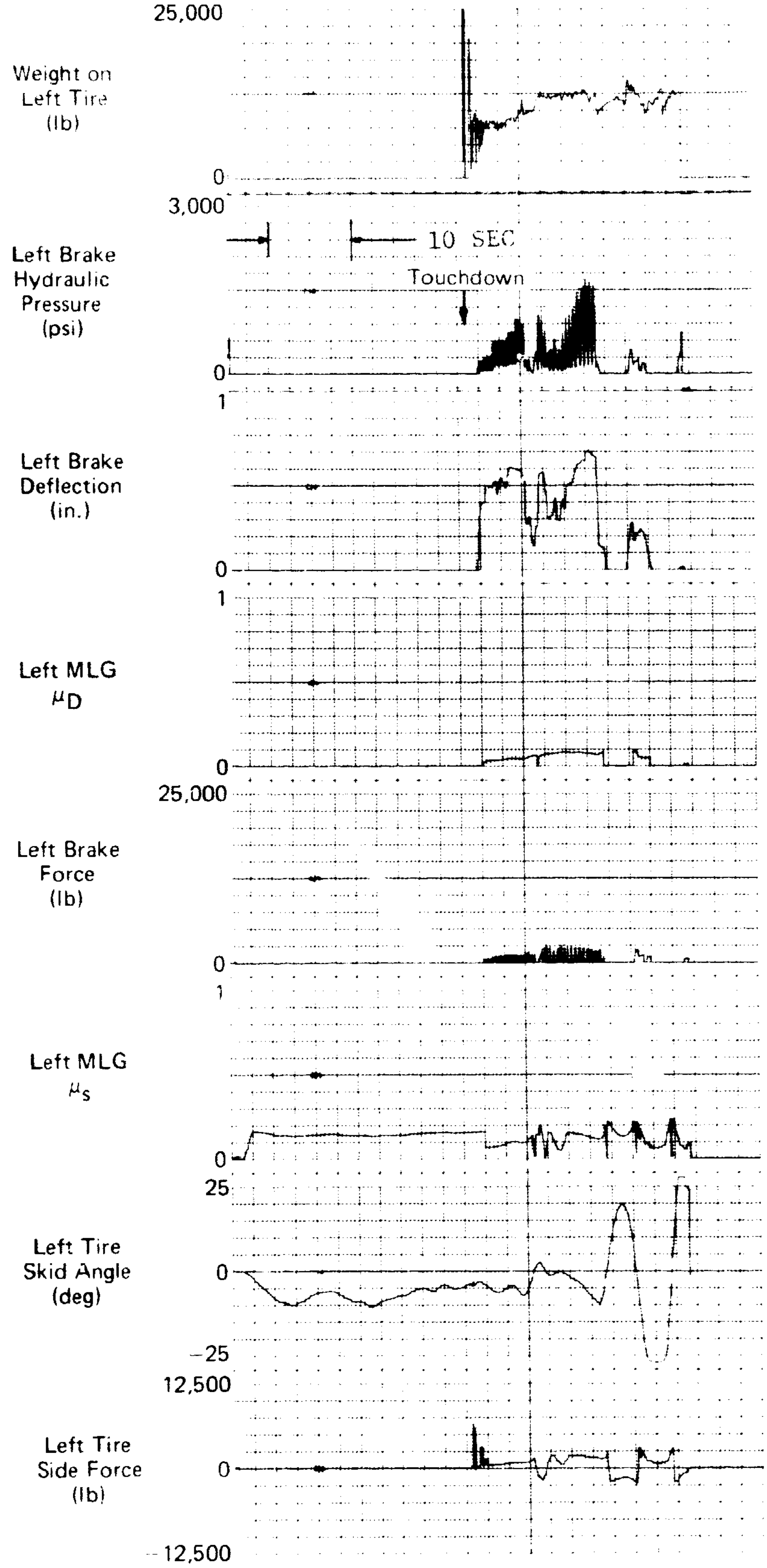

FIGURE 6-8 (Continued)
TYPICAL LANDING ON WET RUNWAY
Demonstration Run No. 90

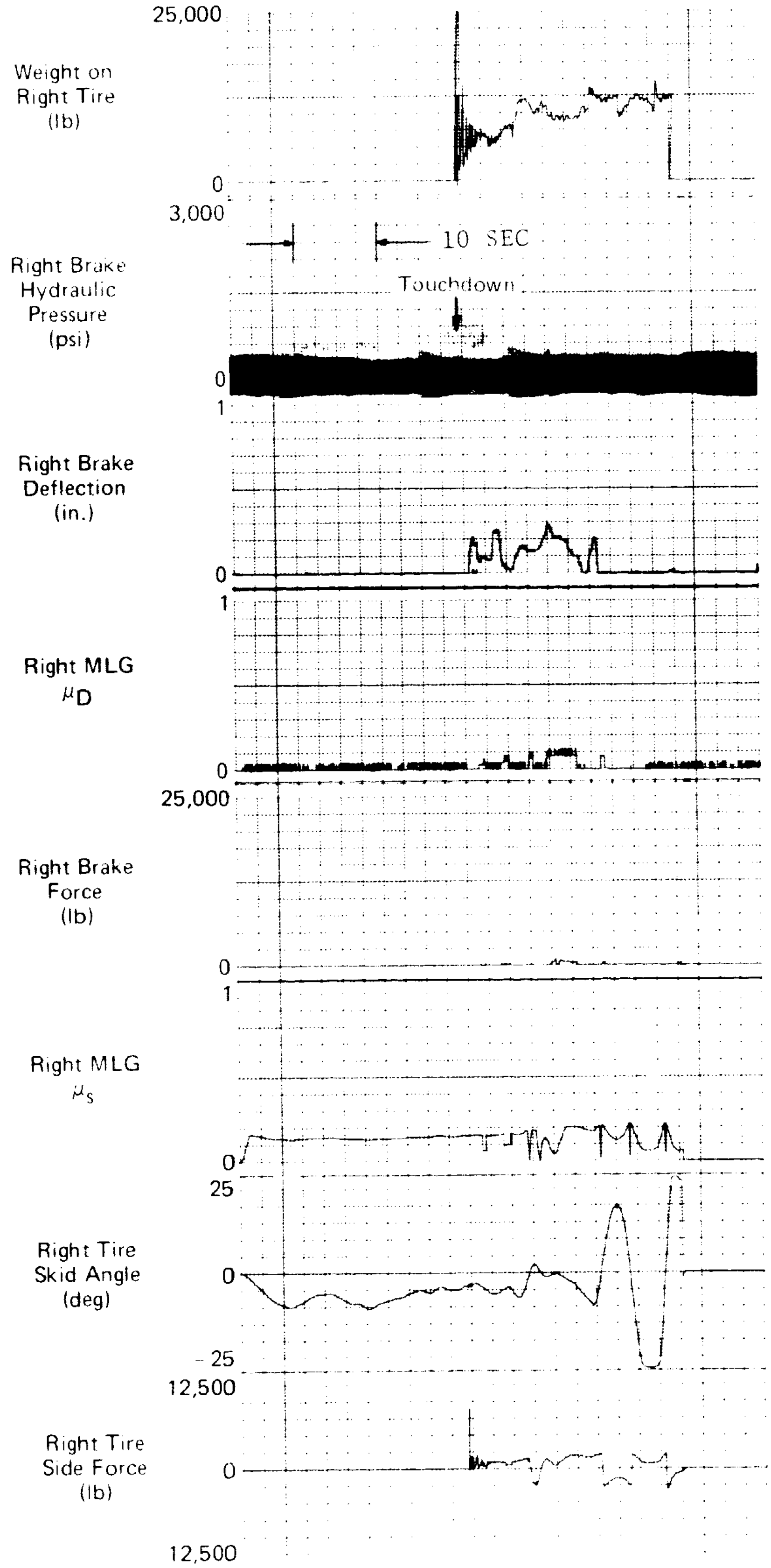

FIGURE 6-8 (Continued)
TYPICAL LANDING ON WET RUNWAY
Demonstration Run No. 90

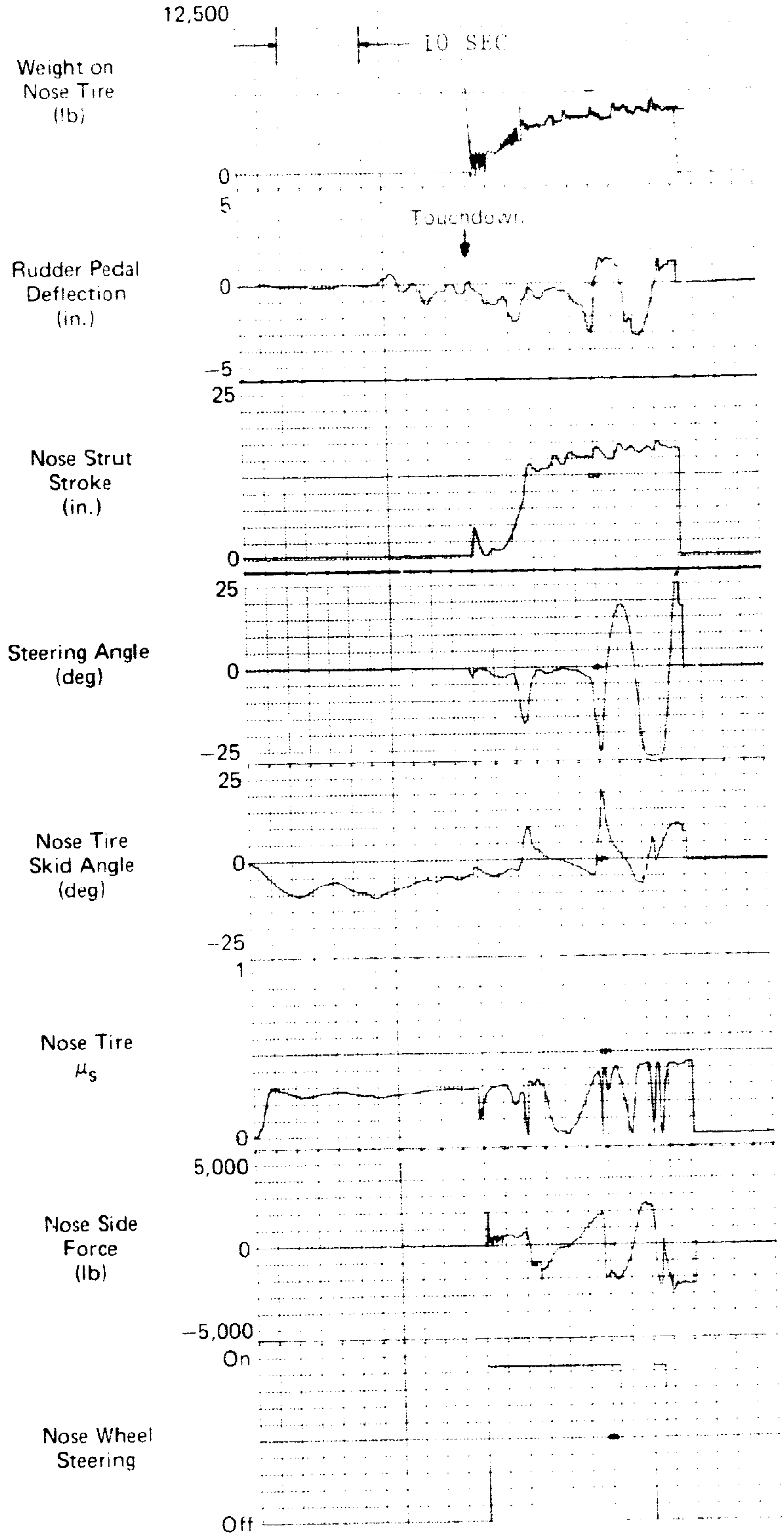

FIGURE 6-8 (Concluded)
TYPICAL LANDING ON WET RUNWAY
Demonstration Run No. 90

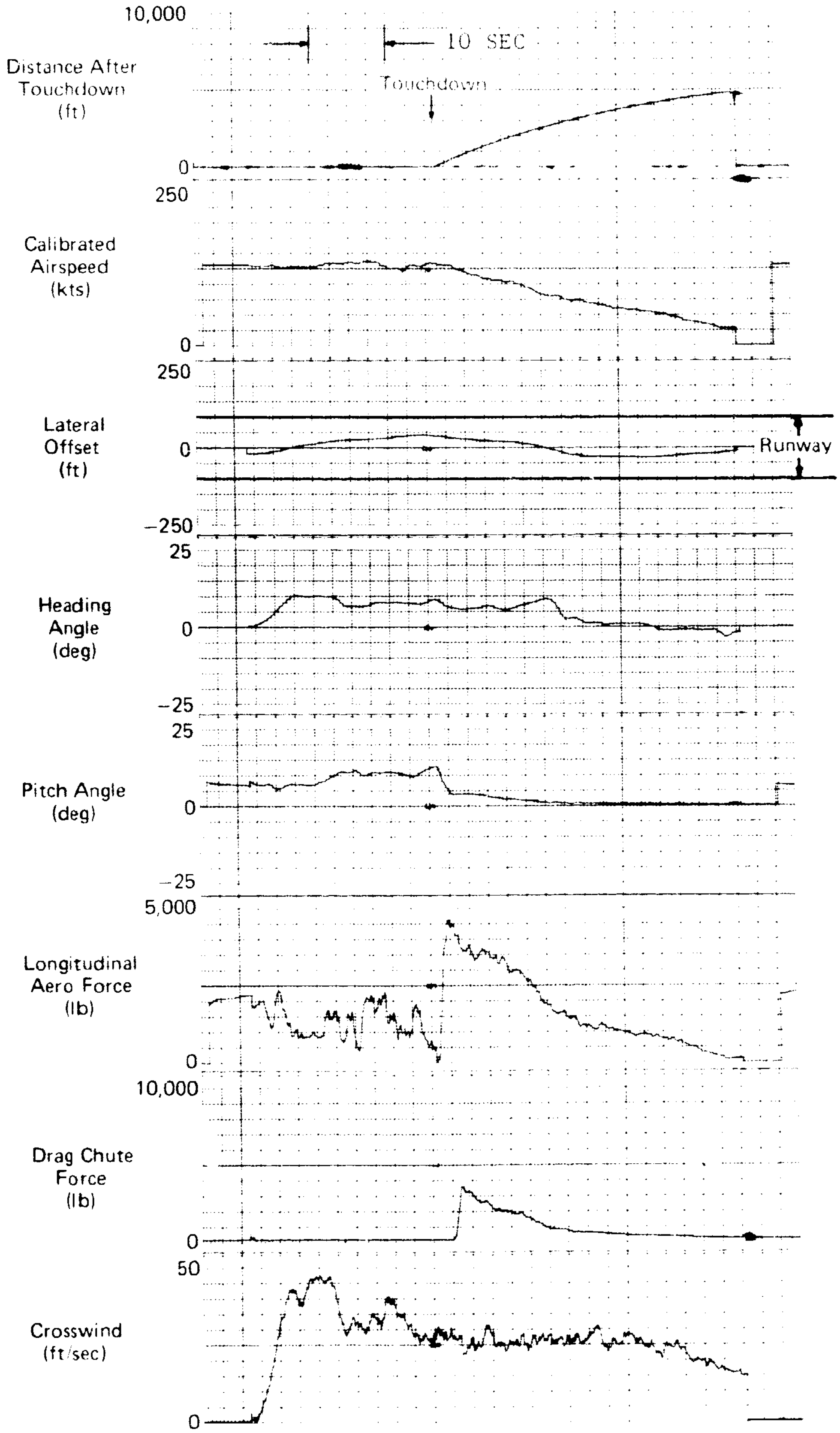

FIGURE 6-9
TYPICAL LANDING ON FLOODED RUNWAY
Demonstration Run No. 101 See Table 6-1

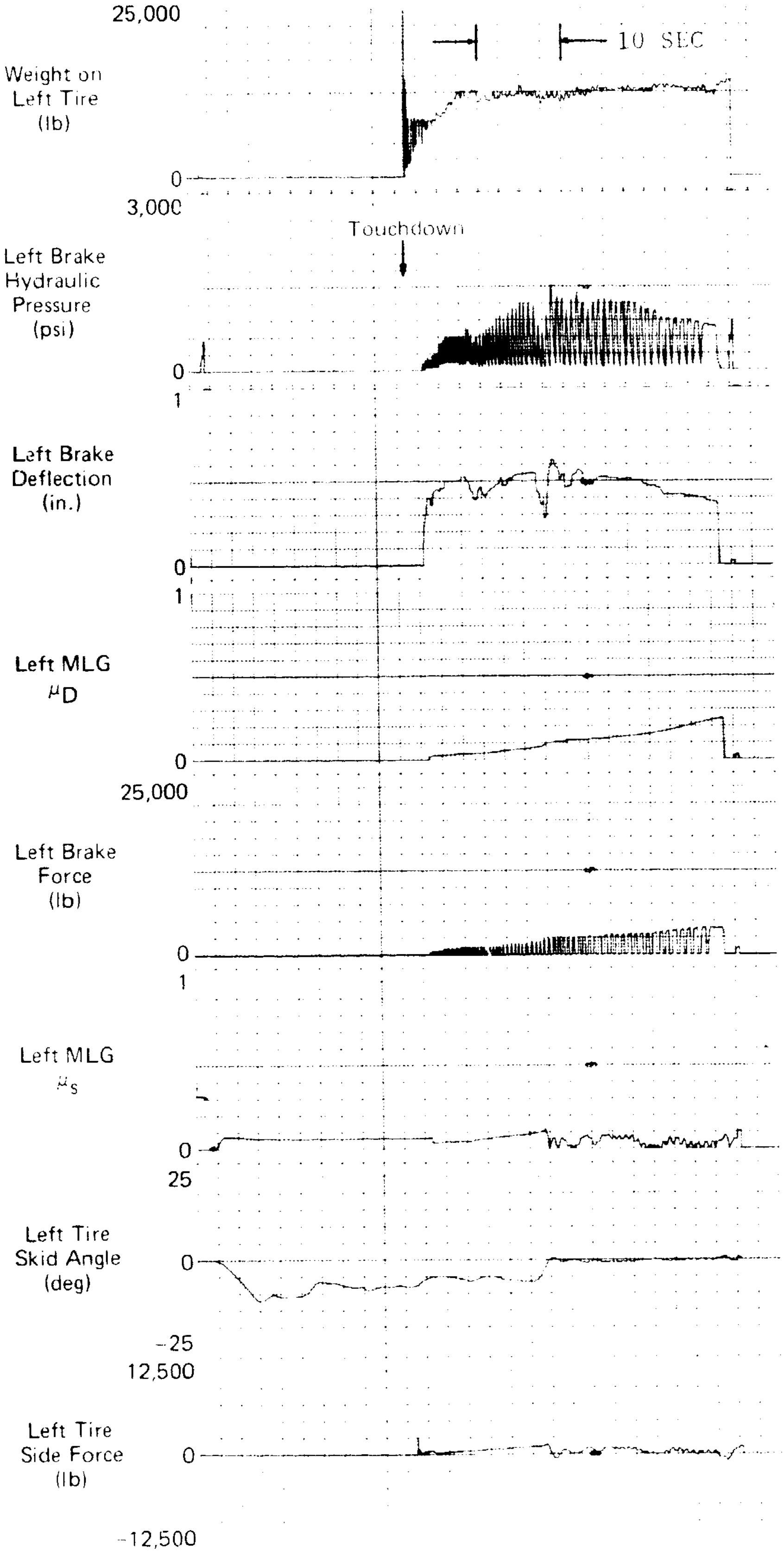

FIGURE 6-9 (Continued)
TYPICAL LANDING ON FLOODED RUNWAY
Demonstration Run No. 101

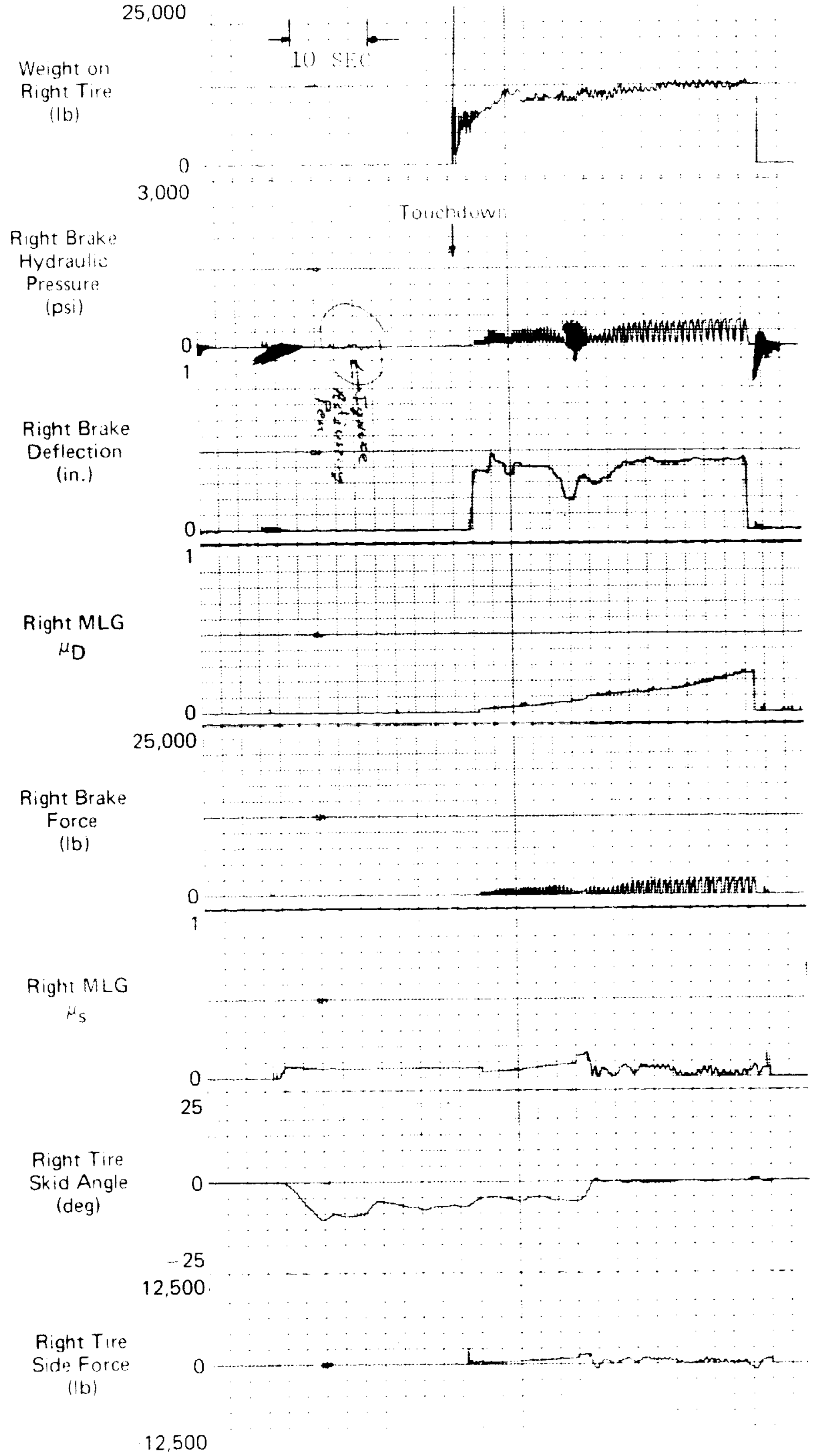

FIGURE 6-9 (Continued)
TYPICAL LANDING ON FLOODED RUNWAY
Demonstration Run No. 101

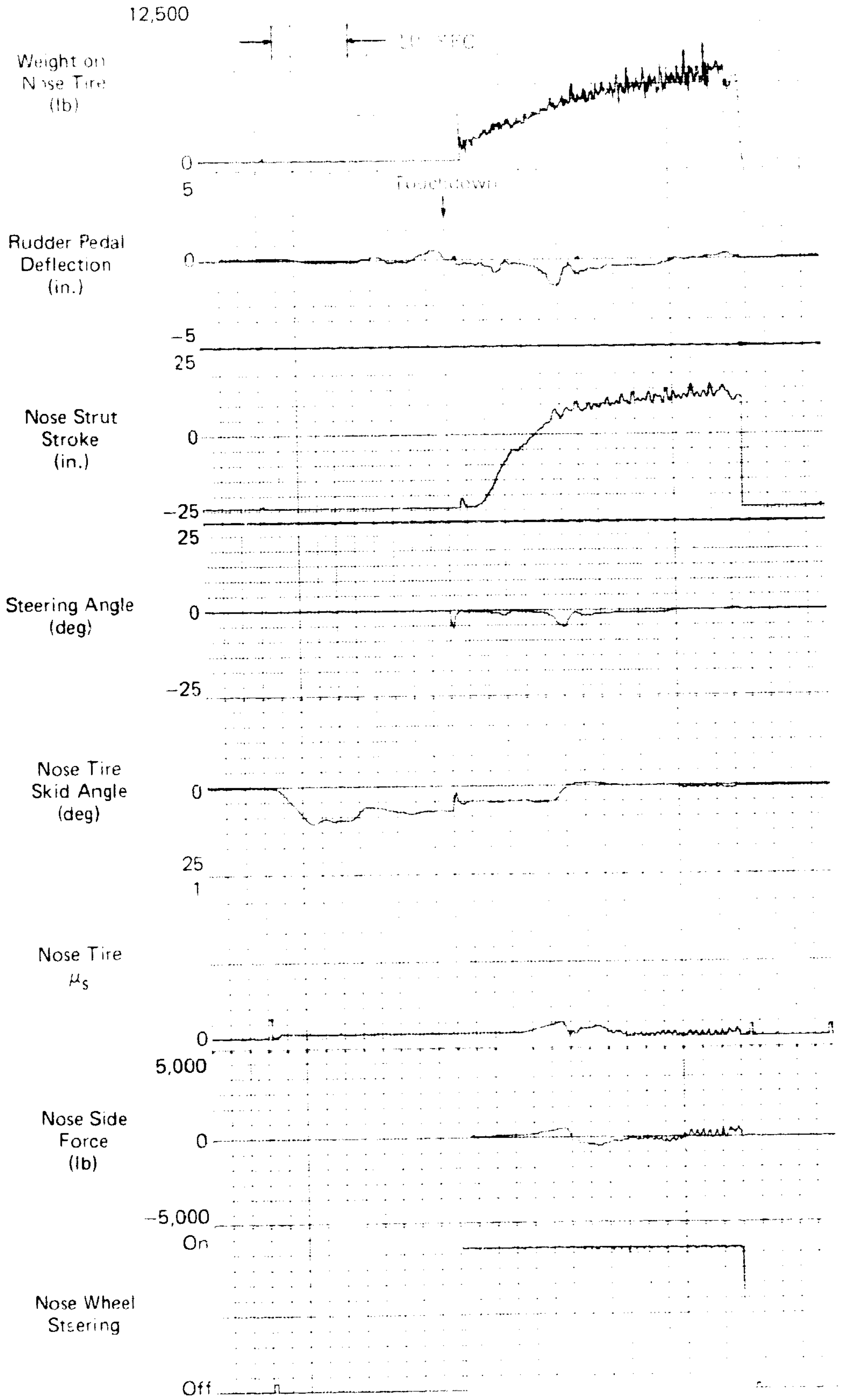

FIGURE 6-9 (Concluded)
TYPICAL LANDING ON FLOODED RUNWAY
Demonstration Run No. 101

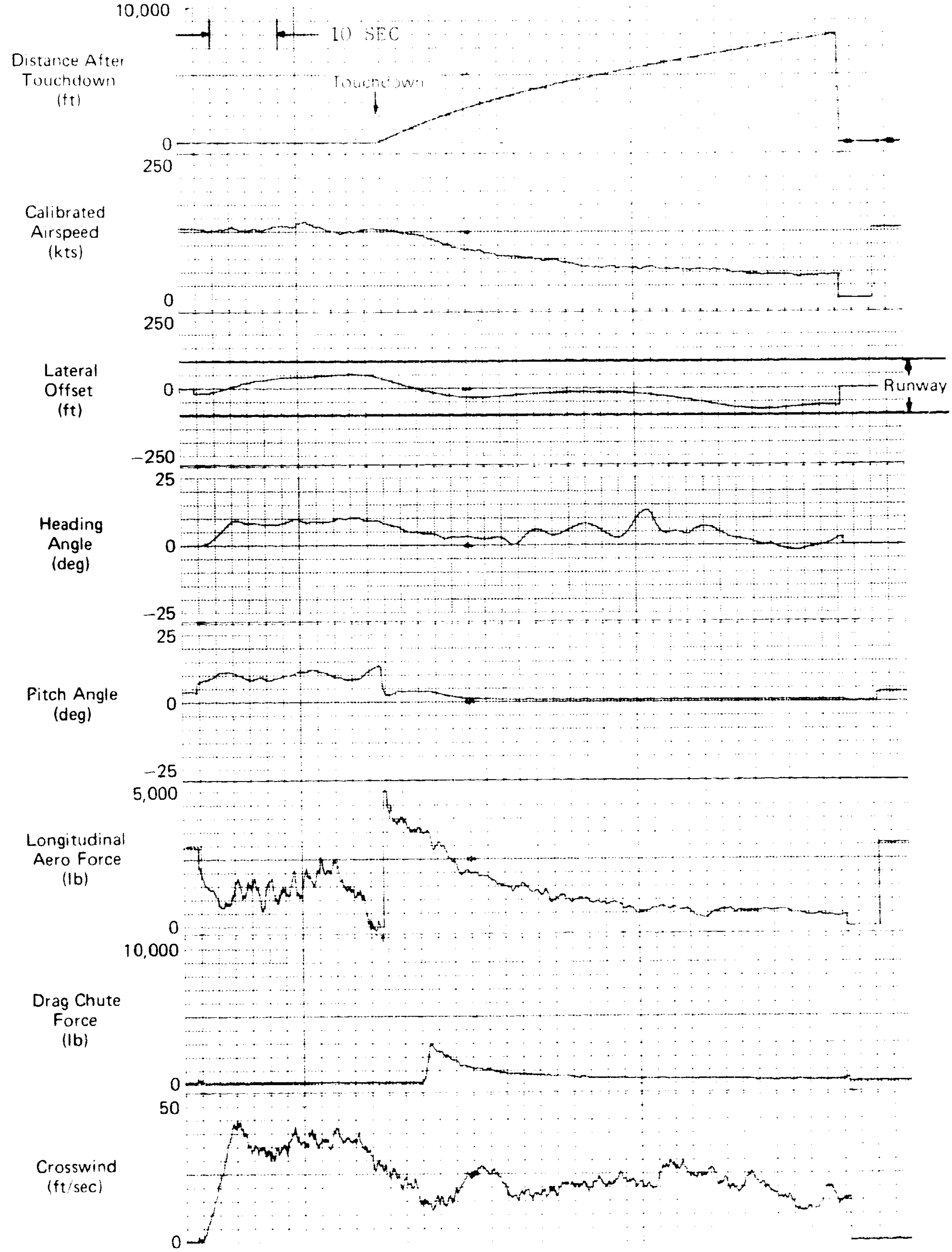

FIGURE 6-10
TYPICAL LANDING ON ICY RUNWAY
Demonstration Run No. 76 See Table 6-1

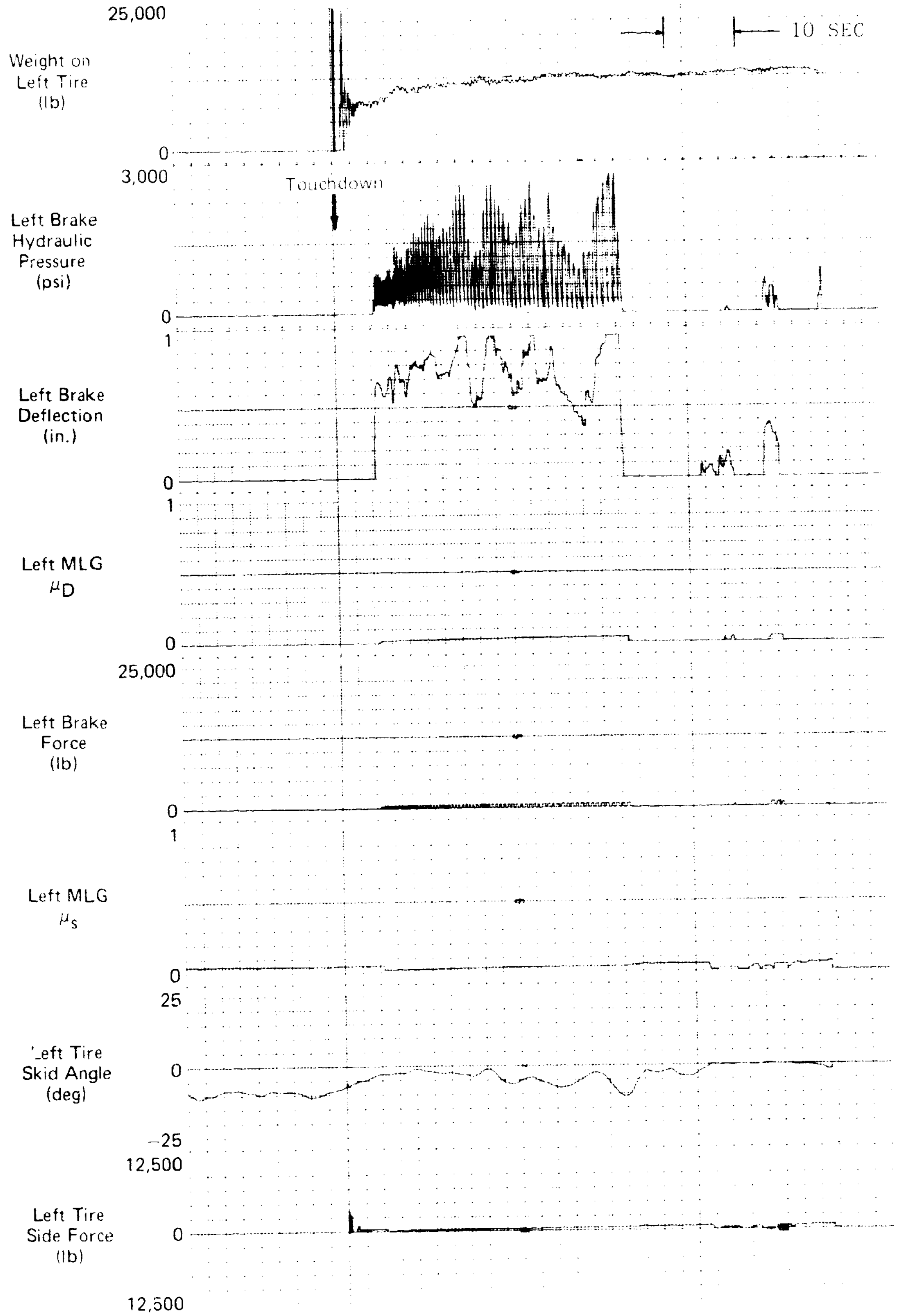

FIGURE 6-10 (Continued)
TYPICAL LANDING ON ICY RUNWAY
Demonstration Run No. 76

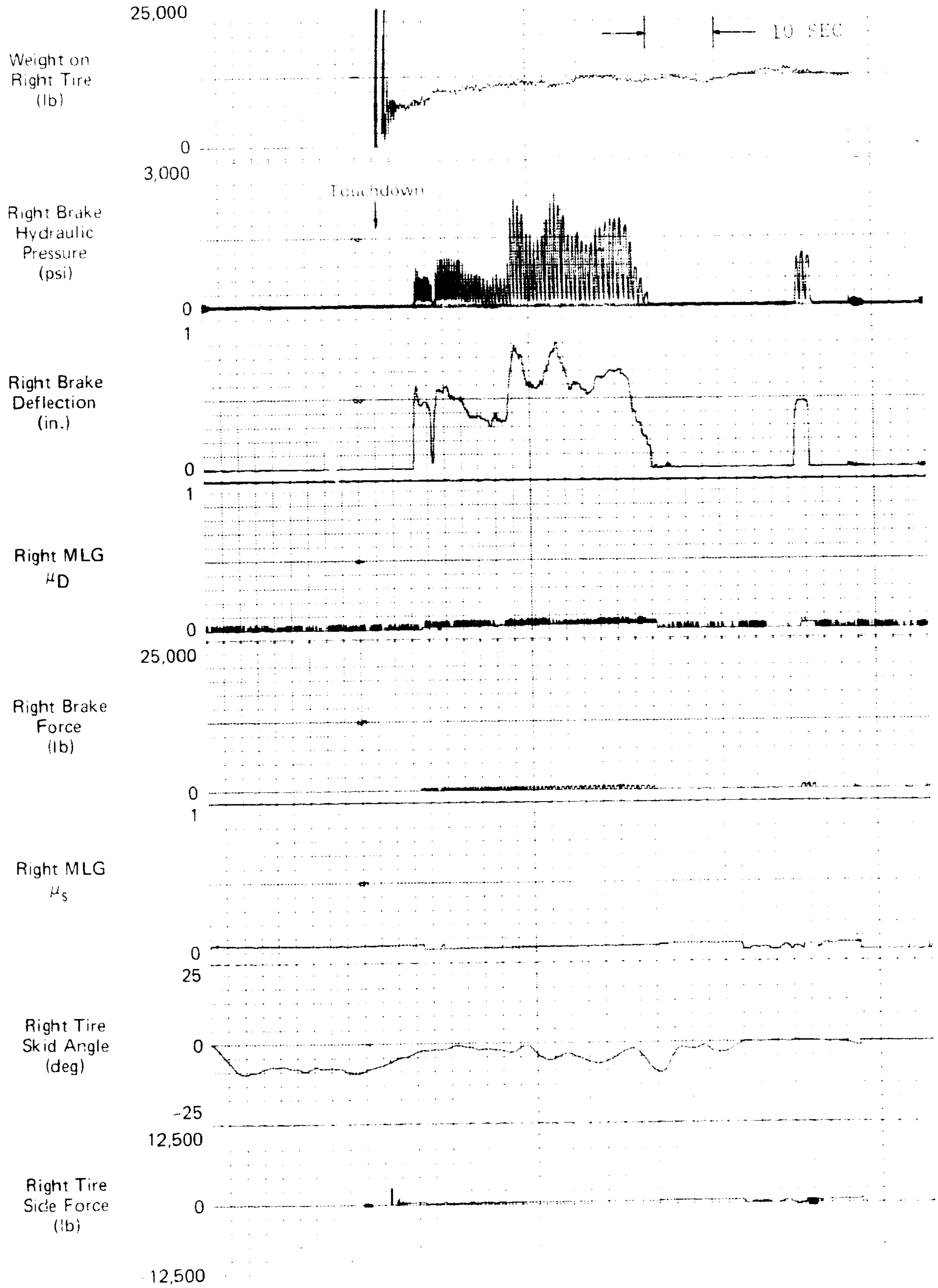

FIGURE 6-10 (Continued)
TYPICAL LANDING ON ICY RUNWAY
Demonstration Run No. 76

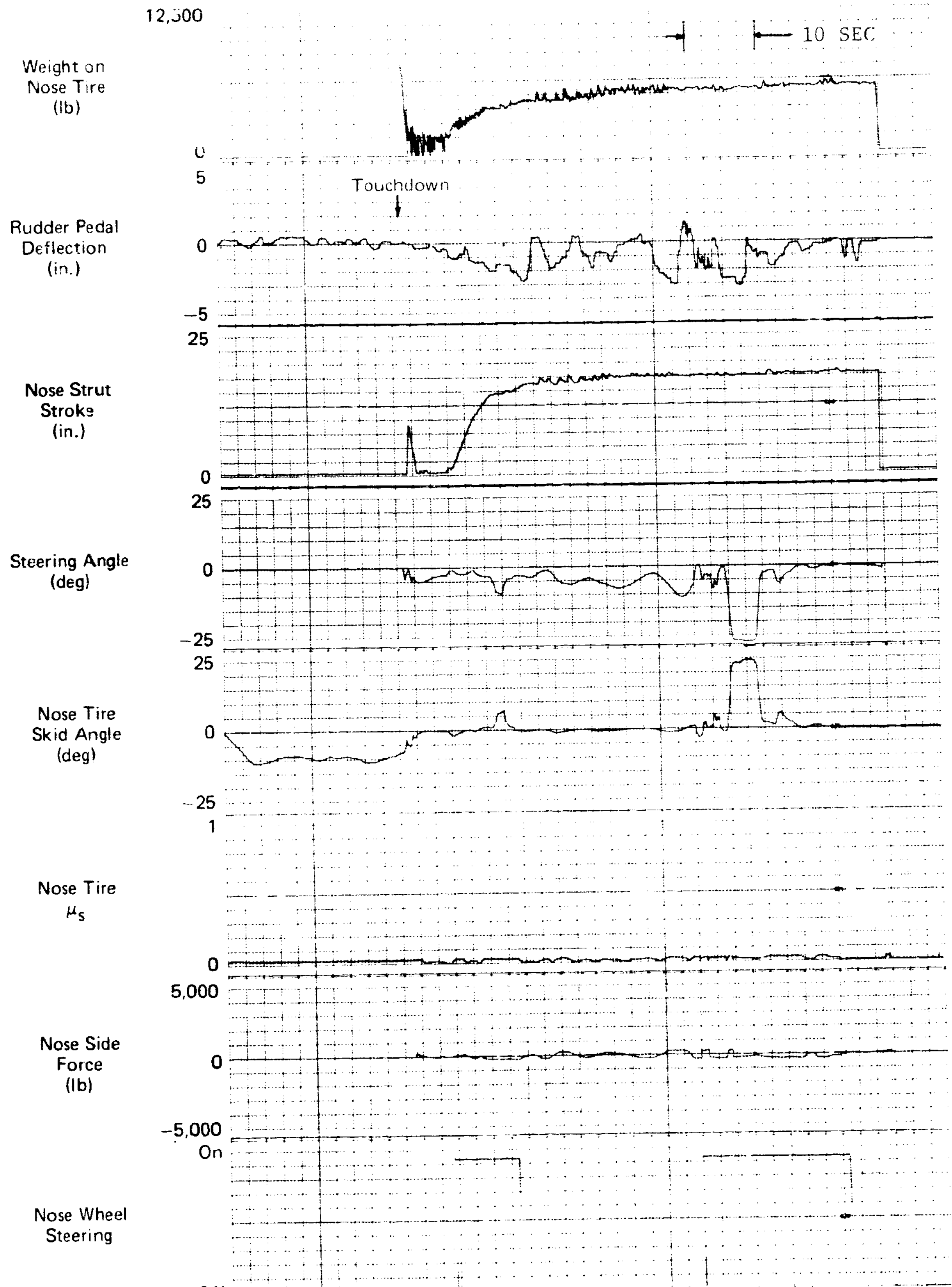

FIGURE 6-10 (Concluded)
TYPICAL LANDING ON ICY RUNWAY
Demonstration Run No. 76

GP75 0012 43

C.2

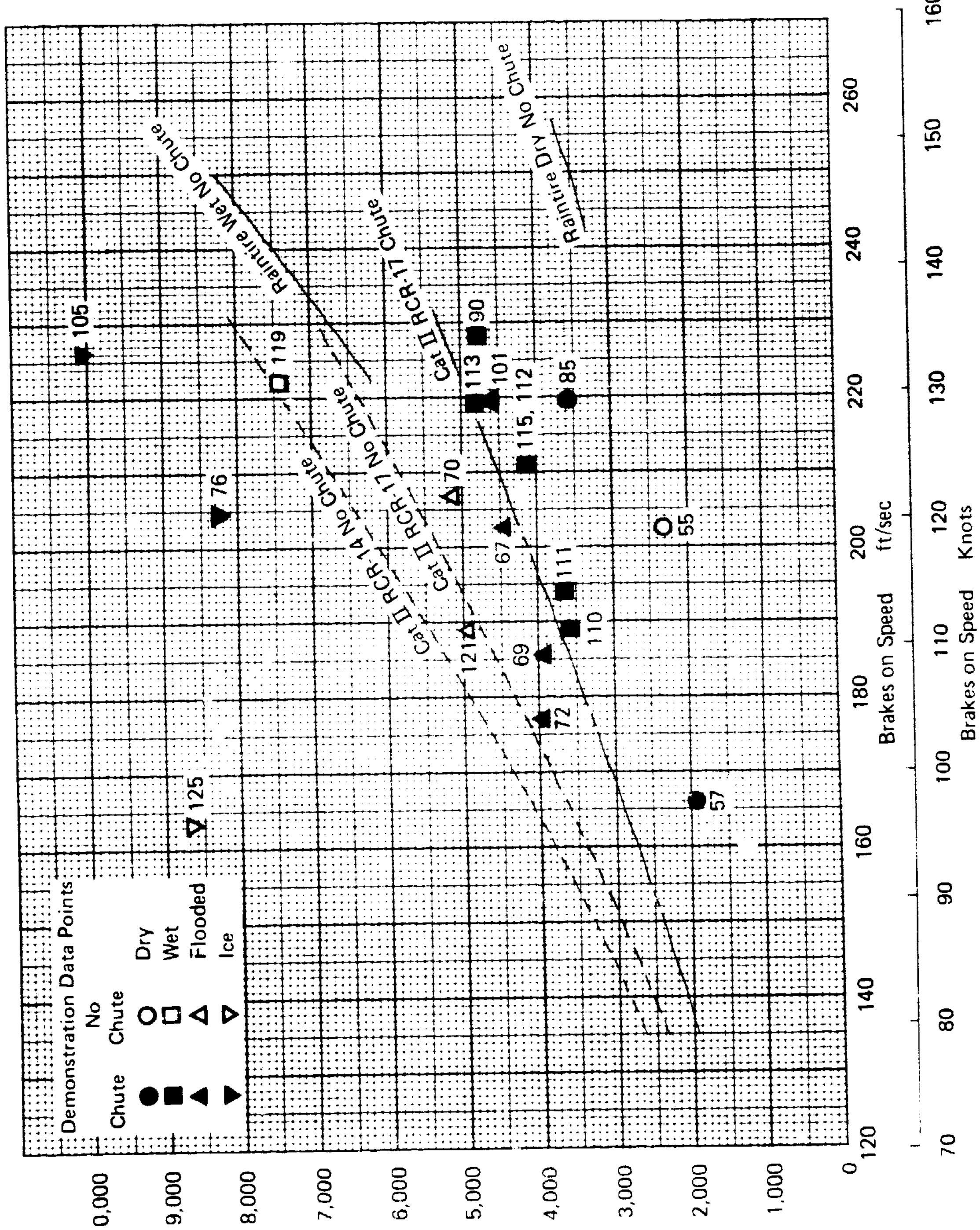

FIGURE 6-11
STOPPING DISTANCE FOR SIMULATOR vs AIRCRAFT

"My general feelings, for all conditions evaluated, were that the motions on the visual display reduced the overall capability considerably from that available with a good simulation of this type. My ratings ignore this "poor" factor because I am aware there is an effort underway to provide a new translator in the near future.

One other point: The "spring-feel" brake pedals detract from the F-4 similarity standpoint. Too bad we can't get that "hydraulic feel" instead! Another remark on overall simulation: Excellent capability for engineering evaluation and for training purposes. The difficulty I had in a crosswind, parabrake extended, full braking, on solid ice was very realistic. (Although I have not had the personal experience in the F-4). Extrapolating my F-4 experience on patchy ice (and other aircraft on solid ice) leaves me with that impression.

I think the crown effect is needed, as well as undulations of surface. All things considered, very good simulation!"

George Mills, MCAIR

**FIGURE 6-12
POST DEMONSTRATION
PILOT COMMENTS**

RUNWAY CONDITION: DRY_X_ WET_X_ FLOODED_X_ ICY_X_

ITEM	(EXCELLENT) 1	2	3	4	5	6	7	8	9	(POOR) 10
1. AERODYANMIC STEERING										
2. NOSEWHEEL STEERING										
3. COMBINED NW & AERO STEERING										
4. BRAKING EFFECTIVENESS										
5. CROSSWIND										
6. YAW CONTROL										
7. YAW STABILITY										
8. DRAG CHUTE										
9. OTHER										

Pilot: George Mills - MCAIR

Note: All runs were made without motion for this pilot, due to maintenance on the MBS.

FIGURE 6-13
PILOT RATING - POST DEMONSTRATION

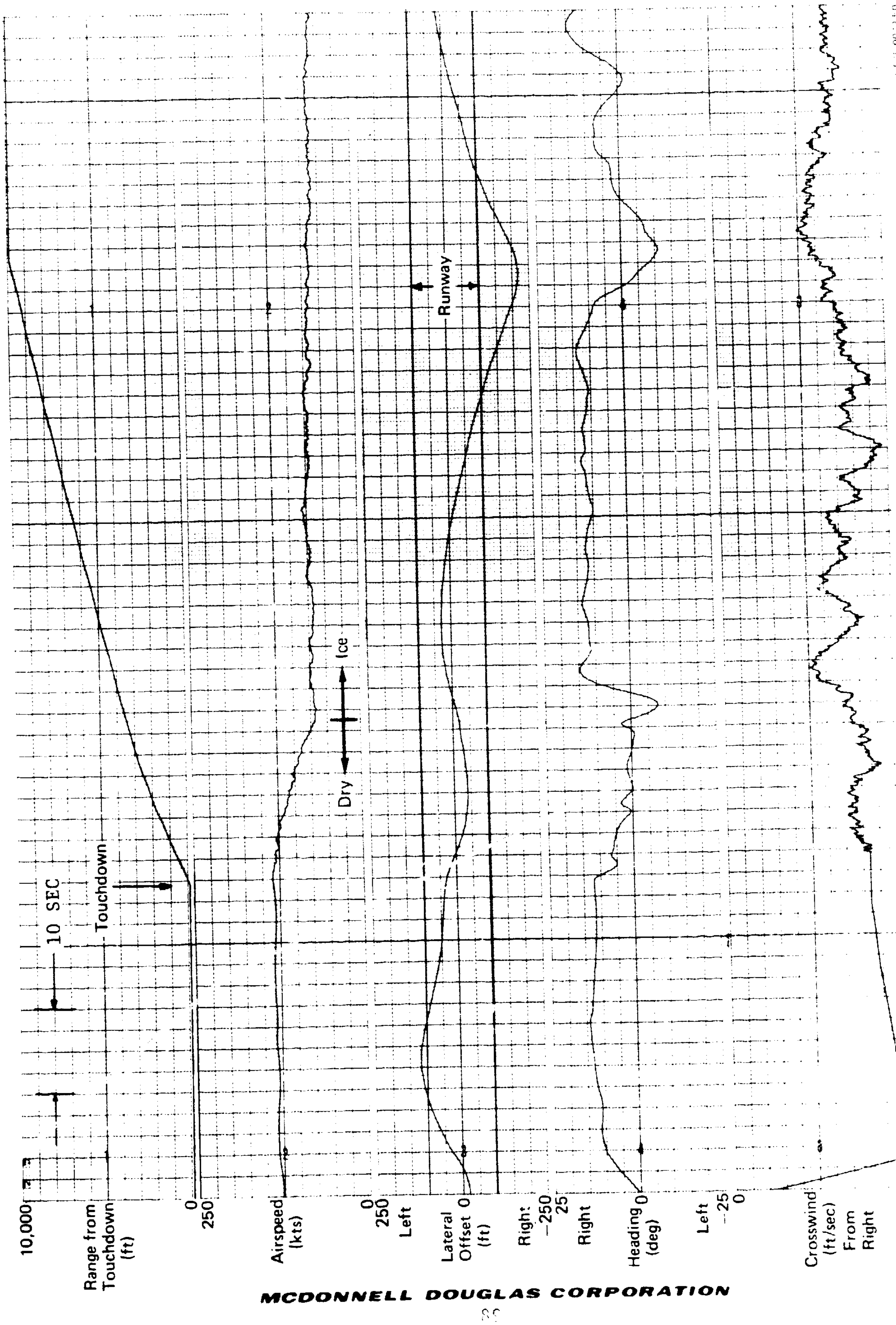

FIGURE 6-14
TYPICAL LANDING ON SIMULATED WALLOPS ISLAND PROFILE
Post Demonstration Matrix II Run 36

TABLE 6-1
DEMONSTRATION MATRIX

Run No.	Runway	Crosswind	Braking	Chute	Steering	Pilot
1	Dry	None	●			Meyers
2	↓	↓				↓
3	↓	↓	●			↓
4	↓	↓			●	↓
5	↓	↓	●		●	↓
6	Wet	↓	●		●	↓
7	↓	↓	●	●	●	↓
8	Flooded	↓	●	●	●	↓
9	↓	↓	●	●	●	↓
10	↓	↓	●	●	●	↓
11	↓	15 Knots - Steady	●	●	●	↓
12	↓	↓		●		↓
13	↓	↓	●	●		↓
14	Ice	None	●	●	●	↓
15	↓	↓	●	●	●	↓
16	↓	15 Knots - Steady	●		●	↓
17	↓	↓	●		●	↓
18	↓	15 Knots - Gusts	●		●	↓
19	Wet	None				Higgs
20	↓	↓	●			↓
21	↓	↓				↓
22	↓	↓	●			↓
23	↓	↓	●		●	↓
24	↓	↓	●	●		↓
25	↓	↓		●		↓
26	↓	↓				↓
27	↓	↓	●	●		↓
28	Dry	↓	●	●		↓
29	↓	↓	●	●	●	↓
30	Flooded	↓				↓
31	↓	↓		●		↓
32	↓	↓	●	●	●	↓
33	Ice	↓				↓
34	↓	↓	●	●	●	↓
35	↓	↓	●	●		↓
36	Wet	15 Knots		●	●	↓
37	↓	↓	●	●	●	↓
38	Flooded	↓	●	●	●	↓
39	↓	None			●	Tinsley
40	↓	↓	●			↓
41	Wet	↓	●	●	●	↓
42	↓	↓	●	●	●	↓
43	↓	↓	●	●	●	↓
44	Ice	↓	●	●	●	↓
45	↓	↓	●	●	●	↓

● Indicates brake application, chute deployed, steering engaged, skid control model operating

GP75 0072 44

TABLE 6-1 (Continued)
DEMONSTRATION MATRIX

Run No.	Runway	Crosswind*	Braking	Chute	Steering	Pilot
46	Ice	15 Knots	•	•	•	Tinsley
47	↓	None	•	•	•	↓
48	Dry	15 Knots				
49	↓	↓				
50			•		•	↓
51	↓	None	•	•		↓
52	Dry	No	•			Meyers
53	↓	↓			•	↓
54						
55			•			
56	↓	Yes - Turbulence		•	•	↓
57		↓	•	•	•	
58	Wet	None		•		
59	↓	↓	•	•	•	
60		Yes - Turbulence		•	•	
61	↓	Yes		•		↓
62		Yes - Turbulence	•	•	•	
63		↓	•	•	•	
64			•		•	
65					•	
66	Flooded	No		•	•	↓
67	↓	No	•	•		
68		Yes - Turbulence		•		
69		↓	•	•	•	
70			•		•	
71	↓	↓			•	↓
72			•	•	•	
73	Ice	No		•	•	
74	↓	No	•	•	•	
75		25-15 Knots - Turbulence		•	•	
76	↓	↓	•	•	•	↓
77						
78			•			
79	Dry	No		•		Tinsley
80	↓	25-15 Knots				↓
81	↓	25-15 Knots - Turbulence	•	•		↓
82		No				
83		No	•		•	
84		25-15 Knots - Turbulence		•	•	
85		↓	•	•	•	
86	Wet	No		•	•	↓
87	↓	No	•	•	•	
88		25-15 Knots - Turbulence		•	•	
89		↓		•	•	
90			•	•	•	

End Day 1 (between runs 51 and 52)

GP75 0072 45

*Crosswind Ramp Input 25 Knots down to 15 for Wind Shear.

TABLE 6-1 (Concluded)
DEMONSTRATION MATRIX

Run No.	Runway	Crosswind*	Braking	Chute	Steering	Pilot
91	↓	↓	•			Tinsley
92	↓	↓	•		•	↓
93	↓	25-15 Knots - Turbulence			•	↓
94	Flooded	No		•		↓
95		No	•	•	•	↓
96	↓	25-15 Knots - Turbulence		•		↓
97	Dry	↓		•		↓
98	↓	↓	•	•	•	↓
99	↓	↓	•		•	↓
100	Flooded	↓		•	•	↓
101	↓	↓	•	•	•	↓
102	↓	↓	•		•	↓
103	↓	↓				↓
104	Ice	No		•		↓
105	↓	No	•	•	•	↓
106	↓	25-15 Knots - Turbulence		•	•	↓
107	↓	↓	•	•	•	↓
108	↓	↓				↓
109	↓	↓	•			↓
110	Wet	No	•	•		Higgs
111	↓	No	•	•		↓
112	↓	25-15 Knots - Steady	•	•	•	↓
113	↓	25-15 Knots - Turbulence	•	•		↓
114	↓	No		•		↓
115	↓	No	•	•		↓
116	↓	25-15 Knots - Turbulence		•		↓
117	↓	↓	•	•		↓
118	↓	↓	•	•		↓
119	↓	↓	•			↓
120	Flooded	No		•	•	↓
121	↓	No	•	•		↓
122	↓	25-15 Knots - Turbulence		•		↓
123	↓	↓	•	•		↓
124	↓	↓	•		•	↓
125	Ice	No	•	•		↓
126	↓	No		•		↓
127	↓	25-15 Knots - Turbulence		•		↓
128	↓	↓	•	•		↓
129	↓	↓	•			↓
130	Dry	↓	•	•	•	↓

GP75 0072 46

*Crosswind Ramp Input 25 Knots down to 15 for Wind Shear

TABLE 6-2
DEMONSTRATION COMMENTS PER RUN

Run No.	Pilot Comments
1	Too sensitive in pitch, with stick aft and brakes nose is slow in coming down
2	Too much nose high
4	False sense of skidding
6	Lots of nose bounce
8	Realistic touchdown feel
9	Tendency to overcorrect on NW steer
11	Would expect nose to turn more with chute and crosswind
12	Didn't need to increase rudder with chute deployment, without steering rudder control was not enough
13	Lots of Skid
14	Seems to be plenty of braking at the start
17	Unnatural, chute not strong enough response in the begining at high speed
18	Full rudder
19	Abort
21	Abort
22	Abort
26	Camera reject
30	Camera reject
31	Large nose rise after trimming aircraft
33	Ground abort
36	Dropped chute
37	Dropped chute, awfully wet
38	Dropped chute
39	Abort
41	Steering tended to diverge
48	Camera reject
49	Camera reject
50	Looks good

Note: After run 51 the following changes were made:
(1) Removed runway markers
(2) Adjusted pitch gain and roll gain
(3) Added wind shear

52	Touchdown pitching improved
53	Nose drops just like plane at touchdown, runway visual is off to right
54	Aft stick, ailerons like plane, rudder response a little high at slow speed, turn associated with turn more than plane but pretty good
55	Nose action very good, difficult to feel decel without peripheral vision
56	Effect at drag chute seemed to change
57	Magnitude of drag chute seems low
58	Rudder effectiveness seems very real, aero steering good, drag chute good
59	Nose steering overly sensitive at 60 knots
60	Nose [illegible]ng overly sensitive at 60 knots, requires large roll correction, lateral displacement hard to [illegible]dge
61	Requires large roll correction, PIO problem with sensitive nose steering - high initial response - not typical of aircraft

GP75 0072 4

Note: For run numbers which are omitted there was no comment.

TABLE 6-2 (Continued)
DEMONSTRATION COMMENTS PER RUN

Run No.	Pilot Comments
62	Lost control - turned off steering - probably very realistic - just pilot problem
63	Nose came over with chute (still not enough)
64	Response of nose steering is still high, removal of runway markers make runway seem wider
67	Seems pretty good, no NW steering
68	More turning into wind, rudder is fairly effective, not much different from wet
69	NW steering more realistic on flooded than wet
70	NW steering more realistic on flooded than wet
71	NW and aero steering - realistic, airborne roll still not right
73	Too much nose steering response at high speed
75	NW steering not effective, aero effective, good simulation
76	NW steering not effective, aero effective, good simulation
78	In general low μ simulation was good high μ values
79	Good aileron response, much better in roll made, rudder decay is good
80	Drag chute seems better, runway seems wider with runway markers removed.
81	Good - effective differential braking
82	Stability excellent, runway scene improved
84	Touchdown in right hand crab pulls right
86	Acts like plane, good aileron simulation - decays properly
87	Some yaw oscillation when going through 70-60 knots with brakes on
88	Lost control at 85 knots (large wind gust) - dropped chute - reset
90	Dropped chute - lost control
91	Large gust at - 90 knots - lost control
92	No large gusts this time - no problem
95	Not much difference between wet and flooded
102	Squirrelly at 70 knots
106	More stable than expected
110	Roll not as wild as yesterday
113	Nose gear not bottoming
114	Dropped chute - nose came back properly, seems better - learning curve?
115	Rejected
116	Dropped chute for control, airlerons helped, seemed like airplane
117	Problem steering - lost control
118	No problem steering (no wind)
120	Out of rudder effect began drifting - tried steering
121	Wind shear loads good, delayed NW steering
127	No serious problems
128	Dropped chute, good aileron effects
129	At - 45 aero steering seems too good
130	Steering works fine, applied brakes at - 80 knots

GP75 0072 48

Note: For run numbers which are omitted there was no comment.

TABLE 6-3
POST DEMONSTRATION TEST MATRIX I

Run No.	Runway	Crosswind	Braking	Chute	Steering	Cycling Skid Control	Pilot
1-8	System Checkout						
9	Dry	None					Plumber
10				●	●	●	
11				●		●	
12						●	
13					●	●	
14		25-15 Knots - Steady			●	●	
15					●	●	
16				●	●		
17	Wet	None		●	●		
18				●	●		
19				●	●		
20		25-15 Knots - Steady		●	●		
21				●	●		
22	Flooded			●	●		
23				●	●		
24	Icy	None		●	●		
25		25-15 Knots - Steady		●	●		
26		25-15 Knots - Turbulence		●	●		
27				●	●		
28				●	●		
29	Dry - Flood(A)	25-15 Knots - Steady			●	●	
30		25-15 Knots - Turbulence			●	●	
31	Flooded				●	●	
32	Dry - Flood(A)				●	●	
33					●	●	
34	Dry	None			●	●	

GP75 0072 52

Note:
(A) Dry changed to flooded at 80 kts
● Indicates brake application, chute deployed, steering engaged, skid control model operating

TABLE 6-4
POST DEMONSTRATION TEST MATRIX II

Run No.	Runway	Crosswind	Braking	Chute	Steering	Cycling Skid Control	Pilot
1-8	← System Checkout →						
9	Dry	25-15 Knots - Steady	●		●	●	Mills
10	Wet	None	●		●	●	↓
11	↓	↓	●		●	●	↓
12	↓	↓	●	●	●	●	↓
13	↓	25-15 Knots - Steady	●	●	●	●	↓
14	↓	↓	●	●		●	↓
15	Flooded	↓	●	●		●	↓
16	↓	None	●	●		●	↓
17	↓	↓	●	●	●	●	↓
18	↓	↓	●		●	●	↓
19	↓	25-15 Knots - Steady	●	●	●	●	↓
20	↓	↓	●	●	●	●	↓
21	↓	35-25 Knots - Turbulence	●	●	●	●	↓
22	Icy	None	●	●	●	●	↓
23	↓	35-25 Knots - Steady	●	●	●	●	↓
24	↓	↓	●	●	●	●	↓
25	Dry - Flooded(A)	↓	●			●	↓
26	Dry - Flooded(B)	↓	●			●	↓
27	Dry - Flooded(A)	↓	●			●	↓
28	Dry - Flooded(B)	↓	●			●	↓
29	Dry - Flooded(A)	↓	●			●	↓
30	Dry - Flooded(B)	↓	●			●	↓
31	Dry - Flooded(A)	35-25 Knots - Turbulence	●			●	↓
32	Dry - Flooded(B)	↓	●			●	↓
33	← Abort →						
34	Dry - Flooded(A)	↓	●	●		●	↓
35	Dry - Flooded(B)	↓	●	●	●	●	↓
36	Dry - Icy(C)	↓	●		●	●	↓
37	Dry - Icy(D)	↓	●	●	●	●	↓
38	Dry - Icy(D)	↓	●	●	●	●	↓

GP75 0072 51

Notes:
(A) Dry changed to flooded at 80 kts
(B) Dry changed to flooded at 100 kts
(C) Dry changed to ice at 80 kts
(D) Dry changed to ice at 100 kts
● Indicates brake application, chute deployed, steering engaged, skid control model operating

7.0 CONCLUSIONS AND RECOMMENDATIONS

7.1 General

This study is a first step to expand the ground handling simulation such that a high degree of confidence will be developed for simulations of all types and sizes of aircraft (flown and unflown, existing and future). This confidence will be created with the philosophy of step by step technological expansion of more and more actual aircraft and environmental parameters representing several increasingly complex aircraft. During the expansion, the influence of parameters on performance must be understood in the interest of developing an economically feasible simulation capability. To maintain a reasonable cost the trend toward developing complex mathematical models should be tempered so that the minimum of complexity needed to adequately simulate the desired aircraft is used.

7.2 Improvements in Simulation Hardware

This phase of study indicated a need for improvements in "down the runway" deceleration cues. Adding the sixth degree of freedom to the cockpit will not in itself appropriately simulate the 20 to 30 seconds of deceleration during braking. MCAIR is currently making improvements to the translator hardware and terrain map will provide smooth visual stopping action, scaled runway markings and a view of the runway with the pilot's eye position at the appropriately scaled height above the runway. Additional cues which can be easily added are "g" suit inflation and/or tilting the cockpit to place a forward force component on the pilot. Other cues which could be added with some difficulty in the present cockpit are controlled shoulder harness tension during braking and rotating drums for peripheral vision effects.

7.3 Improvements in Modeling

MCAIR recommends future modeling be upgraded to include runway crown and roughness, skid control system hardware and actual tire-runway friction characteristics. With the smooth, flat runway used during this program, aircraft motion down the runway was disturbed only by the gusty winds and not by the real life effects of runway undulations, friction variations, and crown effects. The addition of skid control system hardware to the simulation will enable using unmodified tire-runway friction models and will provide increased confidence in future aircraft simulations.

7.4 Expansion to Other Known Aircraft

Another reasonable step in gaining simulation technology confidence is to include additional aircraft while progressing from simple to complex vehicles. Appropriate methods must be developed for simulating complex aircraft effectively but economically.

7.5 Problem Solving

Future effort should also contain problem solving demonstrations preferably where known aircraft deficiencies or limitations have been improved with known aircraft changes. The effects of nose wheel steering rate changes upon the F-4 fishtailing characteristics is an example of problem solving which should be pursued.

7.6 Hardware Performance Definition

The hardware parameters used in this study are those which are generally available to system designers and component manufacturers. The study did reinforce the need for the complete tire-runway friction definition in both cornering and braking throughout the yaw angles expected for the aircraft.

8.0 REFERENCES

1. Flying Qualities of Piloted Airplanes, MIL-F-8785, 7 August 1969.

2. W. J. Bonnie and C. R. Niemann: Model F/RF-4B-C Aerodynamic Derivatives, McDonnell Aircraft Company Report MDC 9842.

3. Robert F. Smiley and Walter B. Horne: Mechanical Properties of Pneumatic Tires with Special Reference to Modern Aircraft Tires, NASA TR R-64, 1960.

4. Richard H. Danhof and Herauld G. Gentry: RF-4C Wet Runway Performance Evaluation, FTC-TR-66-6, May 1966.

5. Thomas A. Byrdsong: Experimental Investigation of the Directional Control Capability of 18x5.5, Type VII, Aircraft Tires on Wet Surfaces, NASA TN D-6202, March 1971.

6. Thomas J. Yager, W. Pelham Phillips, Walter B. Horne, Howard C. Sparks: A Comparison of Aircraft and Ground Vehicle Stopping Performance on Dry, Wet, Flooded, Slush-, Snow-, and Ice-Covered Runways, NASA TN D-6098, November 1970.

7. Robert C. Dreher and John A. Tanner: Experimental Investigation of Braking and Cornering Characteristics of 30x11.5-14.5, Type VII, Aircraft Tires with Different Tread Patterns, NASA TN D-7743, 1974.

8. Robert C. Dreher and John A. Tanner: Experimental Investigation of Cornering Characteristics of 18x5.5, Type VII, Aircraft Tires with Different Tread Patterns, NASA TN D-7815, 1974.

9. W. W. Macy and R. W. Palmer: Effects of Skid Control, Tires, and Steering on Aircraft Ground Performance (Raintire), McDonnell Aircraft Company Report MDC A2683, February 1974.

10. Model F-4C Landing Gear Design Data, McDonnell Aircraft Company Report 8581 (including unincorporated changes).

11. Nose Landing Gear Metering Tube Development, McDonnell Aircraft Company Laboratory Test Report J32-152.10.

12. Main Landing Gear Metering Tube Development, Bendix Test Report EAL-66-47.

END

DATE

FILMED

NOV 18 1976